



Promoting heart regeneration via cardiomyocyte-specific OSKM-expression

INAUGURAL-DISSERTATION

Zur Erlangung des Doktorgrades der Naturwissenschaften

-Doctor rerum naturalium-

(Dr. rer. nat.)

vorgelegt dem

Fachbereich 08 – Biologie und Chemie der

Justus-Liebig-Universität Gießen

Durchgeführt am Max-Planck-Institut für Herz-und Lungenforschung,

W.G. Kerckhoff-Institut Bad Nauheim

vorgelegt von

Yanpu Chen

aus Leshan, China

Gießen (2022)

Die Untersuchungen zur vorliegenden Arbeit wurden am Max-Planck-Institut für Herz-und Lungenforschung (W. G. Kerckhoff-Institut) in Bad Nauheim unter Leitung von Prof. Dr. Dr. Thomas Braun durchgeführt.

Vom Fachbereich 08-Biologie der Justus-Liebig-Universität Gießen angenommen

Erstgutachter:

Prof. Dr. Dr. Thomas Braun

Abteilung für Entwicklung und Umbau des Herzens

Max-Planck-Institut für Herz-und Lungenforschung

Ludwigstraße 43D-61231 Bad Nauheim

Zweitgutachter:

Prof. Dr. Thomas Böttger

Abteilung für Entwicklung und Umbau des Herzens

Max-Planck-Institut für Herz-und Lungenforschung

Ludwigstraße 43D-61231 Bad Nauheim

Declaration

I declare that the dissertation here submitted is entirely my own work, written without any illegitimate help by any third party and solely with materials as indicated in the dissertation. I have indicated in the text where I have used texts from already published sources, either word for word or in substance, and where I have made statements based on oral information given to me. At all times during the investigations carried out by me and described in the dissertation, I have followed the principles of good scientific practice as defined in the “Statutes of the Justus Liebig University Gießen for the Safeguarding of Good Scientific Practice”.

Place, Date

Original Signature

Publications relating to this dissertation

Yanpu Chen, Felipe F. Lüttmann, Eric Schoger, Hans R. Schöler, Laura C. Zelarayán, Kee-Pyo Kim Jody J. Haigh Johnny Kim and Thomas Braun. Reversible reprogramming of cardiomyocytes to a fetal state drives adult heart regeneration in mice. *Science*. 373(6562):1537-1540 (2021). DOI: [10.1126/science.abg5159](https://doi.org/10.1126/science.abg5159)

Contents

Summary	4
Zusammenfassung.....	6
1. Introduction	8
1.1. Heart and heart attack.....	8
1.1.1. General aspects.....	8
1.1.2. Heart development	8
1.1.3. Heart and circulatory system.....	10
1.1.4. Heart attack	12
1.2. Regeneration.....	13
1.3. Heart regeneration	15
1.4.1. Cardiac transdifferentiation.....	17
1.4.2. Cell therapy	18
1.4.3. Promotion of cardiomyocyte proliferation.....	20
1.5. OSKM-dependent reprogramming	23
1.6. Molecular rejuvenation through OSKM-dependent reprogramming	24
2. Aim of this project.....	26
3. Materials	27
3.1. Chemicals	27
3.2. Antibodies.....	28
3.3. Primers.....	29
3.4. Plasmids.....	30
3.5. Kits	33
3.6. Equipment.....	34
4. Methods	36
4.1. Cloning and constructs	36
4.2. Cell culture	36
4.3. Isolation and culturing of neonatal, juvenile (P5) and adult cardiomyocyte isolation.	36
4.4. OSKM induction of cardiomyocyte and time-lapse imaging.....	37
4.5. Lentiviral production and transduction	37
4.6. Isolation of cardiomyocytes from fixed hearts	37
4.7. RNA samples preparation and cDNA synthesis.....	38
4.8. Quantitative real time polymerase chain reaction (qRT-PCR).....	38
4.9. Protein sample preparation	39
4.10. Sodium dodecyl sulfate-polyacrylamide gel electrophoresis	39
4.11. Western blot.....	40
4.12. Frozen samples and cryosections preparation	40
4.13. Immunocytochemistry and histology	40
4.14. WGA staining and cardiomyocyte size quantification.....	41
4.15. Blood cTnI measurements	41
4.16. Scar quantification.....	41

4.17. LAD ligation.....	41
4.18. Cardiac apical resection.....	42
4.19. Magnetic resonance imaging	42
4.20. RNA sequencing and analysis	42
4.21. Mouse models.....	43
4.22. Statistics.....	43
5. Results	45
5.1. OSKM expression promotes proliferation of neonatal cardiomyocytes and facilitates their reprogramming.....	45
5.2. OSKM expression enables adult cardiomyocytes to re-enter cell-cycle	49
5.3. OSKM expression promotes neonatal and juvenile (P7) cardiomyocyte dedifferentiation and proliferation in vivo	50
5.4. OSKM expression promotes adult cardiomyocyte dedifferentiation and proliferation in vivo.....	53
5.5. Transcriptome of adult cardiomyocyte is reverted to a fetal-like state upon OSKM expression.....	57
5.6. Sustained OSKM expression can reprogram adult cardiomyocyte to iPSC-like cells in vivo.....	60
5.7. Temporarily-restricted OSKM expression promotes cardiomyocyte de-differentiation, proliferation and re-differentiation.....	63
5.8. Partial OSKM expression promotes juvenile (P7) heart regeneration following apical resection	68
5.9. Partial OSKM expression promotes adult heart regeneration and restore function following myocardial infarction.....	69
6. Discussion.....	76
6.1. Proliferation of cardiomyocytes	76
6.1.1. OSKM-induced dedifferentiation of cardiomyocytes	76
6.1.2. Cytokinesis of bi-nucleated cardiomyocytes.....	78
6.2. Cardiomyocyte reprogramming.....	78
6.2.1. OSKM induced heart tumors.....	78
6.2.2. The cells in cardiomyocytes derived heart tumor	80
6.2.3. Morphological and molecular changes during cardiomyocytes reprogramming	81
6.2.4. Tissue environment and cardiomyocyte reprogramming.....	82
6.3. Reversibility of OSKM-dependent dedifferentiation	83
6.4. Perspectives	85
6.4.1. Mechanism of partial cardiomyocyte reprogramming.....	85
6.4.2. Timing of OSKM expression for heart regeneration	88
Acknowledgements.....	91
List of abbreviation.....	92
Unit.....	92
Materials	92
Gene and protein.....	93

Cell	95
Other abbreviations	95
References	96

Summary

Cardiomyocytes are critically responsible for heart contraction and the pumping of blood through the circulatory system. In adult mice and humans, the rate of cardiomyocyte division is extremely low. In addition, dedicated cardiac stem cells that support myocardial renewal do not exist. Therefore, cardiomyocytes that are lost upon heart damage cannot be replenished. The inability to recover from cardiac injury, such as a myocardial infarction, is a leading cause of morbidity and mortality worldwide. Obviously, it is of great biomedical interest to find ways for enabling heart regeneration by restoration of lost cardiomyocytes.

Previous reports have suggested that dedifferentiation of adult cardiomyocytes, which concurs with reactivation of fetal gene expression programs, is a prerequisite to enable adult cardiomyocytes to reenter the cell-cycle. Continuous forced expression of reprogramming factors known as OSKM (Oct4, Sox2, Klf4 and c-Myc) causes stepwise dedifferentiation of somatic cells and acquisition of pluripotency. More recently, it was shown that short-term OSKM-expression allows partial reprogramming of cells without the loss of cellular identity, improving the regenerative potential of tissues. The aim of this thesis was to investigate whether OSKM-expression in cardiomyocytes enforces cardiomyocyte dedifferentiation and proliferation, and to establish a cardiomyocyte-specific partial reprogramming strategy that might enable heart regeneration.

To this end, two transgenic mouse lines designated $i4F^{\text{Heart}}$ and $i4F^{\text{Heart/mCherry}}$ were generated and analyzed in this study. These animal models allow control of OSKM expression specifically in fluorescently labelled cardiomyocytes. Here, it was found that OSKM-expression facilitates division of both neonatal and adult cardiomyocytes in vitro. Furthermore, cardiomyocyte-specific OSKM-expression results in dedifferentiation and enhanced proliferation of cardiomyocytes in neonatal, juvenile and adult hearts in vivo. Sustained OSKM-expression leads to complete cardiomyocyte reprogramming and heart tumor formation. Transient OSKM-expression in the adult heart dedifferentiates adult cardiomyocytes to fetal-like cardiomyocytes and allows subsequent reversion to the previous differentiated state. Transient OSKM-expression in juvenile mice enables heart regeneration after resection of the heart apex. In adult mice, transient OSKM-expression before and during myocardial infarction facilitates heart regeneration and ameliorates heart failure.

Keywords: cardiomyocytes, dedifferentiation, proliferation, re-differentiation, reprogramming, OSKM, regeneration

Zusammenfassung

Kardiomyozyten sind entscheidend für die Kontraktion des Herzens und für die Aufrechterhaltung der Funktion des Kreislaufsystems. Bei erwachsenen Mäusen und Menschen ist die Teilungsrate der Kardiomyozyten extrem niedrig. Zudem existieren keine regenerativen kardialen Stammzellen zur Organerneuerung. Daher können Kardiomyozyten, die bei einer Schädigung des Herzens verloren gehen, nicht wiederhergestellt werden. Die Unfähigkeit, die Herzfunktion nach Myokardinfarkt vollständig wieder herzustellen, ist weltweit eine der Hauptursachen für Morbidität und Mortalität. Daher ist es von großem biomedizinischen Interesse, Wege zu finden, die Regeneration des Herzens durch Wiederherstellung verlorener Kardiomyozyten zu ermöglichen.

Aus früheren Berichten geht hervor, dass die Dedifferenzierung erwachsener Kardiomyozyten, die mit der Reaktivierung fötaler Genexpressionsprogramme einhergeht, eine Voraussetzung dafür ist, dass erwachsene Kardiomyozyten wieder in den Zellzyklus eintreten können. Die kontinuierliche, forcierte Expression von Reprogrammierungsfaktoren, die als OSKM (Oct4, Sox2, Klf4 und c-Myc) bekannt sind, bewirkt eine schrittweise Dedifferenzierung somatischer Zellen und den Erwerb von Pluripotenz. Kürzlich wurde gezeigt, dass eine kurzzeitige OSKM-Expression eine partielle Reprogrammierung von Zellen ohne Verlust der zellulären Identität ermöglicht, was zu einer Verbesserung des Regenerationspotenzials führt. Ziel dieser Arbeit war es zu untersuchen, ob die OSKM-Expression in Kardiomyozyten die Dedifferenzierung und Proliferation von Kardiomyozyten verstärken kann, und eine Kardiomyozyten-spezifische partielle Reprogrammierungsstrategie zu etablieren, die eine Herzregeneration ermöglicht.

Zu diesem Zweck wurden zwei transgene Mauslinien mit der Bezeichnung $i4F^{\text{Heart}}$ und $i4F^{\text{Heart/mCherry}}$ erzeugt und in dieser Studie analysiert. Diese Modelle erlauben es, die Expression von OSKM spezifisch in fluoreszenzmarkierten Kardiomyozyten zu kontrollieren. Dabei wurde festgestellt, dass die OSKM-Expression die Teilung sowohl neonataler als auch adulter Kardiomyozyten *in vitro* verstärkt. Außerdem wurde festgestellt, dass die Kardiomyozyten-spezifische OSKM-Expression zu einer Dedifferenzierung und verstärkter Proliferation von Kardiomyozyten im neonatalen, jugendlichen und erwachsenen Herzen *in vivo* führt. Eine anhaltende OSKM-Expression führt zu einer vollständigen Reprogrammierung der

Kardiomyozyten und zur Bildung von Herztumoren. Eine vorübergehende OSKM-Expression im adulten Herzen führt zu einer partiellen Dedifferenzierung adulter Kardiomyozyten, welche Charakteristika fötaler Kardiomyozyten annehmen, und zu einer anschließenden Reversion in den zuvor differenzierten Zustand. In jungen Mäusen ermöglicht eine transiente OSKM-Expression die Regeneration des Herzens nach Resektion des kardialen Apex. Bei erwachsenen Mäusen ermöglicht eine transiente OSKM-Expression vor und während eines Myokardinfarkts die Herzregeneration und verbessert die Herzfunktion.

Schlüsselwörter: Kardiomyozyten, Dedifferenzierung, Proliferation, Re-Differenzierung, Reprogrammierung, OSKM, Regeneration

1. Introduction

1.1. Heart and heart attack

1.1.1. General aspects

The heart is a critical organ of the circulatory system [1]. It consists of various cell types including cardiomyocytes, fibroblasts, endothelial cells, adipocytes, smooth muscle cells and neuronal cells [2]. The cooperative interaction of these cells is necessary to maintain rhythmical pumping of blood through the circulatory system [3]. Heart contraction is mediated by cardiomyocytes, which comprise 70-85% of the myocardium. Cardiomyocytes beat approximately 7.3×10^8 times per lifetime and continuously for virtually all mammalian species [4]. Cardiovascular diseases (CVD) which include myocardial infarction (commonly known as heart attack) cause cardiomyocyte death, compromising heart contraction and impairing function of the cardiovascular system. The rate of cardiomyocyte division in adult mammal is extremely low [5]. Lost cardiomyocytes that die following a heart attack cannot be replenished. This consequently results in severe morbidity and/or mortality [6].

1.1.2. Heart development

The heart is the first organ to develop in mammals. Heart development is initiated through migration and differentiation of different progenitor cell types that delaminate and migrate from the mesoderm, proepicardium and the neural crest [7]. At around gestational day 22 in humans and E7.5 in mice, cardiomyocytes begin to differentiate from the anterior mesoderm forming two major progenitor cell groups on either side of the midline [8] designated as first heart field (FHF) and second heart field (SHF) [9].

At this stage, the horseshoe-shaped cardiac crescent emerges. The FHF progenitor cells fuse at the midline to form the primitive heart tube, which acquires the shape of an inverted 'Y', organized by an inner endocardial cell and outer cardiomyocyte layers [10]. Subsequently, SHF progenitors lying dorsal to the primary heart tube, continuously differentiate to cardiomyocytes thereby increasing the length of heart tube [7]. The elongated straight heart

tube then undergoes further morphological changes and transforms into a twisted loop. In the end of looping stage, endocardial layer forms sprouts which ingress through multiple matrix-rich areas (ECM bubbles) and towards myocardium. The ECM bubbles are progressively reduced with myocardial layer protruding to form trabeculae [11]. This process is referred to as trabeculation. Mitotic cardiomyocytes divide in the direction of the developing lumen thereby providing orientation trabeculation [12]. At around eight weeks of development in humans and E14.5 in mice the trabeculated structures undergo significant compaction which transforms them from spongy to solid [13]. Cardiac compaction is then followed by septation, by which left and right atria and ventricles are separated. Septation results in the emergence of the four chambered mammalian heart comprising two atria and two ventricles.

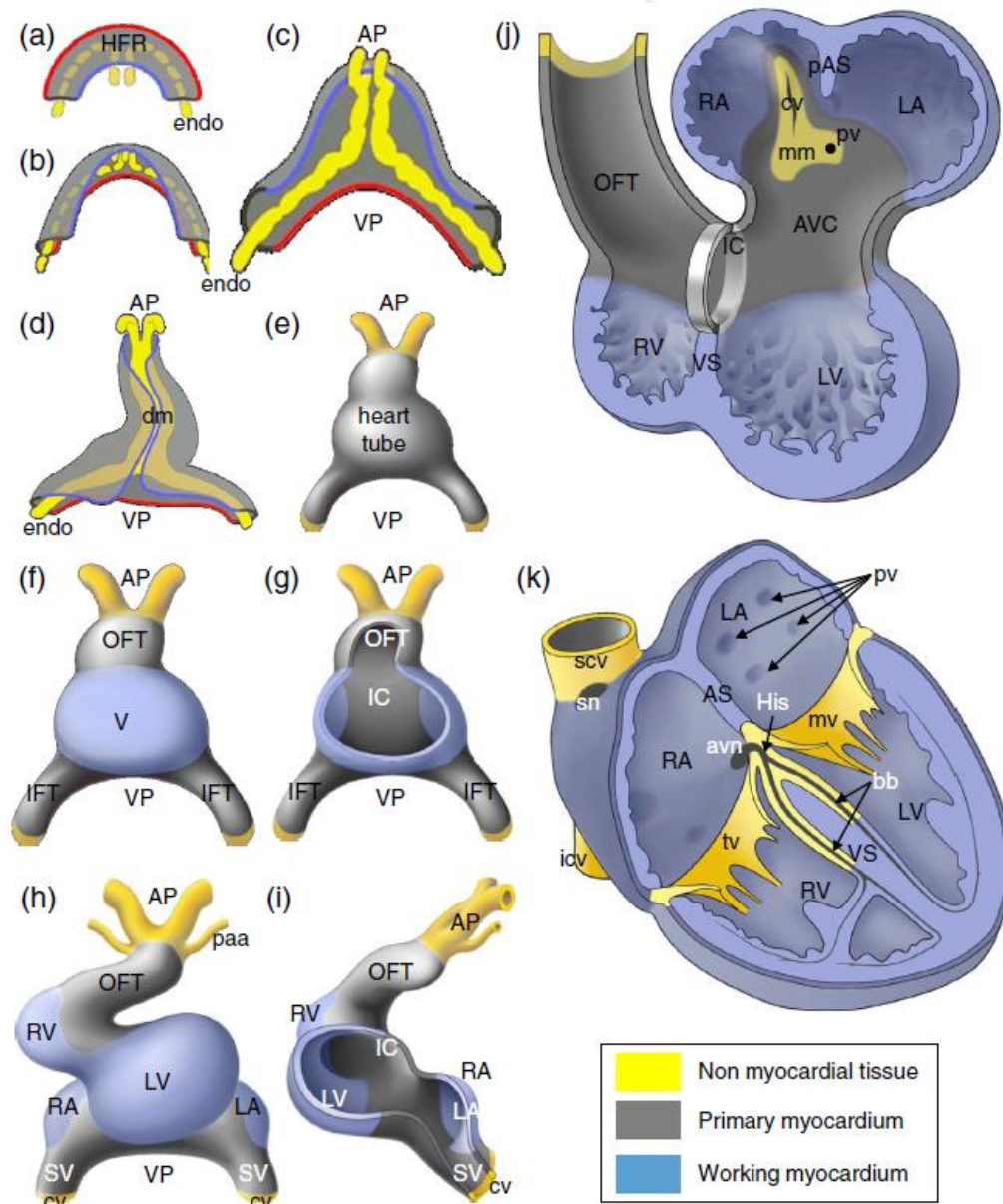


Fig. 1 Schematic representation of mammalian heart development [14].

Heart forming region (HFR), embryonic ventricle (V), inner curvature (IC), inflow tract (IFT), outflow tract (OFT), right ventricle (RV), left atrium (LA), right atrium (RA), cardinal vein (cv), pharyngeal arch arteries (paa), primary atrial septum (pAS), ventricular septum (VS), pulmonary vein (pv), bundle branches (bb), superior and inferior caval veins (scv and icv), mitral valve (mv), tricuspid valve (tv).

1.1.3. Heart and circulatory system

The atria and ventricles have different functions. The atria pump blood into the ventricles. The ventricles pump blood out of the heart into the peripheral vasculature. The right atrium

receives deoxygenated blood from the superior vena cava, inferior vena cava, and anterior cardiac veins as well as the smallest cardiac veins and the coronary sinus. The deoxygenated blood passed to the right ventricle is pumped through the pulmonary arteries to the lungs for re-oxygenation. Oxygenated blood is then pumped through the pulmonary veins into the left atrium and then left ventricle and finally out of the heart through the aorta and the major arteries [15]. The contraction phase by which blood is pumped out of the heart is called systole, the relaxation phase called diastole. A heart beat is the contraction cycle from systole to systole. The volume of blood within in the left ventricle at the end of diastole is termed end-diastolic volume (EDV). The end-systolic volume (ESV) is the volume of blood within the right or left ventricle at the end of systole. The blood volume pumped from right or left ventricle in one heartbeat, $EDV-ESV$, is termed as stroke volume (SV) while the ejection fraction (EF) calculated as $SV/EDV \times 100$ [%] describes the pumping efficiency of the heart. Cardiac output (CO) describes the stroke volume in relationship to the heart rate:
 $CO=SV \times HR$.

Blood circulation through the myocardium is called coronary circulation. Oxygenated blood diffuses into the heart muscle via left and right coronary arteries. The left coronary artery has two main branches, which distribute oxygenated blood to the left ventricle, atrium and septum. The circumflex artery arises from the left coronary artery and follows the coronary sulcus. Another major branch is the larger anterior interventricular artery, which is also known as the left anterior descending artery (LAD). Numerous smaller arterioles branches from LAD perfuse entire anterior wall of left ventricle, 2/3 of septum and left ventricular apex (Fig. 2). Because LAD supply blood for major portion of heart and it still the most common occluded artery in comparison with right coronary artery and circumflex artery [16], the blockage of it can result in myocardial infarction due to shortage of oxygenated blood supply.

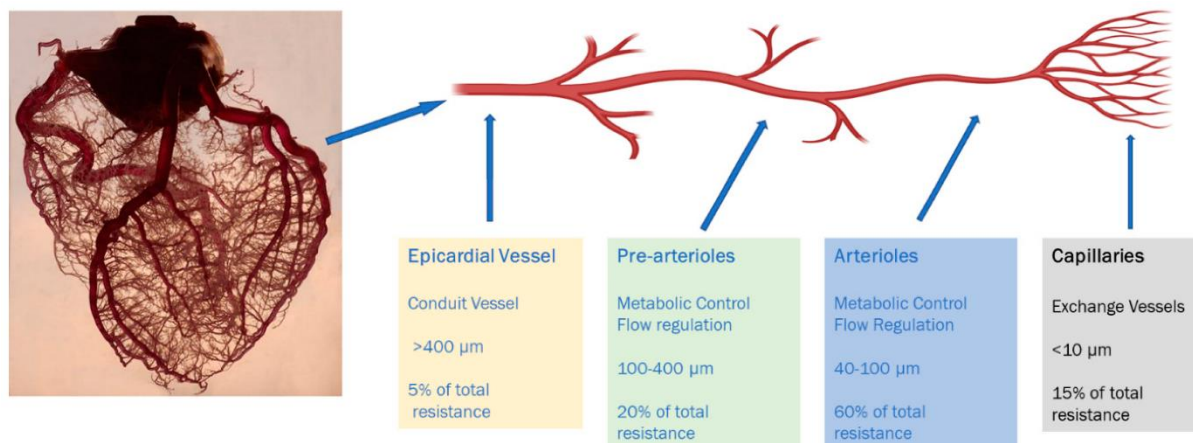


Fig. 2 Anatomical and functional classification of the coronary macro and micro-arterial system [6]. Blood perfusion of the myocardium is achieved by a system of larger epicardial vessels, serving as conduits to supply pre-arterioles and arterioles, which are subject to metabolic control and flow regulations. Arterioles transport oxygenated blood to capillaries, which are responsible for exchange of oxygen and nutrients to the myocardium. Resistance to blood flow is mainly supplied by arterioles, although pre-arterioles and capillaries contribute as well.

1.1.4. Heart attack

Heart attack, also called myocardial infarction (MI), is an irreversible injury of the myocardium that results from severe and sustained myocardial ischemia. During myocardial infarction, blood flow through coronal arteries is severely reduced or blocked resulting in insufficient supply of oxygenated blood and consequent death of cardiomyocytes distal to the blockage within the myocardium. Adult cardiomyocytes do not divide and therefore cardiomyocytes that are lost in MI will not be replenished by new cardiomyocytes. Instead, they are replaced by scar tissue, which is formed by cardiac fibroblasts at the site of damage. The scarring in turn triggers chronic neurohumoral activation and remodeling of the heart. Cardiac remodeling often leads to thinning of the ventricular wall, ischemic mitral regurgitation and further loss of cardiomyocytes. In severe cases of MI, cardiac remodeling can progressively affect the subepicardium even after longer time periods [17]. This often results in lethal ventricular arrhythmias, cardiogenic shock and sudden death [18]. Ultimately, the loss of cardiomyocytes culminates in heart failure [19], which is associated with reduced stroke volume and reduced ejection fraction. In recent years, significant advances to salvage immediate consequences of myocardial ischemia have been made. However, although most patients can survive MI nowadays through timely reperfusion and surgical restoration of

coronary blood flow, cardiomyocytes that are lost during MI cannot be restored leading to cardiovascular disease that accounts for at least 15 million deaths per year[20]. Therefore, profound interest lies in finding ways to replace lost cardiomyocytes as a means to restore heart function and to ameliorate cardiovascular disease.

1.2. Regeneration

Regeneration is the process of replacing lost or damaged tissues. For longer-lived organisms regeneration is essential for maintenance of tissue homeostasis and survival [21]. All organisms have the ability to repair wounds. However, the capacity to regenerate tissues varies considerably not only across tissues within a regenerative organism but also across species. Invertebrates, such as planarians [22], crinoid echinoderm [23], annelids and *Hydra* [24, 25], display remarkable regenerative potential and can regenerate an entire organism from a tiny body segment. Specifically, planarians have the capacity to regenerate entirely from only $\sim 1/279$ of its original body [22]. Some non-mammalian vertebrates, such as newts, axolotls and zebrafish can regenerate entire extremities following amputation including limbs or fins. Furthermore, these organisms also have the remarkable capacity to regenerate different types of internal organs including the heart [26-28]. Although mammals do not have the same potency to regenerate complex structures such as whole organs as some invertebrates, they can efficiently regenerate certain tissues upon damage. Examples of highly regenerative tissues in mammals, including humans, are skeletal muscle [29], liver [30-32], skin [33], blood vessels [34], intestinal mucosa [35] nailbeds [36, 37] and bone marrow [38]. In contrast, some organs and tissues including the brain, spinal cord, joints and heart are almost completely devoid of regeneration capacity and cannot fully recover when they are injured. This inability to regenerate these tissues can lead to many types of human disease such as heart failure, atrophy and neural degeneration. Hence, it is considered certain that understanding fundamental mechanisms of tissue regeneration will aid in developing novel treatments to conquer various human diseases and to prolong human healthspan.

Regeneration can be divided mainly into two modes: morphallaxis and epimorphosis. Morphallaxis has only been observed in invertebrates such as hydra and involves the re-organization and re-arrangement on an existing tissue that can transform to take on the identity of another tissue without the need of cell proliferation.

In contrast to morphallaxis, epimorphosis involves cell proliferation. Epimorphosis-based regeneration is subcategorized into blastemal and non-blastemal regeneration. Blastemal-

based regeneration is intensively investigated in urodeles such as axolotl and zebrafish that can regenerate many organs following amputation, including limbs, tail and intestine [39-41]. In blastemal regeneration, a so called blastema consisting of an aggregation of undifferentiated cells forms from coordinated dedifferentiation of cells immediately adjacent to the injury site. These dedifferentiated cells acquire the ability to proliferate, migrate and differentiate to undergo profound morphological organization in three dimensions. Whole body or organ parts can be formed from a blastema in some animals [42]. A common feature of blastemal regeneration is the reactivation of genetic programs that are normally required for organ formation during early development.

Blastema formation as a mode of regeneration after injury occurs only very rarely in mammals. Some examples include skin regeneration in African spiny mice [43], closure of ear punctures in rabbits and some rodents [44, 45], regrowth of deer antlers [46] and digit tip regeneration in perinatal mammals including rodents, monkeys and even humans [47-49]. Comprehensive molecular analyses have revealed that blastemal regeneration of amputated axolotl limbs critically involves the coordinated dedifferentiation of connective tissue cells immediately adjacent to the amputation. During blastema formation these cells form a relatively homogeneous population of multipotent cells that are strikingly similar to those cells that enable limb bud formation in early development [50]. Therefore, an instrumental aspect of blastemal regeneration appears to be the ability of cells to acquire an embryonic, dedifferentiated state. Interestingly, it has been shown that blastemal regeneration during digit tip regeneration in mice is not associated with emergence of germline lineage boundaries like in axolotls but is instead mediated by resident stem/progenitors adjacent to the injury site [51-55].

Non-blastema-based regeneration is the major mode of regeneration in mammals. It almost always relies on tissue resident stem cells with exception of the liver. Interestingly, the skeletal muscle, which is the only other type of striated muscle in mammals next to the heart, displays quite remarkable regenerative ability. For many years, skeletal muscle regeneration has been studied to understand the process of striated muscle regeneration, not only as to understand skeletal muscle regeneration per se; but essentially to understand how one type of striated muscle can regenerate while the other cannot. It is widely accepted that the adult mammalian heart cannot regenerate, not only because adult cardiomyocyte are incapable of division, but also because the heart does not contain cardiac stem cells [56]. In contrast, the skeletal muscle does contain highly regenerative muscle stem cells (MuSCs), which are also

commonly referred to as satellite cells. MuSCs display remarkable proliferation and differentiation capacity to support muscle repair following muscle injury [57]. However, in this context it is noteworthy to mention that regenerative tissues such as the skeletal muscle are vulnerable towards tumor formation [58, 59]. In contrast, while the heart cannot regenerate it virtually never forms tumors [60-62].

1.3. Heart regeneration

Some non-mammalian vertebrates, such as zebrafish, newts, and axolotls can regenerate an injured heart in adulthood. Heart regeneration in these animals does not appear to rely on cardiac stem cells or progenitors. Instead it relies on the ability of cardiomyocytes to proliferate upon an inflicting injury [28, 63-66]. Along this line, Poss and colleagues found that cardiomyocytes next to the injury zone can reactivate the expression cell-cycle genes and reenter the cell cycle in zebrafish. Interestingly, this appears to go along with cardiomyocyte dedifferentiation by virtue of concomitant re-expression of embryonic sarcomere genes [67]. Remarkably, in zebrafish, the dedifferentiated proliferation competent cardiomyocytes can subsequently re-differentiate to completely restore the loss of cardiomyocytes even following amputation of up to 20% of the ventricle [28] or after genetic obliteration of 60% of the cardiomyocyte population [68].

It has been formally proven that cardiac stem cells do not exist in the adult mammalian heart [56, 69]. Cardiomyocyte renewal does occur in humans but at an extremely low rate. It is estimated in the adult human heart approximately 0.5-1% of the cardiomyocyte population renews per year [70, 71]. Newly formed cardiomyocytes are not generated by cardiac progenitor cells but instead by the very rare division of pre-existing cardiomyocytes [72, 73]. The potential of adult cardiomyocytes to divide is so low, that it does not suffice to restore the loss of cardiomyocytes, for example upon a myocardial infarction during which up to 25% of cardiomyocytes within the left ventricle die within only a few hours [74].

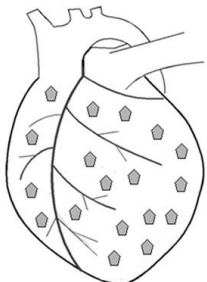


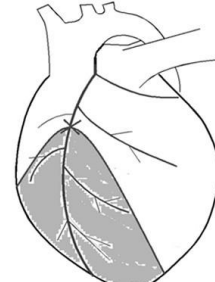
			
Genetic ablation	Cryoinjury Cautery injury Mechanical injury	Ventricular resection	LAD ligation
TYPE OF DAMAGE			
CM specific death	Cardiac damage by freezing, burning, squeezing or electrical shock	Removal of ventricular tissue	Ligation of the left anterior descending coronary artery
EXTENT OF TISSUE REMOVAL			
60 % CMs in the global myocardium	10 to 30 % of the ventricle	10 to 20 % of the ventricle	75 % CMs are lost below the ligation
INFLAMMATION and ECM DEPOSITION			
No	Variable	Yes	Yes
HEART REGENERATIVE CAPACITY			
YES zebrafish larvae YES adult zebrafish YES embryonic mouse YES neonatal mouse	YES newt YES axolotl YES adult zebrafish YES giant danio YES goldfish YES polypterus YES neonatal rat YES embryonic rabbit YES neonatal mouse (NTC) NO neonatal mouse (TC) NO adult mouse NO adult rabbit	YES newt YES axolotl YES adult zebrafish YES neonatal mouse YES neonatal rat NO medaka NO adult mouse NO adult rat	YES embryonic sheep YES neonatal mouse NO adult mouse NO adult sheep NO adult rabbit NO adult rat

Fig. 3 The regenerative capacity of hearts differs across various species.

Different approaches were used to study cardiac regeneration in vertebrates. Cardiac damage ranges from 10-30% to 75%. Depending on the method used. Several aquatic animals such as newts and zebrafish show remarkable regenerative capacity, although some fish species such as medaka fish are not able to undergo heart regeneration. NTC, non-transmural cryoinjury; TC, transmural cryoinjury [1].

1.4. Current strategies for heart regeneration

Heart transplantation remains a therapeutic option for end-stage heart failure. If successful, it can significantly improve the quality of life of affected patients [75-77]. However, apart from the fact that costs are very high, other critical drawbacks and difficulties of heart transplantation therapy remain, including the limited number of heart donors, the requirement for continuous immunosuppressant therapy, and the complexity of the operation procedure [78]. In recent years much research has been dedicated towards three alternative approaches, all aiming to restore loss of cardiomyocyte numbers including 1) direct transdifferentiation of other cell types within the heart into cardiomyocytes 2) transplantation of cardiogenic cells or cardiac tissue and 3) stimulation of cardiomyocyte proliferation.

1.4.1. Cardiac transdifferentiation

Transdifferentiation is the process of directly converting one cell type into another without going through an intermediate state such as that of a less differentiated progenitor cell or even pluripotent cell. Several examples of physiological transdifferentiation have been reported in vitro and in vivo [79, 80]. For example, following liver injury in mammals, hepatocytes can change fate and transdifferentiate into biliary epithelial cells. This coincides with a profound shift of both transcriptome and cellular morphology without an intermediate dedifferentiation step [81, 82]. In addition, it was recently shown that glucagon-producing α -cells in pancreatic islets can transdifferentiate into insulin-producing β -like cells after pancreatic damage when β -cells are lost [83].

Forced transdifferentiation was first described by Davis et al., who showed that 10T1/2 mouse fibroblasts can be directly converted into myoblasts by overexpression of the myogenic transcription factor MyoD [84]. Later Murry et al. showed that MyoD overexpression can convert rat cardiac fibroblasts into myoblasts which can subsequently differentiate into contractile myotubes in vitro. Furthermore, direct reprogramming of cardiac fibroblasts into cardiomyocytes in vivo was reported by the groups of Srivastava and Olson in 2012. This is achieved by forced retroviral overexpression of the transcription factors Gata4, Mef2c, and Tbx5 (GMT) [85]. Interestingly, transdifferentiation efficiency could be increased both in vitro and in vivo by introducing Hand2 to the GMT combination [86]. In both studies it was shown that transdifferentiation of cardiac fibroblasts into cardiomyocytes can reduce scar formation and improve cardiac function following myocardial infarction. Later, three

independent groups reported that human cardiomyocyte-like cells can be generated via transdifferentiation of fibroblast through different combinatorial approaches including 1) overexpression of GMTH, microRNAs miR-1, and miR133 [87], 2) overexpression of GMT and MYOCD [88] , and 3) overexpression of GMT, ESRRG, MESP1, MYOCD, and ZFPM2 [89].

Instead of forced-expression of exogenous transcription factors, it has recently been shown that cardiac transdifferentiation can also be achieved with chemical approaches. Specifically, Ding and colleagues demonstrated that a combination of nine chemicals (C9) can convert human fibroblasts into cardiomyocyte-like cells. These cells uniformly contract and resemble human cardiomyocytes, although not completely, in respect to their transcriptional and epigenetic profiles as well as their electrophysiological properties. Interestingly, fibroblasts that are exposed to C9 for short periods of time (such that they had not yet transdifferentiated into cardiomyocyte-like cells) begin to transdifferentiate *in vivo* when transplanted into infarcted mouse hearts, indicating that the heart environment promotes cardiogenesis [90]. Transdifferentiation provides some important advantages as a means for cardiac regeneration in comparison to other approaches. It appears that transdifferentiation is a relatively fast process and the incidence of tumor formation is low. It is also noteworthy to mention that transdifferentiation as a therapeutic means does not raise ethical issues. However, although transcription factors, miRNAs, and small molecules can transdifferentiate fibroblasts into cardiomyocytes, the major drawback is that transdifferentiation is inefficient. Moreover, transdifferentiated cardiomyocytes appear to be immature and their cardiac properties are instable [91]. Furthermore, it needs to be noted that generating cardiomyocytes by transdifferentiation *in vivo* naturally occurs at the expense of losing a different cell type, of which the consequences are not known. Finally, the molecular mechanisms of cardiac transdifferentiation remain poorly understood and the risks and benefits still require large animal studies before venturing into clinical applications.

1.4.2. Cell therapy

Cell based therapies involve transplantation of cells or tissues that can either be suspended cells or engineered tissues. Prominent examples of widely used cell based therapies include the transplantation of hematopoietic stem cells and/or bone marrow cells in general as well as skin grafts [92]. In recent years, much research has been devoted to cardiac cell based

therapies, which hold great promise to treat ischemic heart disease and to enable restoration of cardiomyocytes that are lost in cardiovascular disease.

Like other cell based therapies, cardiac cell based therapies involve transplantation of in vitro generated heart tissues or transplantation of suspended cells. A wide range of cell types have been used for cardiac cell-based therapy in pre-clinical and clinical studies. In some studies adult-derived cells have been used for transplantation including skeletal muscle stem cells or myoblasts [93-96], bone marrow-derived mononuclear cells (MNCs) [97-100] or bone marrow-derived (stromal) mesenchymal stem cells (MSCs) [101-103]. More recently, intense research efforts have been devoted to replace lost cardiomyocytes with pluripotent stem cell-derived cardiomyocytes (PSC-CM). For such studies, PSC-CM are usually derived from embryonic stem cells (ESC-CM) [104], or induced pluripotent stem cells (iPSC-CM) [105]. Significant advances have been made in the past two decades not only in pre-clinical models but also in clinical trials. The clinical trials have mostly involved the transplantation of adult cells. However, many discrepancies exist concerning the therapeutic effect of transplanting adult-derived cells, regardless of their origin. Reported outcomes are often been ambiguous, especially in respect to the efficacy of cardiac differentiation and the degree of cell engraftment as well the degree of heart regeneration [56].

In contrast to transplantation of non-cardiomyocyte cell types, the transplantation of PSC-cardiomyocytes seems to be a more effective approach to restore numbers of lost cardiomyocytes. Several pre-clinical studies in various animal models have indicated that PSC-CM can efficiently repair injured myocardium by remuscularization [106-112]. In 2018, Murry and colleagues reported efficient remuscularization of infarcted hearts in a non-human primate model. Importantly, the remuscularized hearts also displayed significant improvement of cardiac functions including increased contractility in contrast to infarcted controls [110, 113]. However, the engrafted animals displayed significant cardiac arrhythmias indicating insufficient or incomplete electrical coupling to the recipient myocardium. As an alternative to the injection of suspended cells, other cardiac cell based therapy strategies involve transplantation of engineered cardiac tissues. For example, it was recently shown that sheets of cardiomyocytes can engraft into infarcted hearts. Compared to injection of single cell suspensions, aggregation and necrosis of the grafted cells within the transplanted cardiac sheets do not occur. A significant advantage in the transplantation of engineered heart tissues is that the shape and size of the transplanted tissue can be controlled and engrafted into a precise anatomical location [114]. Indeed, Sawa and colleagues recently demonstrated that

human iPSC-CM derived cardiac sheets can engraft in porcine hearts and improve heart function following MI [112, 115, 116].

As with transdifferentiation approaches, several critical aspects require definitive clarification before entering clinical trials. At current, immune rejection remains an important issue that needs to be consider in cell based therapies [117], although it may be possible to overcome this issue using biobanks of PSC-CMs, comprising a wide variety of distinct haplotypes. Other important issues include improvement of engraftment efficiency, ensuring differentiation of transplanted tissues and/or PSC-CMs, and securing the purity of PSC-CMs to exclude the possibility of tumor formation, since PSC-CMs bare the risk of retaining residual proliferative capacity.

1.4.3. Promotion of cardiomyocyte proliferation

Notably, cell based therapies require obtaining sufficient material amounts for transplantation ex vivo regardless whether artificially generated cardiac tissues or PSC-CMs are used. Thereby, undifferentiated, but highly proliferative cells are differentiated into mature and non-mitotic cardiomyocytes. In some non-mammalian vertebrates however, mature adult cardiomyocytes still possess proliferative capacity which enables these organisms to regenerate their hearts after injury [28, 118]. It has been demonstrated that cardiomyocytes in neonatal mammals including mice, pigs and humans still display proliferative capacity. However, it has been shown in mice that this proliferative capacity is progressively lost shortly after birth until cardiomyocytes have fully matured at around one week of age [119-121]. These observations have fueled the idea to facilitate mammalian heart regeneration by identifying factors that might promote adult cardiomyocytes to reenter the cell cycle. Many approaches to promote cardiomyocyte proliferation are rooted in the identification of growth factors, transcription factors, signaling pathways and other cell cycle regulators that play an important role during cardiac development as cardiomyocytes transit from hyperplastic to hypertrophic growth and stop to proliferate.

Along this line, it has been shown that several growth factors can stimulate DNA synthesis in cardiomyocytes and induce cardiac hypertrophy but most of them are not able to stimulate cardiomyocyte proliferation. However, one growth factor that can stimulate cardiomyocyte proliferation is the growth factor Neuregulin1 (NRG1), the receptors of which are ErbB2 and ErbB4. Activation of the NRG1/ErbB2/4 axis can induce mononucleated adult cardiomyocytes to reenter the cell-cycle through activating the phosphatidylinositol-3-OH

kinase (PI3K) pathway, which suffices to ameliorate heart function following myocardial infarction [122, 123].

PI3K and phosphoinositide-dependent kinase (PDK1) mediates activation of Yes-associated protein 1 (Yap1) which is associated with the core Hippo pathway-kinase complex [124]. This is important because the highly conserved Hippo signaling pathway has been shown to regulate cell proliferation and growth of a wide variety of organs including the heart [125]. Specifically, it has been shown that hyperactivation of Yap1 or inactivation of its effectors Salv and Lats1/2 results in enhanced cardiomyocyte proliferation [126]. Several studies have reported that direct disruption of the Hippo pathway or activating Yap1 function could provide a promising strategy to promote adult cardiomyocyte proliferation and heart regeneration [127-130]. Indeed, a variety of means that have been shown to promote cardiomyocyte proliferation seem to be functionally connected with the Hippo-Yap pathway, including inactivation of thyroid hormone signaling [131], administration of the extracellular matrix protein Agrin [132], and regulated expression of specific micro-RNAs [133-136].

Manipulation of Hippo-Yap pathway seems to be a center for cardiomyocyte proliferation and heart regeneration, which regulates the expression and activity of many downstream genes related to cell cycle terminally. The cell cycle is a well investigated process that is divided into four steps: Gap1(G1), DNA synthesis(S), Gap2(G2) and mitosis(M). Each of these four stages are tightly regulated at so called checkpoints, which are mediated by specific cyclins, cyclin-dependent kinases (CDKs) and cyclin-dependent kinase inhibitors (CDKIs). It has been shown that alteration of these factors can override checkpoints [137]. Thereby cell division can be inhibited or facilitated. Therefore, numerous research groups have attempted to modulate the expression or functions of cyclins, CDKs and CDKIs as a means to promote cardiomyocyte proliferation. For example, it has been shown that overexpression of the cell cycle activators Cyclin D [138], Cyclin B [139], Cyclin A2[140] or inhibition of the cell cycle inhibitors p21^{Waf1}, p27^{Kip1} and p57^{Kip2} [141] can promote cardiomyocytes to reenter the cell-cycle. Notably, except for overexpression of Cyclin A2, none of these approaches are sufficient to elicit complete cardiomyocyte division. Recently, Srivastava's group found that combinatorial overexpression of CDK1, CDK4, cyclin B1, and cyclin D1 could efficiently induce cell division in mouse, rat and human post-mitotic cardiomyocytes [142]. Hsieh and colleagues found that forced expression of FoxM1 and Id1 and simultaneously inactivation of the Jun-dependent kinase Jnk3 inhibits expression of the cell cycle inhibitors p16, p21, p27

and induces upregulated expression of CDK4 and CDK2. This approach designated as FIJ-induced reprogramming is sufficient to induce cardiomyocyte cell-cycle reentry [143].

In 2005, Braun and colleagues found that direct expression of transcription factor E2Fs enable to induce division of primary isolated newborn mouse and rat cardiomyocyte, along with inhibition of CDKs and activation of p15INK, p16INK, and p19INK [144]. More recently, it was shown that the transcription factor Meis1 induces expression of the CDKs p15, p16 and p21 in cardiomyocytes shortly after birth, which results in rapid termination of cardiomyocyte proliferation. Consistently, knockout of Meis1 in mice is sufficient to extend the postnatal proliferative window of cardiomyocyte and reactivates cardiomyocyte mitosis in adult hearts [145]. These observations were extended by the findings that the transcription factor Hoxb13 is a cofactor of Meis1 and plays an important role in postnatal cardiomyocyte cell cycle arrest. Double-knockout of Meis1 and Hoxb13 in adult cardiomyocytes outperformed induced rates of cardiomyocyte mitosis compared with the single knock-outs. Interestingly, even though Meis1/Hoxb13 double knockout mice exhibited significant sarcomere disassembly they exhibited improved heart function after myocardial infarction compared to controls [146].

In summary, different strategies have provided proof of concept that cardiomyocyte proliferation can be induced and thereby facilitate heart regeneration in adult mammals. Although yet far away from clinical application, these studies strongly indicate that induction of cardiomyocyte proliferation may provide a promising means to enable endogenous heart regeneration in the future. However, by any means described to date, the induced rates of cardiomyocyte proliferation, and cytokinesis in particular, are very low. It also needs to be considered that in all cases reported so far, the induction of cardiomyocyte proliferation is mediated by permanent gain or loss of gene expression. In other words, the artificial overexpression or inactivation of genes is permanent, which might result in devastating outcomes since the desired effect is to induce cellular proliferation. Lastly, inducing cardiomyocyte proliferation specifically in discrete areas where the heart is damaged and not in healthy myocardium will be an additional important aspect that needs to be solved before entering clinical trials.

An underlying feature of almost all studies reporting successful induction of cardiomyocyte proliferation appears to be that it is accompanied with a loss of differentiated features (such as the loss of sarcomeres and cytoskeletal components), massive metabolic changes, and the re-

expression of some embryonic genes. Such a process has been collectively coined simply as “dedifferentiation”. It has been suggested that three separable and consecutive processes need to be fulfilled to enable cardiomyocyte division for heart regeneration: i) induction of cardiomyocyte dedifferentiation, ii) proliferation and iii) redifferentiation wherein disassembled sarcomeres are reestablished and contractile function is fully restored [147]. These requirements for heart regeneration are similarly fulfilled in lower regenerative vertebrates wherein the acquisition of proliferative potential is preceded by cellular dedifferentiation. Incidentally, an artificial process that can enforce progressive cellular dedifferentiation of a wide range of differentiated somatic cell types is OSKM-dependent reprogramming. This involves forced combinatorial expression of the pluripotency factors Oct4, Sox2, Klf4, and cMyc, which are collectively abbreviated as OSKM or 4F.

1.5. OSKM-dependent reprogramming

In their landmark study in 2006, Takahashi and Yamanaka demonstrated that forced expression of Oct4, Sox2, Klf4, and cMyc (OSKM) can directly convert mouse embryonic fibroblasts (MEF) into induced pluripotent cells (iPSCs) that resemble pluripotent embryonic stem cells [148]. In a series of subsequent studies the process of iPSC formation by forced OSKM expression was recapitulated in various species including mice and humans and in a wide range of different somatic cell types such as fibroblasts [148], keratinocytes [149], blood cells [150], hepatocytes [151] pancreatic islet beta cells [152], mesoangioblasts [153], astrocytes [154], and even cancer cells [155, 156]. Owing to its striking nature, much research was and remains devoted to understanding the molecular mechanisms that orchestrate the reprogramming process [157]. The transcription factors Oct4 and Sox2 are instrumental for reprogramming by virtue of their profound epigenomic rewiring functions that are largely mediated by their pioneering activities [158, 159]. It has been shown that mesenchymal to epithelial transition (MET) is required for reprogramming and is enforced by the presence of KLF4 and cMYC in reprogramming cocktails [160]. cMYC in addition enhances cell division rates albeit at the expense of cell survival [161]. More generally, the reprogramming process can be divided into two phases. The first phase is a long stochastic phase in which cell proliferation rates increase. Thereby, cells that dedifferentiate appear to acquire pluripotency randomly. Increasing rates of cell division is a key parameter that affects the stochastic phase of the reprogramming process and is highly amenable to acceleration [162]. The second phase is a shorter deterministic phase when those cells that have dedifferentiated sufficiently activate endogenous Oct4, Sox2, Klf4, and cMyc to maintain a self-sustaining state of

pluripotency that does not require ectopically expressed OSKM anymore [163]. The reprogramming process per se is not a genetic but an epigenetic process that gives rise to pluripotent stem cells, injection of which into blastocysts are capable of chimera formation in foster mothers.

Few studies have investigated OSKM-dependent reprogramming *in vivo*. An example is the generation of genetically engineered i4F mice, in which OSKM expression can be induced in all cells of the body by administration of Doxycycline. Sustained administration of Doxycycline to adult i4F mice leads to the emergence of undifferentiated teratomas within one to two weeks in multiple organs simultaneously including pancreas, kidney, intestine, adipose tissue, liver, intracranial and stomach [164, 165]. Widespread reprogramming in all cells of the body of i4F mice not only results in teratoma formation but consequently results in severe morbidity and mortality by the time teratomas have formed. Notably, teratomas are never detected in the heart within this time frame, likely reflecting the extremely low division rate of adult cardiomyocytes. Interestingly however, it was recently shown that overexpression of OSKM in not yet completely differentiated neonatal cardiomyocytes can increase their residual proliferative capacity and reprogram them to iPS cells *in vitro* [143].

1.6. Molecular rejuvenation through OSKM-dependent reprogramming

A striking feature of somatic cell fate conversion to iPSCs is the epigenetic resetting of molecular age [148]. In fact, many hallmarks of aging can be reversed by OSKM-dependent reprogramming such as elongation of age-dependent shortening of telomeres [166], reduction of DNA damage [167], and enhanced mitochondrial function [168]. Indeed, Lapasset and colleagues could show along this line that forced OSKM expression not only efficiently dedifferentiates old senescent cells to iPS cells but that they are indistinguishable from their much “younger” human ES cell counterparts [169]. Manukyan reported that OSKM expression reverts senescence-based loss of HP1 β mobility. The activity of the epigenetic modifier HP1 β is thought to be tightly correlated with cellular age and senescence. This study not only confirms that derivation of iPSCs is capable from senescent cells, but their study also supports the notion that molecular rejuvenation of cells is possible without altering the differentiated state by incomplete OSKM-dependent reprogramming [170].

In 2016, Belmonte and colleagues reported that transient OSKM expression *in vivo* reverts hallmarks of aging at the molecular, cellular, organ and physiological levels. Intriguingly, they showed that cyclic bouts of OSKM expression for 2 day every week can ameliorate

aging hallmarks and prolong the lifespan in a mouse model of premature aging without teratoma formation [171]. Transient expression of OSKM for a short period of time without fully reprogramming cells to the pluripotent state has since been coined as “partial reprogramming”. This discovery not only sparked a profound interest to restore youthfulness but also to restore or even instate regenerative potential artificially by partial reprogramming. Indeed, more recently it was shown that short-term expression of reprogramming factors in aged mouse retinal ganglion cells restores youthful DNA methylation patterns and transcriptomes. More intriguingly, it was shown that partial reprogramming with OSK enables regeneration of injured axons and can restore vision loss in a mouse model of aged-related glaucoma [172]. Similarly, partial reprogramming has been shown to revert features of aging in naturally aged human cells [173] as well as in dentate gyrus cells in vivo which results in improvement of memory in mice [174].

The mammalian neonatal heart still owns considerable regenerative capacity, which is inferred by cardiomyocytes that are not yet fully differentiated and still retain residual proliferation capacity. Since molecular rejuvenation is a hallmark of partial reprogramming, it seems conceivable to test whether it could rewire adult cardiomyocytes to a juvenile, division competent, and hence regenerative, state. However, this has never been explored.

2. Aim of this project

The main goal of this project was to test the potential to promote proliferation of adult cardiomyocytes by forced expression of the reprogramming factors OSKM. This idea is based on the fact that OSKM-dependent reprogramming induces pluripotency by progressive dedifferentiation of somatic cells. Since cardiomyocyte proliferation is almost always associated with dedifferentiation, I tested the hypothesis whether overexpression of OSKM dedifferentiates adult cardiomyocytes is sufficient to facilitate cardiomyocyte cell cycle re-entry. If true, this strategy might be useful to restore cardiac function after myocardial infarction. To this end, the effects of OSKM expression in fluorescently labelled cardiomyocytes were investigated both in vitro and in vivo.

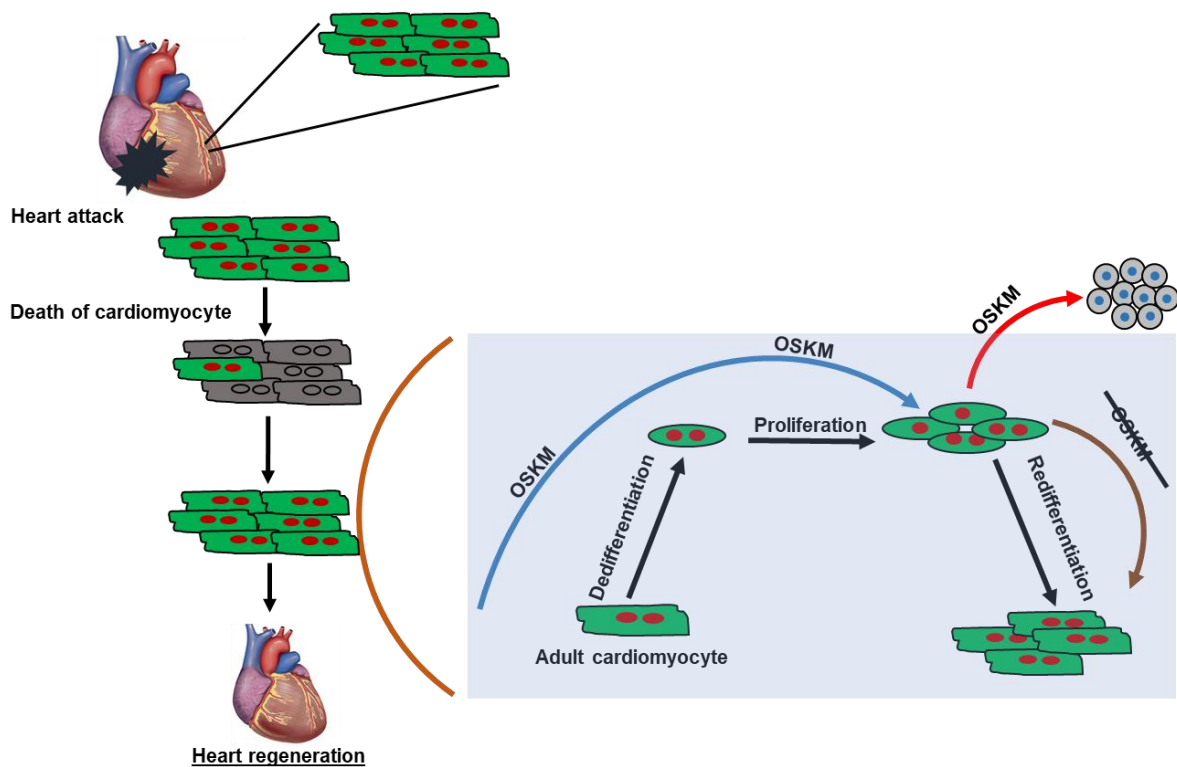


Fig. 4 Schematic outline of the approach to stimulate heart regeneration by transient overexpression of OSKM.

Death of cardiomyocytes is caused by myocardial infarction, induced by permanent LAD ligation. Hypothetically, transient OSKM expression may induce dedifferentiation and subsequent cardiomyocyte proliferation to enable heart regeneration and improve cardiac function without iPSCs formation.

3. Materials

3.1. Chemicals

Table 1. List of materials and chemicals

Chemicals	Provider (Catalogue Number)
BSA, Fraction V	Merck (112018)
Bromophenol blue	Merck (1081220005)
Cell culture dishes	Nunc and Greiner
Trypsin from porcine pancreas	Sigma (T6567)
Collagenase typeII	Worthington Biochemicals
DAPI	Invitrogen (D1306)
Ethidium bromide	AppliChem (A1152,0100)
Falcon®Cell strainer (100µM, 70µM,40µM)	BD Biosciences
MES running buffer	Invitrogen (NP0002)
Mowiol	Merck (475904)
NuPAGE®Novex®PAGE gel	Invitrogen
Paraformaldenhyde, PFA	Merck (1040051000)
Polybrene	Sigma (107689)
Protein standard marker	Invitrogen (LC5800)
Proteinase inhibitor cocktail tablets	Roche (04693116001)
PVDF membrane	Sigma (3010040001)
Puromycine	Sigma (P8833)
Red Alert® buffer	Novagen (710783)
Super signal west® femto	Thermo fisher scientific (34095)
SYBR Green fluorescein qPCR mix(2x)	Thermo fisher scientific (k0241)
TRIzol® Reagent	Invitrogen (15596026)

M.O.M.® (Mouse on Mouse) Blocking Reagent	Vector Laboratories (MKB-2213)
Signal Enhancer HIKARI for Western Blotting and ELISA	Nacalai tesque (02267-41)
Doxycycline hyclate	Sigma (D9891)
5-Ethynyl-2'-deoxyuridine	Sigma (900584)
Polyethylenimine	Polysciences (23966-100)

3.2. Antibodies

A list of primary and secondary antibodies is provided in Tab. 2 and Tab. 3 respectively.

The providers and working dilutions for their specific applications are included. (ICC: immunocytochemistry, IHC: immunohistochemistry, WB: Western Blot).

Table 2. List of primary antibodies.

Reactivity	Provider (Catalogue Number)	Dilution	Application
Alpha Smooth Muscle Actin Cy3	Sigma (C6198)	1:500	ICC
Cardiac Troponin T Monoclonal antibody	ThermoFisher (MA5-12960)	1:500	ICC
Phospho-Histone H3 (Ser10)	Cell Signaling (9701)	1:300	ICC
Anti-Aurora B antibody	Abcam (ab2254)	1:200	ICC
Anti-Nanog antibody	Abcam (ab80892)	1:500	ICC
E-cadherin Polyclonal antibody	Proteintech (20874-1-AP)	1:500	ICC
cleaved caspase-3	Cell Signaling (9661)	1:500	ICC
CD45 antibody	TheromFisher (11-0451-82)	1:50	ICC
CD31 antibody	BD Biosciences (550274)	1:50	ICC
Oct4 antibody	Santa Cruz (sc-5279)	1:200	WB, ICC
c-Myc antibody	ThermoScientific (132500)	1:500	WB, ICC
Vimentin antibody	Abcam (ab8978)	1:500	ICC

Pericentriolar material 1	Sigma (HPA023374)	1:200	ICC
---------------------------	-------------------	-------	-----

Table 3. List of secondary antibodies.

Reactivity	Provider (Catalogue Number)	Dilution	Application
Mouse HRP	Pierce (1858413)	1:2000	WB
Rabbit HRP	Pierce (31460)	1:2000	WB
Mouse Alexa 594	Invitrogen (A11005)	1:500	ICC
Mouse Alexa 488	Invitrogen (A11001)	1:500	ICC
Mouse Alexa 680	Invitrogen (A21057)	1:500	ICC
Rabbit Alexa 594	Invitrogen (A11012)	1:500	ICC
Rabbit Alexa 488	Invitrogen (A11070)	1:500	ICC
Rabbit Alexa 680	Invitrogen (A21076)	1:500	ICC
Rat Alexa 488	Invitrogen (A21208)	1:500	ICC
Rat Alexa 594	Invitrogen (A21209)	1:500	ICC

Table 4. List of enzymes used for molecular cloning.

Enzyme	Provider / Catalogue Number
EcoRI	NEB (R0101)
AgeI	NEB (R0552)
T4 DNA Ligase	Progma (9PIM80)
Pfu DNA polymerase	Promega (M774A)

3.3. Primers

All primers were synthesized and ordered from Sigma-Aldrich

Table 5. List of primer sequences used for genotyping.

Allele	Sequence
ROSA26 OSKM	Rosa-FA: AAAGTCGCTCTGAGTTGTTAT Rosa-RF: GGAGCGGGAGAAATGGATATG Rosa-4F2A: TTGCTCAGCGGTGCTGTCCA
aMHC MCM	MCMint 784 s: CAACATGAAATGCAAGAACG MCMint 1200 as: GGAAACCATTTCCGGTTATT
OSKM	OSKM fw: GGCTCTCCCATGCATTCAAACG OSKM rev: GCTTCAGCTCCGTCTCCATCATGT
H2B-mCherry	Cherry FWD2: CATGTACGGCTCCAAGGCC Cherry REV2: CCTTCAGCTTCAGCCTCTGC
ROSA26	Rosa-FA: AAAGTCGCTCTGAGTTGTTAT Rosa-RF: GGAGCGGGAGAAATGGATATG Rosa-SpliAC: CATCAAGGAAACCCTGGACTACATG
Xmhc2 Cre	MH61-Cre: GACCAGGTTTCGTTCACTCATGG MH63-Cre: AGGCTAAGTGCCTTCTCTACAC

Table 6. List of primer sequences used for qRT-PCR.

Gene	Sequence / Catalogue number
GAPDH	mm999999915_g1
Myh7	Mm00600555_m1
Acta2	Mm00725412_s1
Transgenic OSKM	Forward: GGCTCTCCCATGCATTCAAACG Reverse: GCTTCAGCTCCGTCTCCATCATGT
Tnni1	Forward: GCACTTTGAGCCCTCTTCAC Reverse: AGCATCAGGCTCTTCAGCAT
beta-Actin	Forward: ATGGTGACGTTGACATCCGTA Reverse: GCCAGAGCAGTAATCTCCTTCT

3.4. Plasmids

Table 7. List of plasmids.

Name	Insertion fragment	Backbone
------	--------------------	----------

pLVX-TetOne-Puro	NA	pLVX-TetOne
pLVX-TetOne-Puro-OSK	Oct4-T2A-Sox2-P2A-Klf4	pLVX-TetOne
pLVX-TetOne-Puro-cMyc	cMyc	pLVX-TetOne
pLVX-TetOne-Puro-OSKM	Oct4-T2A-Sox2-P2A-Klf4-F2A-cMyc	pLVX-TetOne

Table 8. List of bacterial strains.

Bacterial strain	Genetic background
DH5 α	F- ϕ 80lacZ Δ M15 Δ (lacZYA-argF) U169 deoR recA1 endA1 hsdR17(rK ⁻ , mK ⁺) phoA supE44 λ -thi-1 gyrA96 relA1
Stbl3	F-mcrB mrr hsdS20 (rB ⁻ , mB ⁻) recA13 supE44 ara14 galK2 lacY1 proA2 rpsL20 (StrR) xyl5 λ -leu mtl1

Table 9. List of cell lines.

Cell line	Description
HEK 293 ATCC ® CRL-1573 TM	Human Embryonic Kidney Cells 293
HEK 293T ATCC ® CRL-11268 TM	HEK293 cells constitutively express the simian virus 40 (SV40) large T antigen

Table 10. List of growth medium.

Growth medium/Cell type	Composition
Complete DMEM medium	DMEM (ThermoFisher) 10% FCS (Gibco) 1 x Penicillin / Streptomycin (Sigma)
Adult cardiomyocytes plating medium	M199 (ThermoFisher) 5 % FBS (Gibco) 10 mM BDM (Sigma) 1 x Penicillin / Streptomycin (Sigma)
Adult cardiomyocyte culture medium	M199 (ThermoFisher) 5 % BSA (Gibco) 1 x ITS (ThermoFisher)

	1 x CD lipid (ThermoFisher) 10 mM BDM (Sigma) 1 x Penicillin / Streptomycin (Sigma)
KSR medium	Knockout DMEM (ThermoFisher) 2% FBS (Gibco) 10% KSR (ThermoFisher) 1 x Penicillin / Streptomycin (Sigma) 100 µM 2-mercaptoethanol (ThermoFisher)
LB medium (liquid) 10%	10% bacto-tryptone 5% yeast extract 10% NaCl (For selection: 100 g/mL Ampicillin, Sigma-Aldrich)
LB medium (agar)	10% bacto-tryptone 5% yeast extract 10% NaCl 10 % agar (For selection: 100 g/mL Ampicillin, Sigma-Aldrich)

Table 11. List of buffers.

Buffer/Purpose	Composition
EDTA buffer	130 mM NaCl 5 mM KCl 10 mM HEPES 0.5 mM NaH ₂ PO ₄ 10 mM Glucose 10 mM 2,3-Butanedione monoxime (BDM) 10 mM Taurine 5mM EDTA
Perfusion buffer	130 mM NaCl 5 mM KCl 10 mM HEPES 0.5 mM NaH ₂ PO ₄ 10 mM Glucose 10 mM 2,3-Butanedione monoxime (BDM) 10 mM Taurine 1mM MgCl ₂
Digestion buffer	Perfusion buffer 1mg/mL collagenase II 0.1 mg/mL pancreas tyrosinase
Stopping buffer	Perfusion buffer 5% FCS

Blocking buffer (ICC)	PBS pH=7.4 3 % BSA 0.05% Triton-X100
Tris-EDTA buffer	10 mM Tris Base 1 mM EDTA 0.05% Tween 20 pH 8.0
Permeabilization buffer	PBS pH=7.4 5% Triton-X100
Lysis buffer	10mM Tris-HCl pH 8.0 1mM EDTA 1% Triton-X 0.1% sodium deoxycholate 0.1% SDS 150mM NaCl
10 % Bis-Tris polyacrylamide Resolving gel	2.3 mL Rotiphorese® Gel 30 (37.5:1) (Roth, 3029.1) 2 mL 3.5 x Bis-Tris pH 6.5 -6.8 2.7 mL Milli-Q H2O 25 µL 10 % Ammoniumperoxodisulfate (APS -Merck, 1.01201) 7 µL TEMED (Roth, 2367.1)
10 % Bis-Tris polyacrylamide Stacking gel	0.29 mL Rotiphorese® Gel 30 (37.5:1) (Roth, 3029.1) 0.5 mL 3.5 x Bis-Tris pH 6.5 -6.8 0.96 mL Milli-Q H2O 8 µL 10 % Ammoniumperoxodisulfate (APS -Merck, 1.01201) 3 µL TEMED (Roth, 2367.1)

3.5. Kits

Table 12. List of kits.

Product	Provider/Catalogue number
Neonatal Cardiomyocyte Isolation kit	Miltenyi Biotec (130-100-825)
Nucleobond AX500 Maxi Kit	Macherey-Nagel (740414.10)
QIAEX II Gel Extraction Kit	Qiagen (20021)
SuperScript™ II Reverse Transcriptase Kit	Invitrogen (18064-014)
Click-iT™ EdU Cell Proliferation Kit	Thermo fisher scientific (C10337)
BCA Protein Quantification Kit	Abcam (ab102536)

Trichrome Stain (Masson) Kit	Sigma (HT15-1KT)
Direct-zol™ RNA MiniPrep Kit	Zymo Research (R2051)
Mouse cardiac troponin I cTnI ELISA Kit	Novateinbio (NB-E20411)

3.6. Equipment

Table 13. List of equipment.

Equipment	Resource
Axiophot2 Z1 fluorescence microscope	Carl Zeiss Jena
ZEISS Axio Observer microscope	Carl Zeiss Jena
Leica SP8	Leica
All-in-one Fluorescence Microscope	Keyence
Master cycler gradient PCR	Eppendorf
StepOnePlus™ Real-Time PCR system	Applied Biosystems
NanoDrop 2000/2000c	Thermo fisher scientific
Bioruptor Sonopuls HD 2070/2200	Diagenode Bandelin
VersaDoc™ 3000	BioRad
7.0 T Bruker Pharmascan	Bruker
gentleMACS Dissociator	Miltenyi Biotec
MiniVent Ventilator	Hugo Sach Elektronik
Heating plate	Agnthos

Incucyte Live-Cell Imaging System	Essen Instruments
Surgical Microscope Leica M841	Leica

Table 14. List of software.

Software	Resource
Axio Vision® 4.8	Carl Zeiss Imaging Solutions, Jena
DNASTAR Lasergene®	DNASTAR Inc. USA
ImageJ	National Institutes of Health. USA
StepOnePlus Software v2.2.2	Applied Biosystems
Cell-by-Cell Analysis Software Module	Essen Instruments
ParaVision 6.0.1	Bruker
Qmass	Medis

4. Methods

4.1. Cloning and constructs

Expression vectors are listed in Table 6. c-Myc, OSK and OSKM were amplified from plasmid FUW-OSKM (Addgene # 20328), and inserted into plasmid pLVX-TetOne-Puro by EcoRI/AgeI.

4.2. Cell culture

All cells were cultured in a cell incubator at 37 °C and 5 % CO₂ with required media listed in Table 10. For cell freezing, trypsinized cell pellets were resuspended in freezing medium and aliquoted into cryovials. Cells were then stored in -80 °C or in liquid nitrogen for short-term and long-term storage, respectively. For cell thawing, aliquoted cells were quickly thawed in 37 °C water baths and washed thrice with 1x PBS before plating into culture dishes. Cells were then maintained in required medium.

4.3. Isolation and culturing of neonatal, juvenile (P5) and adult cardiomyocyte isolation.

Neonatal and juvenile (P5) cardiomyocytes were isolated with the neonatal cardiomyocyte isolation kit (Table 12. List of kits.), according to the manufacturer's protocol. Neonatal and juvenile cardiomyocytes were culturing the complete DMEM medium (Table 10. List of growth medium).

Adult cardiomyocytes were isolated with the Langendorff-free method as described [175], with some modifications. Adult mice were anaesthetized with isoflurane with the open-drop and nose cone method [176]. Following anesthesia, the chest was opened to expose and cut the descending aorta. For perfusion the right ventricle (RV) was injected with 7m EDTA buffer (Table 11. **List of buffers.**). Ascending aorta was clamped by Reynolds forceps. Perfused hearts were then transferred into fresh EDTA buffer. Then 0 mL perfusion buffer (Table 11. **List of buffers.**) was gently injected into the left ventricle (LV). Hearts were then digested by gentle injection of digestion buffer (Table 11. **List of buffers.**) to the LV. Hearts were repeatedly injected (~5 times) with 10mL digestion buffer until they became pale and

soft. Ventricle were separated from atria with forceps and the ventricle was then pulled with the forceps into small pieces. Cellular dissociation was completed by gentle trituration of heart fragments. Digestion process was terminated by addition of 5mL stopping buffer (Table 11. **List of buffers.**). Cells were passed through a 100- μ m filter and collected. The cardiomyocytes were purified by 2 sequential rounds of gravity settling.

For culturing, the calcium was reintroduced in cardiomyocytes following gradient incubation [176]. Then cardiomyocytes were cultured on laminin-coated dishes (5 μ g/mL) in planting medium for 1 hour. Cardiomyocytes were then washed twice and further cultured in cardiomyocyte culture medium.

4.4. OSKM induction of cardiomyocyte and time-lapse imaging

Purified cardiomyocytes were cultured in KSR medium. Induction of OSKM expression was achieved by addition of doxycycline to the culture media (final concentration of 20 ng/mL). Time-lapse imaging was performed using Incucyte Live-Cell Imaging System (Essen Instruments). The Cell-by-Cell Analysis Software Module (Essen Instruments) was used for quantification of cardiomyocyte proliferation.

4.5. Lentiviral production and transduction

Production of lentivirus for c-Myc, OSK, and OSKM overexpression were performed by Polyethylenimine (Polysciences, 23966-100) transfection of HEK293T cells with helper plasmids pMD2.G and psPAX2. Isolated cardiomyocytes were mixed with concentrated supernatants of lentiviruses supplemented with 8mg/ml polybrene in fresh culture medium containing 10%FBS and seeded into 0.2% Gelatin coated culture plates. After 24 hours infected cardiomyocytes were selected by 2 μ g/ml puromycin for 24 hours. Transgene expression was induced by addition of doxycycline at a final concentration of 20 ng/ml.

4.6. Isolation of cardiomyocytes from fixed hearts

Adult mouse hearts were surgically excised immediately after sacrifice and then washed out from blood with PBS. The heart was then cut into small 3 mm pieces and fixed in ice cold fixation buffer (PBS containing 2% paraformaldehyde) for 2 hours. Fixed heart fragments were washed in PBS and exposed to digestion buffer (PBS containing 1 mg/mL collagenase II) at 37° C overnight. Cells were washed at the next day thrice with PBS, counted with a

hemocytometer and plated on SuperFrost Plus adhesion slides (Thermo scientific) for further processing.

4.7. RNA samples preparation and cDNA synthesis

Total RNA was isolated from cells or tissues by using Trizol reagent (life technologies) according to the manufacturer's protocol. For tissue samples, samples were placed in a 2 mL eppendorf tube with a sterile grinding ball (5 mm, Retsch, 22.455.0003). 1 mL Trizol reagent was added and the tube was placed in a tissue homogenizer (Retsch, MM301) for 10 mins at 30/s frequency for homogenization. For cultured cells, cells were washed twice with 1x PBS and then 1 mL Trizol reagent was added to the culture dish. Cells were harvested and collected to a 1.5 mL eppendorf tube by using cell scraper (Sarstedt, 83.1830). 200 μ L chloroform was added to the tube and samples were incubated for 5 mins at room temperature. Following, samples were centrifuged at 4 °C for 10 mins at 12,000 g. The white pellet appeared at bottom of the tube and was washed twice with 1 mL 75 % ethanol. After centrifugation, ethanol was removed and the tubes were put inside the hood until dry. The pellet was re-suspended with 30-50 μ L DEPC water (0.1 % v/v DEPC in water). The dissolved samples were considered as isolated total RNA samples, the concentration was measured with a spectrophotometer (NanoDrop ND-2000c Spectrophotometer).

For cDNA synthesis, >500 ng of purified RNA was reversely transcribed with PrimeScript RT Reagent Kit (Takara bio, RR037B) according to the manufacturer's protocol. Random primers and Oligo DT primers were modified in a usage of in the 1:1 mixture, and the incubation time was adjusted to 30 mins to gain better reverse transcription products. After the reaction, samples were considered as cDNA for further use or stored in -20 °C.

4.8. Quantitative real time polymerase chain reaction (qRT-PCR)

qPCR was used to quantitatively determine the mRNA expression. During the amplification, fluorescent dyes can incorporate into double stranded DNA and were read as signal. For a typical qPCR setup, it contained 10 μ L 2x SYBR Green® mixture, 1 μ L of forward and reserved primers (2.5 pmol), and 5 μ L of diluted cDNA (1:100 diluted) in a total volume of 25 μ L. The PCR conditions were chosen according to the manufactory's protocol and the calculated annealing temperatures of primers. The PCR runs were performed on StepOnePlus real time PCR machine. The relative amount of the target genes and endogenous

housekeeping gene was determined in same plates to avoid deviation. The relative expression level of each genes was calculated with the $2^{-\Delta\Delta CT}$ method as described.

4.9. Protein sample preparation

For tissue samples, samples were briefly freezed with liquid nitrogen and crushed using a mortar and pestle into white powder, and then transferred into a 1.5 mL eppendorf tube containing 300 μ L protein lysis buffer (0.1 M Tris/Hcl pH 8.0, 0.01 M EDTA, 10 % SDS) supplemented with 1x protease inhibitor (ThermoFisher, A32965). Samples were incubated on ice for 10 mins, following with a sonication at 20 kHz for 1 min. After, samples were centrifuged at 12,000 rpm for 10 mins. For cultured cells, the dish was washed twice with 1x PBS and cell lysate was prepared in same way as described for tissues sample. For both, the supernatant containing the protein lysate was transferred to a fresh tube and concentration was measured using Bio-Rad assay (BioRad, Reagent A-500-0113, and Reagent B-500-0114) in a 96 wells plate according to the manufacturer's instruction. Protein concentration was determined by measured and calculated based on the standard curve. For measurement, 200 μ L reagent B and 25 μ L reagent A were mixed with prepared BSA solution or samples. Mixed samples were incubated for 5 mins at room temperature before subjecting for the measurement. The lysates were considered as isolated protein samples used for Western Blot or stored at -80 °C.

4.10. Sodium dodecyl sulfate-polyacrylamide gel electrophoresis

Sodium Dodecyl Sulfate-Polyacrylamide Gel Electrophoresis for western blot were self-made according to recipes shown Table 11. In brief, prepared resolving gel was filled in around 80 % of the NOVEX cassettes (1 mm, Invitrogen, NC2010) and about 1 mL pure ethanol was added on top. The filled cassettes were incubated for 30 mins until the mixtures became set. Following, the ethanol was pulled out, the cassettes were filled with the stacking gel and inserted with comb. For western blot assay, the electrophoresis was performed in a running chamber (NOVEXE electrophoresis Mini-Cell, Invitrogen, EI001) using the MES (2.5 mM MES, 2.5 mM Tris, 0.05 % SDS, 50 mM EDTA) buffer for 2 to 3 hours at 120 volts until the samples were separated accordingly. Protein location was detected with the Protein-Marker VI (Peqlab, 27-2311).

4.11. Western blot

10µg of protein lysates were subjected to SDS-PAGE and western blot using antibodies 1:200 Oct4 (Santa Cruz, sc-5279), 1:500 GAPDH (Cell Signaling Techn. 2118). Protein expression was visualized using an enhanced chemiluminescence detection system (GE Healthcare, Little Chalfont, United Kingdom) and quantified using a ChemiDoc gel documentation system (Bio-Rad).

4.12. Frozen samples and cryosections preparation

Tissues were harvested from mice and kept in a humidified chamber before subjecting for frozen process. 2-methylbutane was poured into an open glass beaker to a depth of approximately 10 cm. The beaker was then put into an insulated container filled with liquid nitrogen. The beaker was ready for sample frozen when the white pellet started forming at bottom. Tissues were then dipped in the beaker for approximately 10 s and put on dry ice for 10 mins for drying. Samples were embedded with OCT at -20 °C for 10 mins. Cryosections were obtained by using a microtome (Leica, RM2125RT) and collected on glass slides (Superfrost Ultra Plus-ThermoFisher, J3800AMNZ). Section slides were immediately used in following staining or stored at -80 °C.

4.13. Immunocytochemistry and histology

For immunostaining sections were permeabilized with Triton X-100 in PBS for 30 min and blocked in M.O.M Immunodetection Kit (Vector Lab, MKB-2213-1) for 1 hour at room temperature. Primary antibody incubations were performed at 4°C overnight, secondary antibody incubations at room temperature for 1 hour. EdU assays was performed with the Click-iT™ EdU Cell Proliferation Kit according to the manufacturer's protocol (ThermoFisher). Antibodies were used at the following Table 2 and

Table 3.). Images were taken using a confocal Leica SP8, Zeiss AxioImager Z1 and ZEISS Axio Observer. Trichrome stainings were performed using the Trichrome Stain (Masson) Kit (Sigma, HT15-1KT). Images were taken and merged by an All-in-one Fluorescence Microscope (Keyence).

4.14. WGA staining and cardiomyocyte size quantification

WGA staining and quantification was performed as previously described [177]. ImageJ was used to quantify the size of cardiomyocytes. At least 100 cells per sample from at least three independent hearts per group with different views and positions across entire heart sections were quantified.

4.15. Blood cTnI measurements

Mouse blood was collected from tail vein after 24 hours of LAD. Mouse cardiac troponin I cTnI ELISA Kit (Novateinbio, NB-E20411) was used to measure the cTnI concentration.

4.16. Scar quantification

All sections were mounted on glass slides and stained with Masson trichrome stain for quantitative analysis of infarct size. Images were acquired using an All-in-one Fluorescence Microscope (Keyence). Scar areas were quantified by imageJ according to Takagawa et al., “Myocardial infarct size measurement in the mouse chronic infarction model: comparison of area- and length-based approaches”

4.17. LAD ligation

Adult mice were injected with buprenorphine (0.05 mg/kg) and anaesthetized using an isoflurane inhalational chamber, then immediately endotracheally intubated using a 20 gauge angiocatheter (Medline), and connected to a MiniVent Ventilator for mice (Harvard Apparatus) while positioned in heating plate (Agnthos). A midline cervical incision was performed under a stereo microscope and the skin, muscle and tissue covering the trachea were separated. A thoracotomy was performed at the left fourth intercostal space to expose the pericardium and LAD. The LAD was ligated using a 7-0 prolene suture (Ethicon), which was verified by evident paling of the left ventricle below the stitch site. The thoracic incisions and skin were closed using a 5-0 suture (SERAFIT Violet). After surgery mice received analgesic treatment via administration of Novalgine (Sanofi) in drinking water (final concentration 0.5 mg/mL) for 3 days.

4.18. Cardiac apical resection

Apical resection of P7 mice was performed as described previously [178] with some modifications. 7 days-old pups were hypothermically anaesthetized by placing mice on a tissue-covered ice-bed under a microscope for 5 min. A transverse skin incision and thoracotomy was performed at the fourth intercostal space. Heart was exteriorized outside the chest by exerting gentle pressure to the abdomen. About 2 mm of the heart apex was resected. Wounds were closed with 7-0 prolene suture. Following surgery, animals were gradually warmed on a heating plate (Agnthos) until recovery and returned back to their mother. Sham procedures excluded apex amputation.

4.19. Magnetic resonance imaging

Cardiac MRI measurements were performed on a 7.0 T Bruker Pharmascan (Bruker, Ettlingen, Germany) and operated using ParaVision 6.0.1, equipped with a 760 mT/m gradient system, a cryogenically cooled four channel phased array element 1H receiver-coil (CryoProbe), a 72 mm room temperature volume resonator for transmission and the IntraGateTM self-gating tool. Measurement were executed with the gradient echo method (repetition time=6.2 ms; echo time=1.3 ms; field of view=2.20x2.20 cm; slice thickness=1.0 mm; matrix=128 x 128; oversampling=100). The imaging plane was localized using scout images showing the two- and four-chamber view of the heart, followed by acquisition in short axis view, orthogonal on the septum in both scouts. Multiple contiguous short axis slices consisting of same slices of same hearts were acquired for complete coverage of the left ventricle. MRI data were analyzed using Qmass digital imaging software (Medis).

4.20. RNA sequencing and analysis

Total RNA was prepared using TRIzol and extracted using the Direct-zolTM RNA MiniPrep kit (Zymo Research). RNA quality and yield were measured using RNA integrity number (RIN) algorithm, using the Fragment Analyzer (Agilent) or LabChip Gx Touch 24 (Perkin Elmer). Samples with 7.0-10.0 RIN value were used for library preparation. 2 µg of total RNA was used as input VAHTS Stranded mRNA-seq Library preparation. Sequencing was performed on a NextSeq500 instrument (Illumina) using v2 chemistry. An average of 31M reads per library had 1x75bp single-end setup. The resulting raw reads were assessed for quality, adapter content and duplication rates with FastQC and Trimmomatic version 0.33 was employed to trim reads after a quality drop below a mean of Q20 in a window of 5

nucleotides. Only reads above 30 nucleotides were cleared for further analyses. Trimmed and filtered reads were aligned versus the Ensembl mouse genome version mm10 (GRCm38) using STAR 2.4.0a with the parameter “--outFilterMismatchNoverLmax 0.1” to increase the maximum ratio of mismatches to mapped length to 10% [179]. The number of reads aligning to genes was counted with featureCounts 1.4.5-p1 tool from the Subread package [180]. Only reads mapping at least partially inside exons were admitted and aggregated per gene. Reads overlapping multiple genes or aligning to multiple regions were excluded. Analysis of differentially expressed genes was performed using DESeq2 [181]. Reanalysis of transcriptomes from E14.5 embryonic cardiomyocytes, neonatal cardiomyocytes, and adult cardiomyocytes (GSE79883) [182] through our pipeline included and Limma's removeBatchEffect.

4.21. Mouse models

All animal experiments were done in accordance with the Guide for the Care and Use of Laboratory Animals published by the US National Institutes of Health (NIH Publication No. 85-23, revised 1996) and according to the regulations issued by the Committee for Animal Rights Protection of the State of Hessen (Regierungspraesidium Darmstadt). The ROSA26-OSKM was obtained from Vascular Cell Biology Unit VIB/Ghent University and described previously [165]. The R26R-H2B-mCherry (RosaH2BmChery) mouse strain (Acc. No. CDB0204K) was obtained from The RIKEN Center for Developmental Biology (Kobe, Japan) [183]. The Tg(myl2-cre)1141Tmhn (Xmlc2Cre) mouse strain was obtained from The Jackson Laboratory (Bar Harbor, ME) [184]. A1cfTg(Myh6-cre/Esr1*)1Jmk (α MHC-MerCreMer) mouse strain was obtained from the Jackson Laboratory (Bar Harbor, ME) [185]. The $i4F^{\text{Heart}}$ mice were generated by cross-breeding of Xmlc2Cre and Rosa26-OSKM mice. The $i4F^{\text{Heart/mCherry}}$ mice were generated by cross-breeding of $i4F^{\text{Heart}}$ mice with RosaH2BmChery mice. The $i4F^{\alpha\text{MHC-MCM}}$ mice were generated by cross-breeding of α MHC-MerCreMer and ROSA26-OSKM mice. All mice were bred on the C57BL/6 background. The age of all adult mice were 9-16 weeks old.

4.22. Statistics

Unpaired two-sided t-test was used for comparisons between two different groups. One-way ANOVA was used for comparisons between more than two groups. Repeated measure one-way ANOVA was performed for weight curves. Two-way ANOVA was used for comparisons

between more than two groups with different treatments and different conditions. Kaplan-Meier estimator was performed for survival curves, followed by the Gehan-Breslow-Wilcoxon test. All statistical tests were performed with GraphPad Prism version 6.0, and $P < 0.05$ was considered statistically significant. (ns $P > 0.05$, * $P < 0.05$, ** $P < 0.01$, *** $P < 0.001$, **** $P < 0.0001$) No statistical methods were used to predetermine sample size. Investigators were not blinded to allocation during experiments and outcome assessment.

5. Results

5.1. OSKM expression promotes proliferation of neonatal cardiomyocytes and facilitates their reprogramming

Forced OSKM expression dedifferentiates a wide range of proliferative somatic cell types to iPSCs, which harbor infinite proliferative capacity [148-156]. Neonatal cardiomyocytes still own residual proliferative capacity and stop to proliferate around 7 days after birth. Therefore, it was tested whether forced OSKM expression maintain proliferation of juvenile cardiomyocytes before acquisition of the post-mitotic state. It was also tested whether overexpression of c-Myc alone sustains juvenile cardiomyocyte proliferation, since c-Myc can function as an oncogene and is also known to promote cell proliferation in other cell types[186]. In addition, it was tested whether overexpression of OSK alone, without c-Myc, dedifferentiates and/or reprograms neonatal cardiomyocytes. It has been shown that OSK alone is sufficient to elicit reprogramming in some cell types [148, 187]. To this end, gene cassettes enabling Doxycycline (Dox) inducible expression of c-Myc, OSK, or OSKM were lentivirally transduced into cultured cardiomyocytes isolated from juvenile mice (P5) in which cardiomyocyte nuclei are genetically labelled with red fluorescence via an H2BmCherry reporter (Fig. 5A). Furthermore, a puromycin selection cassette enabled selection of infected cardiomyocytes. The puromycin selected cardiomyocytes were then treated with Dox for 3 days to induce expression of transgenes. To score for proliferation rates, EdU incorporation rates were measured as an indicator of cardiomyocytes in S phase. In addition, the cardiomyocytes were stained for PH3 (Phospho Histone 3), which labels mitotic cells. Interestingly, c-Myc expression led to an increase of EdU positive cardiomyocytes, consistent with previous reports [188]. However, in contrast to OSK and c-Myc alone, only OSKM expression allowed cardiomyocytes to become both EdU and PH3 positive (Fig. 5B-D). Based on these results, clearly indicating that forced OSKM expression is sufficient to enhance proliferation of cardiomyocytes in vitro, it was tested whether OSKM expression promotes cardiomyocyte proliferation by in vivo.

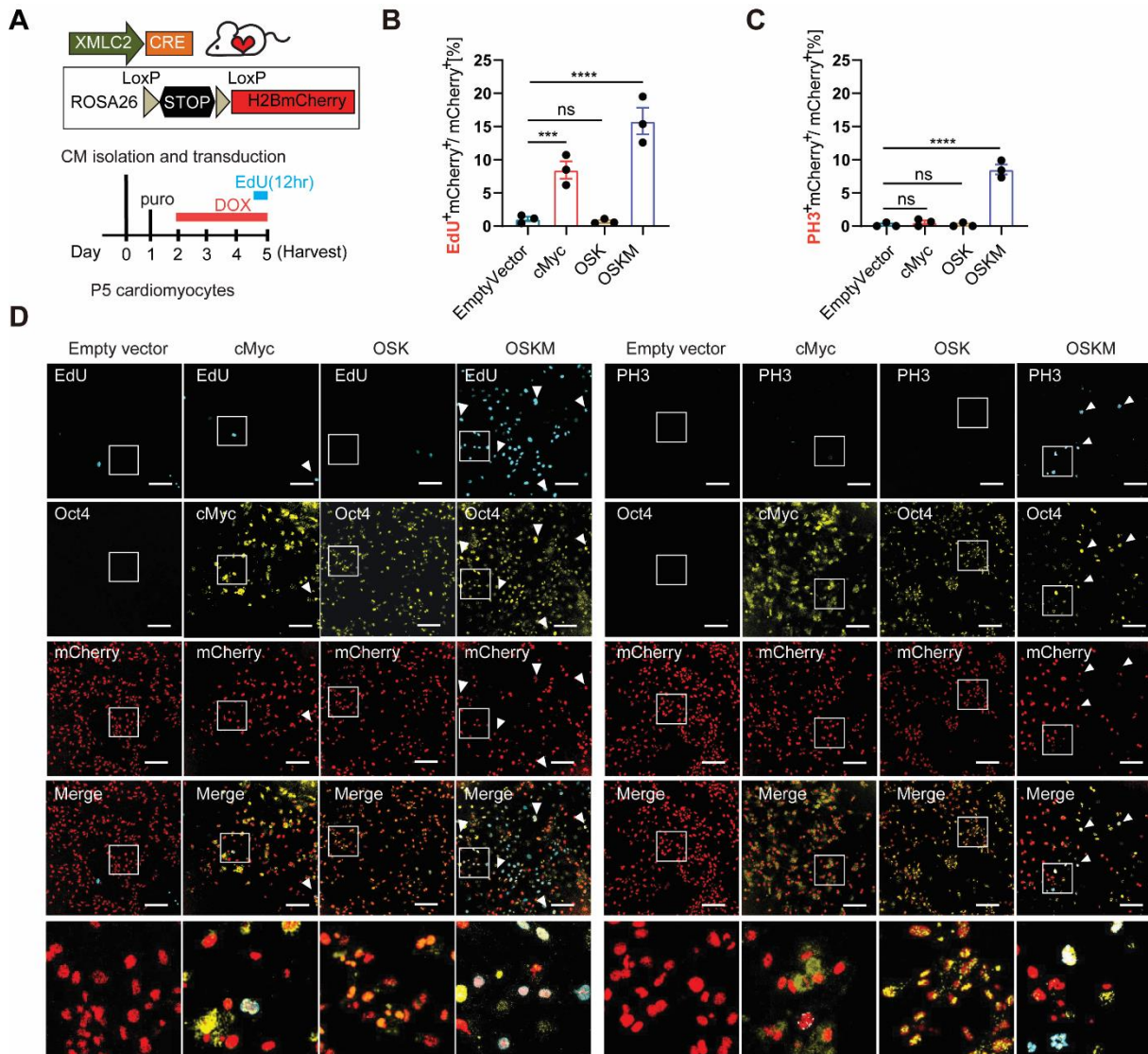


Fig. 5 OSKM expression promotes cardiomyocytes proliferation in vitro.

(A) Schematic outline of lentivirus-mediated expression of c-Myc, OSK and OSKM in P5 cardiomyocytes isolated from Xmlc2Cre-RosaH2BmCherry mouse hearts.

(B and C) Quantification of EdU incorporation (B) and PH3(C) (cyan) in H2B-mCherry labelled P5 cardiomyocytes. Error bars are s.e.m., n=3. p-values were calculated by One-Way ANOVA. ns P>0.05, *P<0.05, **P<0.01, ***P<0.001, ****P<0.0001.

(D) Immunofluorescence and EdU stainings of cardiomyocytes. Scale bar=100 μm.

To this end, mice were generated that harbor a Cre-recombinase specifically expressed in cardiomyocytes [184] and that are homozygous for a bi-directional gene cassette inserted into the Rosa26 locus harboring a LoxP-flanked rtTA and a polycistronic tetO_OSKM-IRES-GFP cassette [165]. These mice are hereafter designated as i4F^{Heart} mice. Essentially, Dox treatment of i4F^{Heart} mice allows cardiomyocyte-specific and reversible expression of OSKM. Notably, this strategy circumvents the problem of early tumor formation and growth in other organs [164]. Crossing of i4F^{Heart} mice with mice harboring a homozygous LoxP-flanked

H2BmCherry cassette in the Rosa26 locus gives rise to $i4F^{\text{Heart/mCherry}}$ mice, in which cardiomyocytes are permanently labelled with red, nuclear localized H2BmCherry fluorescence and express OSKM upon Dox administration. Notably, $i4F^{\text{Heart/mCherry}}$ harbor one H2BmCherry reporter allele and one OSKM allele in contrast to $i4F^{\text{Heart}}$ mice that harbor two OSKM alleles in the Rosa26 locus (Fig.6A).

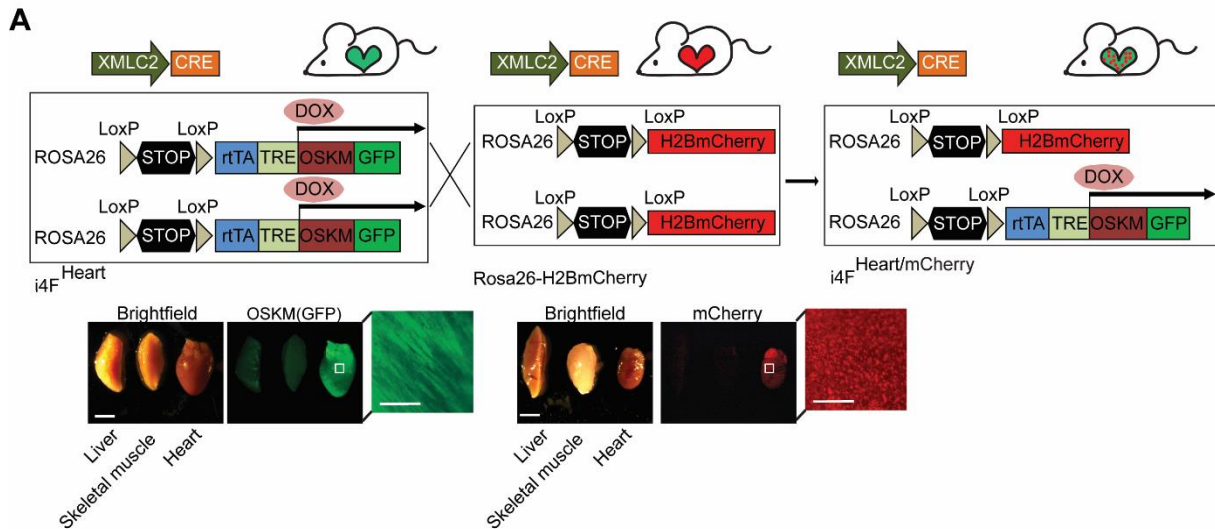


Fig. 6 Schematic outline of the transgenic mouse models.

(A) $i4F^{\text{Heart}}$, Rosa-H2BCherry, $i4F^{\text{Heart/mCherry}}$ mouse models. The fluorescence images indicate the specific expression of OSKM and H2BmCherry in cardiomyocytes.

To test the efficacy of the system, cardiomyocytes were isolated from neonatal $i4F^{\text{Heart/mCherry}}$ mice and treated with Dox in culture. Interestingly, time-lapse imaging revealed that short-term Dox supply for only one or two days did not markedly induce CM proliferation, whereas longer than 3 days of Dox supply increased neonatal cardiomyocyte divisions dramatically (Fig.7A, B). Withdrawal of Dox supply after 3 days attenuated cell division, sustaining Dox supply resulted in continuous divisions and the emergence of Nanog-positive colonies, indicating that cardiomyocytes had acquired pluripotency (Fig. 7C). Indeed, single colonies obtained from these culturing expanded in ES cell medium and maintained Nanog expression in the absence of Dox (Fig. 7C). These data, together with the observation that the colonies stained positive for alkaline phosphatase (AP) (Fig. 7D), strongly indicated that the neonatal cardiomyocytes had been fully reprogrammed to iPSCs. Indeed, upon their injection into blastocysts, chimeric mice developed, thereby confirming that the cardiomyocytes had acquired pluripotency (Fig.7D-E). Taken together, these data demonstrate that OSKM

expression efficiently enhances proliferation of neonatal cardiomyocytes and iPSC formation in vitro.

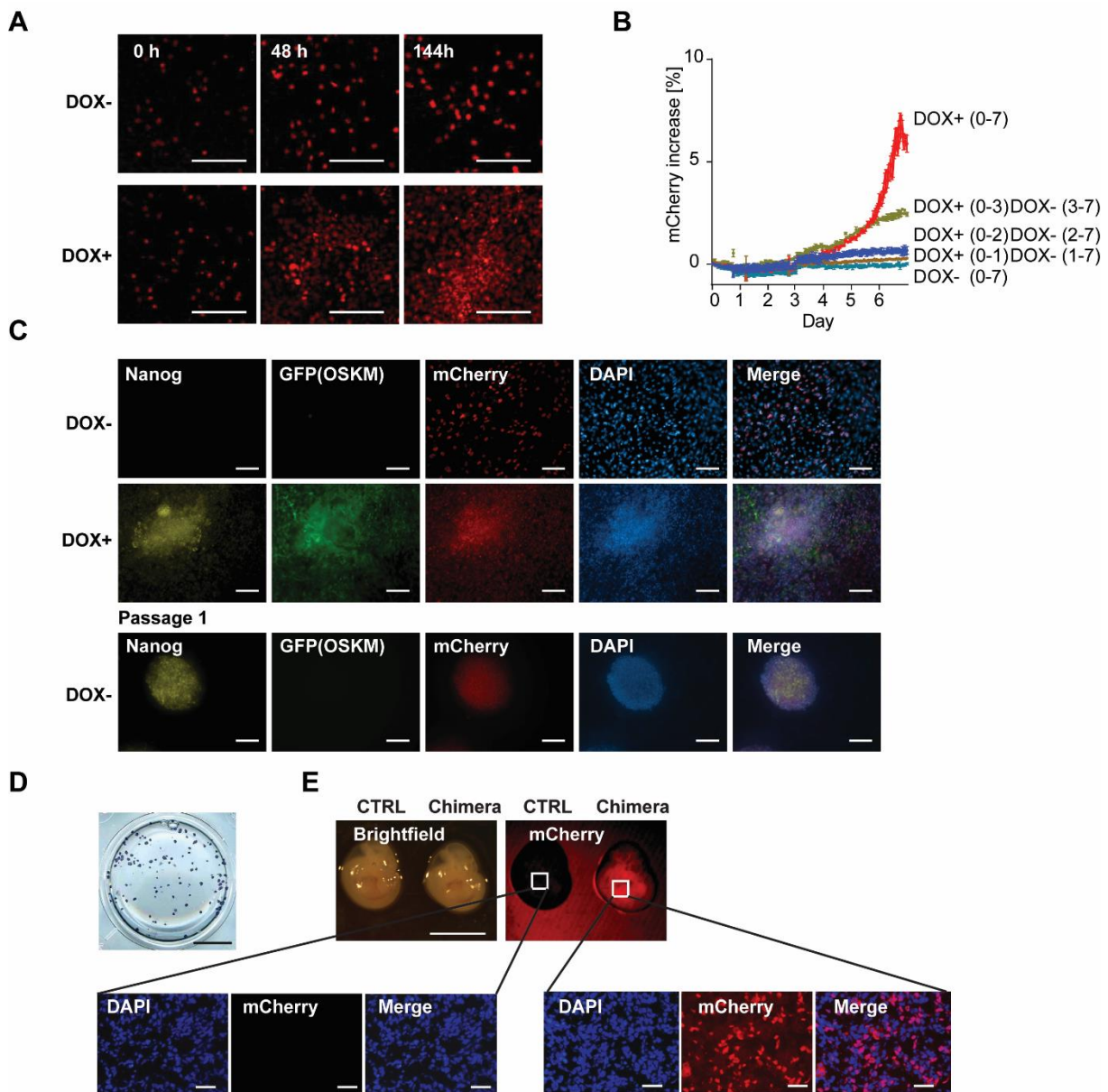


Fig. 7 In vitro generation of iPSCs from neonatal cardiomyocytes by OSKM expression. (A) Time-lapse images of purified, neonatal $i4F^{\text{Heart/mCherry}}$ cardiomyocytes cultured with and without doxycycline, Scale bar=100 μm . (B) Growth rates of purified, neonatal $i4F^{\text{Heart/mCherry}}$ cardiomyocytes cultured with and without doxycycline at indicated times, n=3. (C) Images of colony formation from $i4F^{\text{Heart/mCherry}}$ cardiomyocyte following 10 days of doxycycline treatment. Nanog-expression becomes apparent only in OSKM GFP expressing cells (green) and is sustained after doxycycline withdrawal. Scale bar=50 μm . (D) Alkaline phosphatase staining of passaged colonies derived from $i4F^{\text{Heart/mCherry}}$ cardiomyocytes. Scale bar=2 mm. (E) Formation of mouse chimera after blastocyst injection of $i4F^{\text{Heart/mCherry}}$ cardiomyocyte-derived, Nanog-expressing cells. Scale bar in embryo=1mm. Scale bar in section=50 μm . H2BmCherry is stained in red and DAPI in blue.

5.2. OSKM expression enables adult cardiomyocytes to re-enter cell-cycle

Unlike neonatal cardiomyocytes, adult cardiomyocytes in mammals are considered as post-mitotic [147]. Given the profound rates of division in $i4F^{\text{Heart/mCherry}}$ neonatal cardiomyocytes upon Dox supply, it was next tested if OSKM might also induce proliferation of adult cardiomyocytes. To this end, rod-shape cardiomyocytes isolated from 9~16 week old $i4F^{\text{Heart/mCherry}}$ mice were cultured in the presence of Dox and monitored via time-lapse imaging. Strikingly, Dox-treated adult cardiomyocytes underwent mitosis and completed cytokinesis, (Fig. 8A, B), whereas no divisions were observed in the non-treated group (data not shown). It has been speculated that mono-nucleated adult cardiomyocytes are more susceptible to cell cycle reentry in comparison to bi- or multinucleated cardiomyocytes [189]. Indeed, clear nuclear and cellular divisions of mono-nucleated cardiomyocytes were observed after OSKM expression. Intriguingly however, some bi-nucleated cardiomyocytes also entered mitosis and some directly underwent cytokinesis without nuclear duplication. These data demonstrate that forced OSKM expression is sufficient to induce adult cardiomyocyte cell-cycle reentry even in bi-nucleated cells. Similar to cardiomyocytes from $i4F^{\text{Heart/mCherry}}$, cardiomyocytes derived from $i4F^{\text{Heart}}$ mice also divided after Dox treatment (Fig. 8B). Notably, cardiomyocytes never divided more than once, despite continuous Dox supply and culture periods of up to three months. Consequently, formation of colonies was never observed.

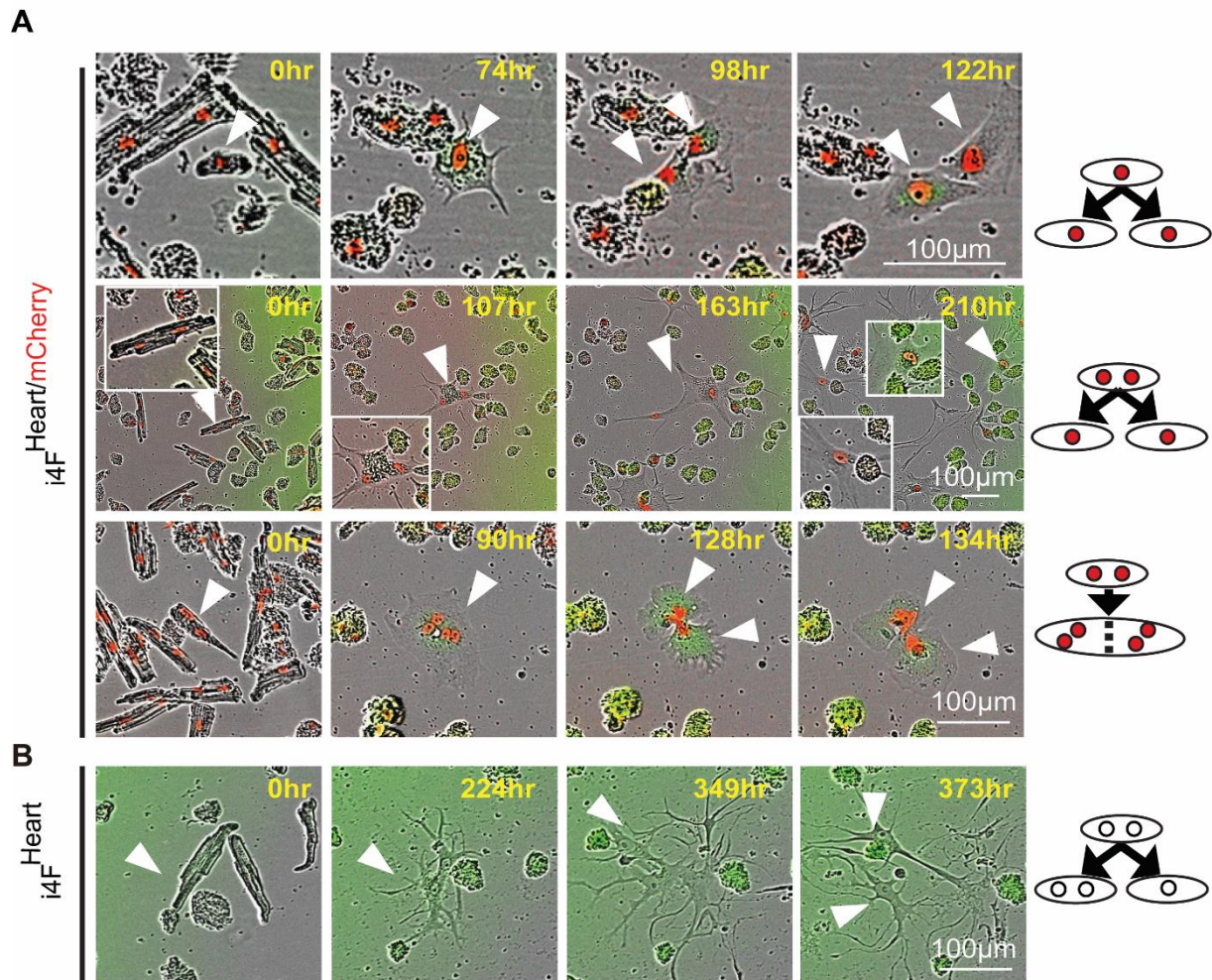


Fig. 8 OSKM expression drives division of mono- and bi-nucleated adult cardiomyocytes.

(A, B) Time-lapse imaging of purified adult cardiomyocytes cultured with DOX, (A) $i4F^{Heart/mCherry}$, (B) $i4F^{Heart}$. H2BmCherry (red), OSKM-GFP (green), arrow points to dividing cardiomyocytes. Scale bar = 100 μm .

5.3. OSKM expression promotes neonatal and juvenile (P7) cardiomyocyte dedifferentiation and proliferation in vivo

Next, it was tested if OSKM expression induces cardiomyocyte proliferation in vivo. More specifically it was tested if OSKM expression sustains CM proliferation and prevents cell cycle exit, since mouse neonatal cardiomyocytes undergo a final round of DNA synthesis around P5 to P7 for bi-nucleation and permanently withdraw from the cell cycle shortly thereafter [190]. Therefore, neonatal (P1) and juvenile (P7) $i4F^{Heart/mCherry}$ mice were injected daily with Dox for one week (Fig. 9A).

Following Dox treatment, strong GFP fluorescence was visible in both neonatal and juvenile $i4F^{\text{Heart/mCherry}}$ mice compared to non-treated controls clearly indicating expression of the OSKM-IRES-GFP transgene. Heart sizes increased massively in Dox-treated $i4F^{\text{Heart/mCherry}}$ mice compared to non-treated controls (Fig. 9B). Immunofluorescent staining revealed markedly decreased expression of the gap junction protein connexin43 (CX43), indicating cardiomyocyte dedifferentiation. Consistently, Dox-treated hearts displayed strong expression of smooth muscle α -actin (aSMA) (Fig. 9C) confirming that OSKM expression induces cardiomyocyte dedifferentiation. Furthermore, a dramatic increase of EdU and PH3 positive cardiomyocyte nuclei was detected in Dox-treated $i4F^{\text{Heart/mCherry}}$ mice (Fig. 9D-H). These data show that OSKM expression elicits cardiomyocyte dedifferentiation, extends the proliferation window of neonatal cardiomyocytes, and inhibits juvenile cardiomyocytes to exit the cell cycle.

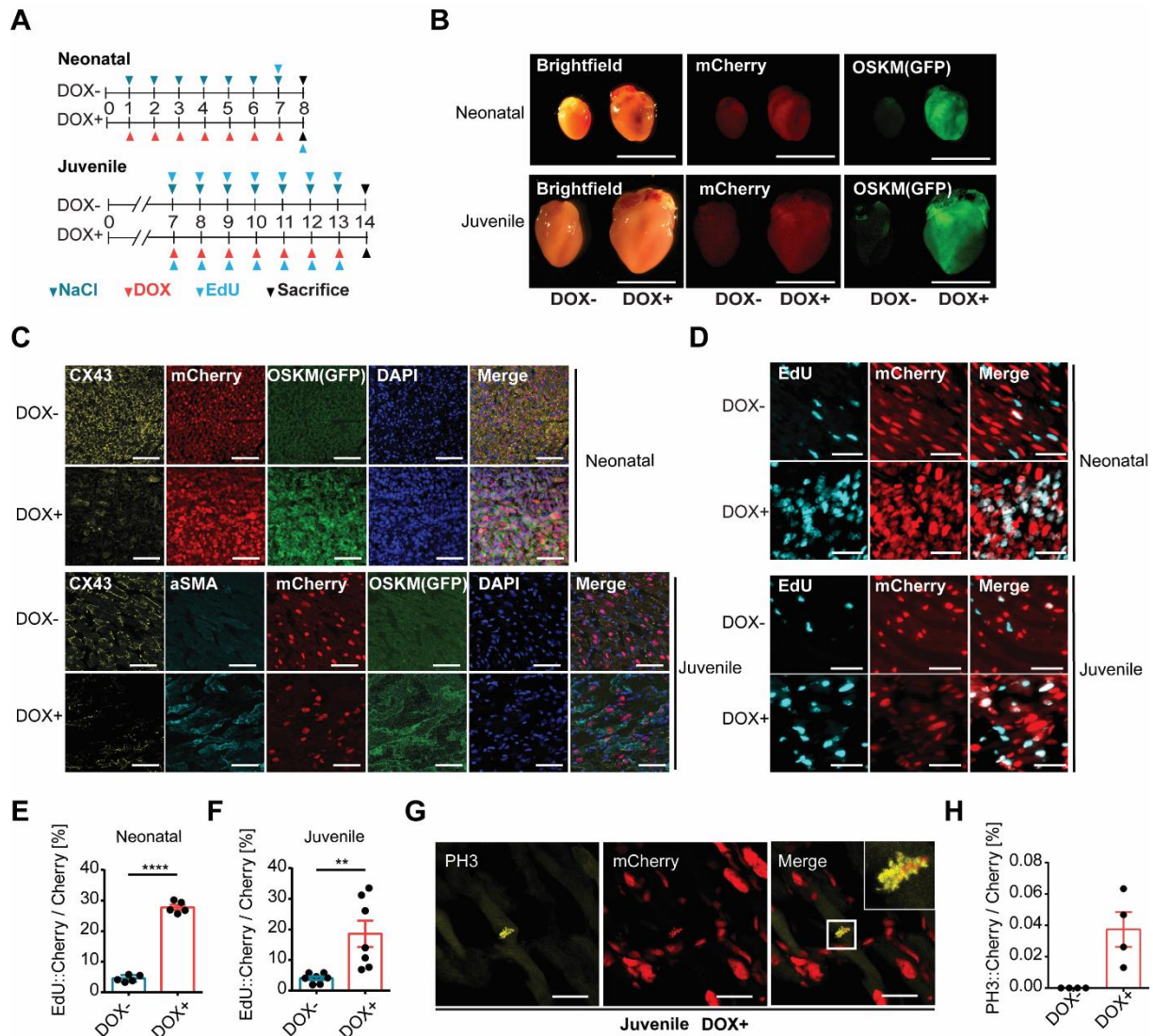


Fig. 9 Transgenic expression of OSKM in neonatal and juvenile hearts induces cell cycle entry and expression of dedifferentiation markers.

(A) Schematic outline of doxycycline treatments of neonatal and juvenile (P7) $i4F^{\text{Heart/mCherry}}$ mice.

(B) Brightfield and fluorescent images of whole hearts isolated from neonatal and juvenile (P7) $i4F^{\text{Heart/mCherry}}$ mice, treated as in (A). Scale bar=1 mm.

(C) Immunostaining of heart cross-sections from neonatal and juvenile (P7) $i4F^{\text{Heart/mCherry}}$ mice treated as in (a). Scale bar=50 μm .

(D, E and F) Images (D) and quantification (E and F) of EdU incorporation (cyan) in H2B-mCherry labelled neonatal cardiomyocytes on heart cross-sections of neonatal and juvenile (P7) $i4F^{\text{Heart/mCherry}}$ mice treated as in (A). Scale bar=50 μm . Error bars are s.e.m., $n=5$. p-values were calculated by the unpaired Student's two-sided t-test. ** $P<0.01$, **** $P<0.0001$.

(G and H) Immunofluorescence staining (G) and quantification (H) of PH3+ (yellow) in H2BmCherry- labelled cardiomyocyte nuclei (red). Note the clear mitotic chromosome separation in the magnified inset. No PH3 was detected in control hearts. Scale bar=50 μm . Error bars in (H) are s.e.m., $n=4$. p-values were calculated by the unpaired Student's two-sided t-test. ** $P<0.01$.

5.4. OSKM expression promotes adult cardiomyocyte dedifferentiation and proliferation in vivo

The pro-proliferative effects of OSKM expression on neonatal and juvenile cardiomyocytes might be due to the fact that cardiomyocytes at this developmental stage are not yet completely dedifferentiated and have not completely lost proliferation competence. To test whether OSKM expression induces dedifferentiation and proliferation of fully differentiated cardiomyocytes, adult $i4F^{\text{Heart/mCherry}}$ mice (9~16 weeks of age), which only carry one copy of the OSKM expression cassette, were treated with Dox (Fig. 10A). After 12 days of Dox supply in the drinking water, heart size heart weight to body weight ratios, and purified cardiomyocyte number of $i4F^{\text{Heart/mCherry}}$ mice did not show any significant differences compared with untreated controls. Notably, GFP fluorescence was also not detected (Fig. 10B-D). No signs of cardiomyocyte dedifferentiation and proliferation was found, as indicated by the absence of α SMA immunofluorescence staining and EdU incorporation in heart cross sections (Fig. 10E).

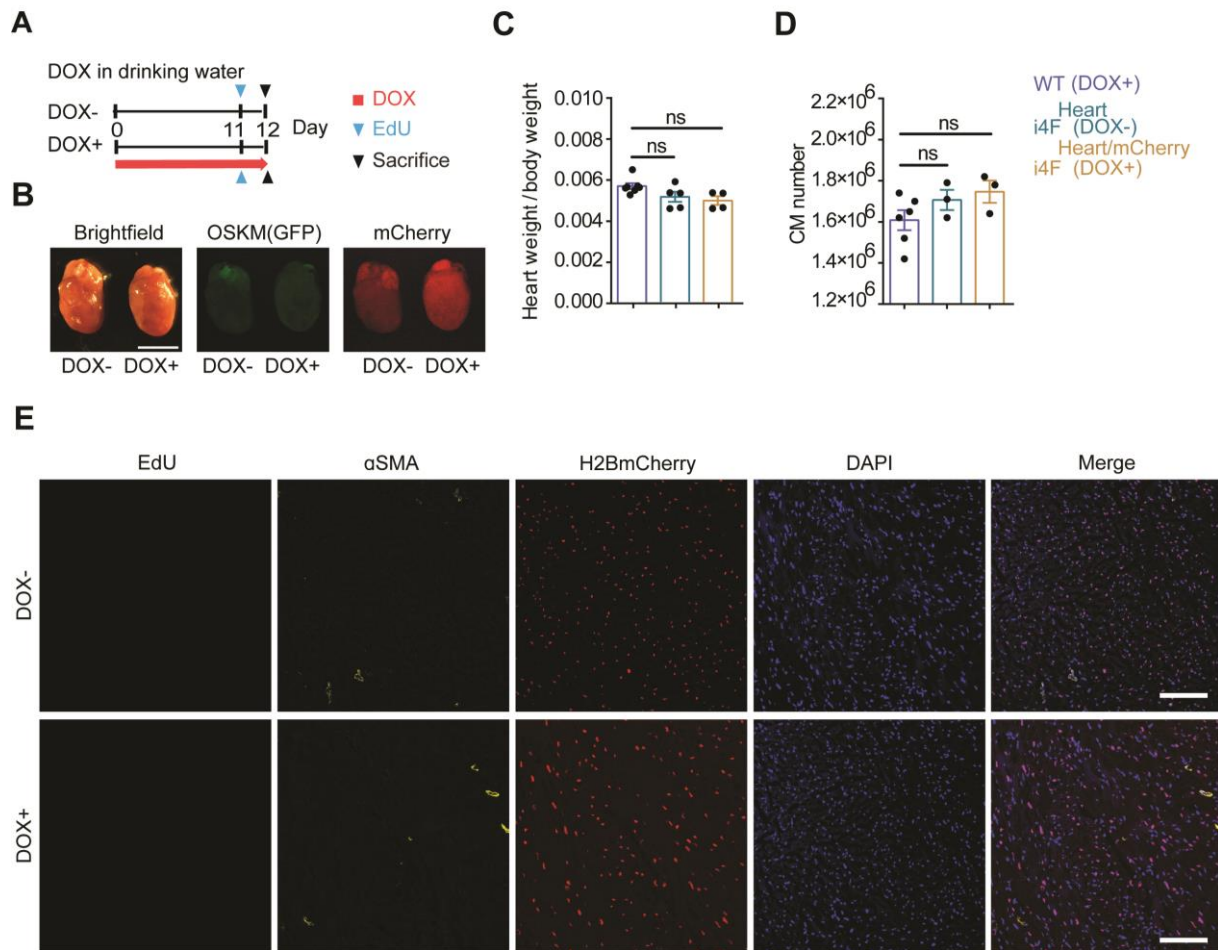


Fig. 10 Dox treatment is unable to induced cardiomyocyte dedifferentiation and proliferation in $i4F^{\text{Heart/mCherry}}$ mice.

(A) Schematic outline of doxycycline treatment to $i4F^{\text{Heart/mCherry}}$ mice.

(B) Brightfield and fluorescent images of whole hearts dissected from $i4F^{\text{Heart/mCherry}}$ mice with and without doxycycline treatment. Scale bar=2 mm.

(C and D) Heart-weight/body ratios (C) and numbers of isolated cardiomyocytes (D) of indicated mouse lines and conditions. Error bars are s.e.m. p-values were calculated by One-Way ANOVA, WT(DOX+)=6, $i4F^{\text{Heart}}$ (DOX-)=5, $i4F^{\text{Heartm/Cherry}}$ (DOX+)=3. ns $P > 0.05$.

(E) EdU (green), immunofluorescent staining of the cardiac dedifferentiation marker α SMA (yellow), and DAPI (blue) and H2B-mCherry labelled adult cardiomyocytes on heart cross-sections (red). DOX+ is the $i4F^{\text{Heart/mCherry}}$ mice with 12-day-Dox treatment and DOX- is the untreated control. Scale bar=100 μ m.

It was previously reported that a single copy of OSKM does not lead to teratoma formation in adult $i4F$ mice [171]. Moreover, the absences of GFP fluorescence in Dox treated adult

$i4F^{\text{Heart/mCherry}}$ mice suggested relatively low expression levels of OSKM, which might not be sufficient to elicit adult cardiomyocyte dedifferentiation and/or proliferation. To increase the level of OSKM expression, homozygous $i4F^{\text{Heart}}$ mice harboring two doxycycline inducible OSKM-IRES-GFP alleles were treated with Dox for 12 days (Fig. 10A and Fig. 6A). In contrast to $i4F^{\text{Heart/mCherry}}$ mice, $i4F^{\text{Heart}}$ mice hearts showed clear GFP fluorescence (Fig. 11B) and $i4F^{\text{Heart}}$ mice displayed a significant increase of induced OSKM expression in comparison to $i4F^{\text{Heart/mCherry}}$ mice (Fig. 11A). In addition, heart sizes of $i4F^{\text{Heart}}$ mice were significantly increased compared to Dox untreated controls (Fig. 11B). Along the same line, Dox treated $i4F^{\text{Heart}}$ mice exhibited a significant increase of heart weight to body weight ratios, an overall increase of cardiomyocyte numbers (Fig. 11B-D) and a significant reduction of cardiomyocyte size (Fig. 11E-F). Interestingly, RT-qPCR analysis revealed that some cardiomyocyte dedifferentiation markers were highly expressed in cardiomyocytes isolated from Dox-treated $i4F^{\text{Heart}}$ mice but not in cardiomyocytes isolated from $i4F^{\text{Heart/mCherry}}$ mice including Myh7, Tnni1, and α SMA (Fig. 11G-I).

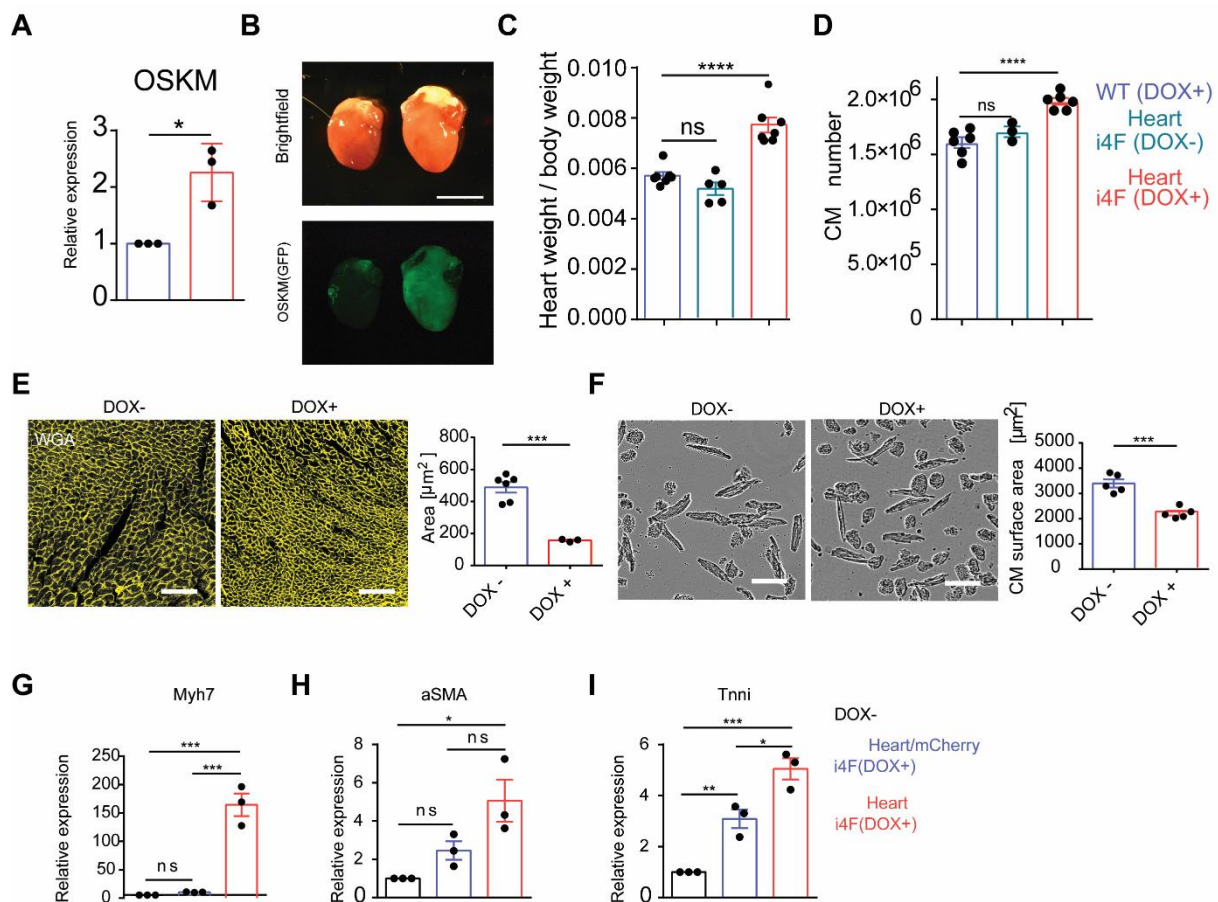


Fig. 11 Forced dedifferentiation increases the number of smaller cardiomyocytes in adult hearts.

(A) Schematic outline of doxycycline treatment to $i4F^{\text{Heart}}$ mice.

(B) Brightfield and fluorescent images of whole hearts dissected from $i4F^{\text{Heart}}$ mice treated with and without doxycycline. Scale bar=2 mm.

(C) Heart-weight/body ratios of indicated mouse lines and conditions. Error bars are s.e.m. p-values were calculated by One-Way ANOVA, n: WT(DOX+)=6, $i4F^{\text{Heart}}$ (DOX-)=5, $i4F^{\text{Heart}}$ (DOX+)=7. ns $P>0.05$, **** $P<0.0001$.

(D) Immunostaining of WGA-stained heart cross-section and quantification of cardiomyocyte size of $i4F^{\text{Heart}}$ mice treated with and without doxycycline. Scale bar=100 μm . Error bars indicate s.e.m, n=3. p-values were calculated by the unpaired Student's two-sided t-test. **** $P<0.001$.

(E) Phase-contrast images and quantification of purified adult cardiomyocytes isolated from $i4F^{\text{Heart}}$ mice treated with and without doxycycline. Scale bar=100 μm . Error bars indicate s.e.m., n=5. p-values were calculated by the unpaired Student's two-sided t-test. **** $P<0.001$.

(F) Total numbers of cardiomyocytes isolated from whole hearts of indicated mouse lines and conditions. Error bars are s.e.m. p-values were calculated by One-Way ANOVA, n: WT(DOX+)=6, $i4F^{\text{Heart}}$ (DOX-)=5, $i4F^{\text{Heart}}$ (DOX+)=7. ns $P>0.05$, **** $P<0.0001$.

(G-I) Relative expression of Myh7 (G), αSMA (H) and Tnni (I) by RT-qPCR. Error bars indicate s.e.m., p-values were calculated by One-Way ANOVA, n=3. ns $P>0.05$, * $P<0.05$, ** $P<0.01$, *** $P<0.001$, **** $P<0.0001$.

Most interestingly, immunofluorescent staining of heart cross-sections isolated from $i4F^{\text{Heart}}$ mice treated with Dox for 12 days showed enhanced expression of αSMA , clearly indicating that cardiomyocytes had undergone dedifferentiation (Fig. 12A). To test whether OSKM-induced dedifferentiation induces cardiomyocytes to enter the cell cycle, heart cross sections were immunostained with various proliferation markers. Strikingly, AuroraB positive foci located between nuclei of cardiomyocytes were clearly detected indicating that prolonged OSKM expression is sufficient to induce cytokinesis of cardiomyocytes in $i4F^{\text{Heart}}$ mice in vivo (Fig. 12B, C). To rule out the possibility that proliferation markers are expression from cells that sit on top of cardiomyocytes in heart sections, immunostaining was performed on freshly purified, rod-shaped cardiomyocytes. Cardiomyocytes positive for EdU, PH3 and AuroraB were clearly detected in the purified cTnT-expressing, rod-shape cardiomyocytes in Dox-treated $i4F^{\text{Heart}}$ mice but not in cardiomyocytes from untreated controls (Fig. 12D-I). Interestingly, sister chromatid separation, indicative of metaphase, was clearly visible in some PH3⁺ $i4F^{\text{Heart}}$ cardiomyocytes (Fig. 12E). Collectively, these observations demonstrate that OSKM expression is sufficient to induce dedifferentiation and proliferation of adult cardiomyocytes, depending on the dosage of OSKM expression.

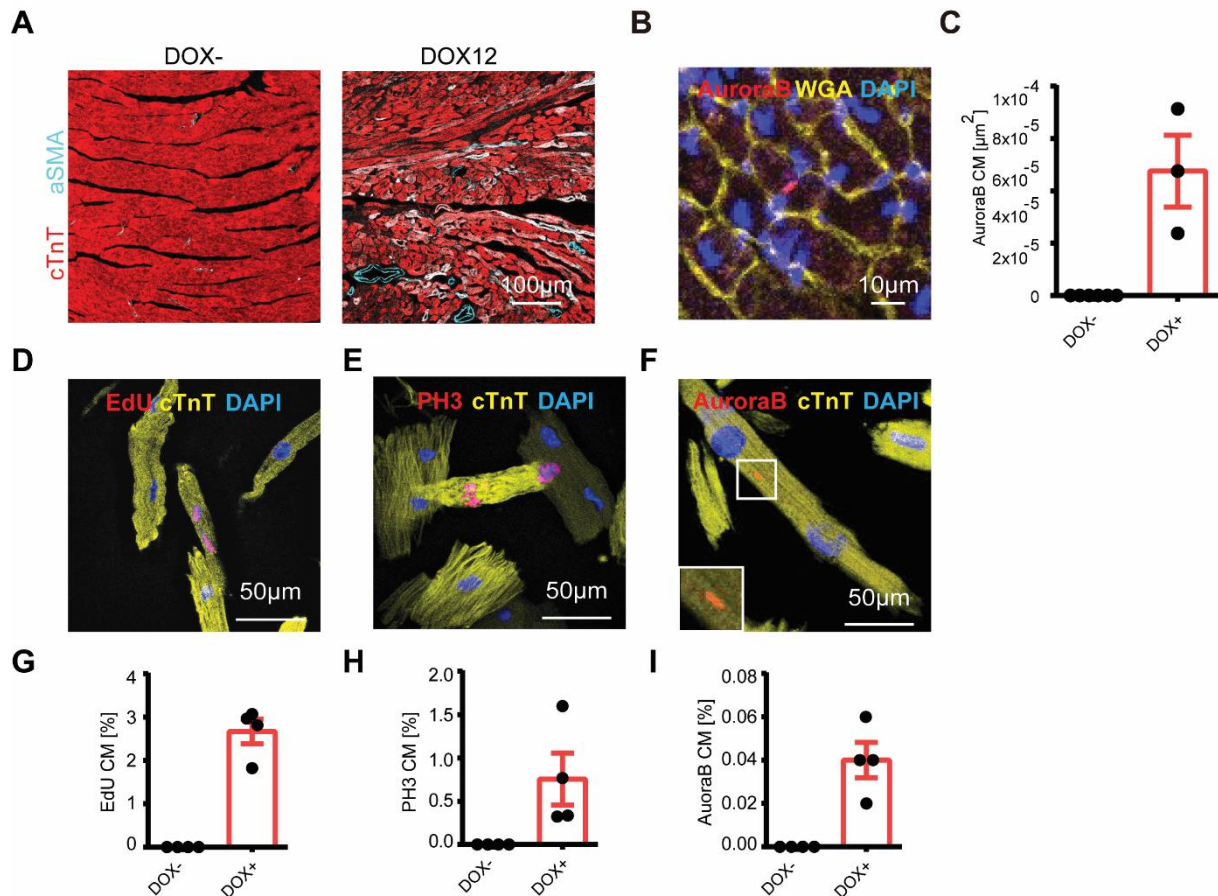


Fig. 12 OSKM expression drives adult cardiomyocyte dedifferentiation and proliferation in vivo.

(A) Immunofluorescent staining of the cardiac dedifferentiation marker a-smooth muscle actin (cyan), and the cardiomyocyte marker cardiac troponin T (red). DOX12 is the $i4F^{\text{Heart}}$ mice with 12-day-Dox treatment and DOX- is the untreated control.

(B, C) Immunostaining of cross-sectioned heart (B) and quantification (C) for Aurora B kinase (red) and WGA (yellow), $n=3$.

(D-I) Immunostaining and relative quantification of isolated cardiomyocytes for fixed adult heart with 12-day-Dox treatment, EdU (D,G), PH3 (E,H), and Aurora B kinase (F,I), $n=4$.

5.5. Transcriptome of adult cardiomyocyte is reverted to a fetal-like state upon OSKM expression

To gain comprehensive insight into molecular processes underlying induced cardiomyocyte dedifferentiation and proliferation, cardiomyocytes purified from untreated and 12 days Dox-treated adult $i4F^{\text{Heart}}$ mice were subjected to RNA sequencing and analysis. Consistent with the immunofluorescent staining (Fig. 12), differential expression analysis followed by gene ontology enrichment revealed that the most strongly upregulated genes in Dox-treated $i4F^{\text{Heart}}$

mice were those related to cell cycle (Fig. 13A, B). Downregulated genes were primarily related to mitochondria or to genes involved in fatty acid oxidation (Fig. 13A, B). Interestingly, genes involved in glycolysis were upregulated. The apparent metabolic shift was of particular interest, since proliferation competent fetal cardiomyocytes show a more glycolytic metabolism [191] (Fig. 13B,C). Consequently, the analysis was extended by including published RNAseq datasets of isolated wildtype E14.5, neonatal (P0) and adult cardiomyocytes [182] to analyze whether and to what extent OSKM-expression might rewind the developmental program. Intriguingly, linear principal component analysis (PCA) and pairwise Pearson correlation of different conditions revealed that continuous OSKM expression for 12 days induced adult $i4F^{\text{Heart}}$ cardiomyocytes to adopt a gene expression profile strikingly similar to neonatal and E14.5 cardiomyocytes (Fig. 13D,E). Separation of conditions was primarily driven by differential expression of genes within PC1 explaining more than 75% of variance. Differential gene expression analysis followed by unsupervised clustering and gene set enrichment analysis (GSEA) revealed that 40% of all genes that are differentially expressed between E14.5 and neonatal cardiomyocytes and between neonatal to adult cardiomyocytes, were inversely expressed upon induction of OSKM expression (Fig. 13F, G). In addition, the top 500 differentially expressed genes across all datasets were isolated and compared. Differential gene expression analysis followed by k-means clustering and gene set enrichment confirmed that genes related to fatty acid metabolic process and muscle contraction were downregulated in adult cardiomyocytes of Dox-treated $i4F^{\text{Heart}}$ mice in comparison to adult cardiomyocytes isolated from untreated $i4F^{\text{Heart}}$ and wildtype controls (Fig. 13H). More importantly, Dox-treated adult $i4F^{\text{Heart}}$ cardiomyocytes adopted gene expression profiles strikingly similar to proliferative neonatal and E14.5 cardiomyocytes (Fig. 13H). Taken together, these data show that forced OSKM-expression induces adult cardiomyocytes to adopt a gene expression profile that resembles an early developmental stage without losing cardiomyocyte identity.

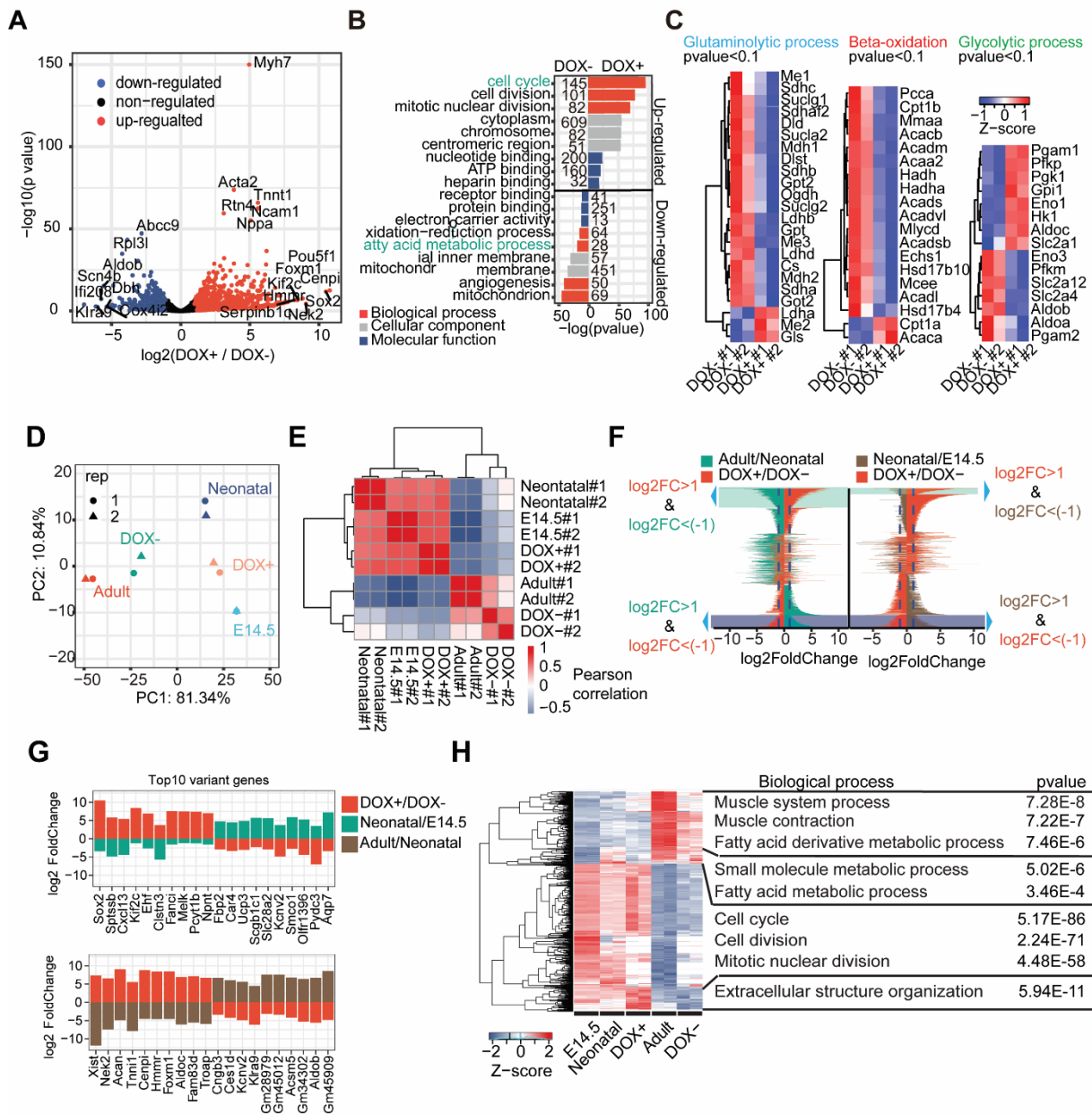


Fig. 13 Transient OSKM expression establishes an embryonic gene expression program in adult cardiomyocytes.

(A) Volcano plot of differentially expressed genes between adult cardiomyocytes isolated from DOX-treated and untreated $i4F^{\text{Heart}}$ mice. Significantly down-regulated genes ($\log_2\text{FC} < -1$) are depicted in red, up-regulated genes ($\log_2\text{FC} > 1$) in blue.

(B) GSEA of differentially regulated genes ($\log_2\text{FC} > 1$, or $\log_2\text{FC} < -1$) between adult cardiomyocytes isolated from DOX-treated and untreated $i4F^{\text{Heart}}$ mice.

(C) Heatmaps of key differentially expressed genes related to different metabolic pathways. (D and E), Principal component analysis (PCA) (D) and corresponding Pearson-correlation (E) of transcriptomes derived from isolated cardiomyocytes of $i4F^{\text{Heart}}$ mice subjected to different doxycycline regimens (E).

(F) Global comparison of differential gene expression between DOX-/DOX+ $i4F^{\text{Heart}}$ versus Neonatal/E14.5 hearts (left), and DOX-/DOX+ $i4F^{\text{Heart}}$ versus Adult/Neonatal (right). Genes are grouped based on $\log_2\text{FC} > 1$ and $\log_2\text{FC} < -1$.

(G) Top 10 differentially expressed genes from (F) between DOX-/DOX+ $i4F^{\text{Heart}}$ versus Neonatal/E14.5 hearts and DOX-/DOX+ $i4F^{\text{Heart}}$ versus Adult/Neonatal hearts.

(H) Heatmap of top 500 differentially expressed genes between all conditions. (FDR < 0.05). GO term classification is based on k-means clustering.

5.6. Sustained OSKM expression can reprogram adult cardiomyocyte to iPSC-like cells in vivo

Notably, in a previous study it was shown that in $i4F$ mice continuous OSKM expression at an organismal level leads to teratoma formation in multiple organs already within one week [164]. In contrast, cardiomyocyte-specific OSKM-expression in $i4F^{\text{Heart}}$ mice appeared to elicit a progressive induction of dedifferentiation and proliferation, which is in principle similar to reprogramming processes observed in other somatic cell types [148]. The fact that $i4F^{\text{Heart}}$ mice remained viable despite prolonged OSKM expression for 12 days raised the question whether cardiomyocytes are eventually reprogrammed when OSKM expression continues for even longer time periods. To test this, $i4F^{\text{Heart}}$ mice were continuously treated with Dox (Fig. 14A). After 3 weeks of continuous Dox treatment, $i4F^{\text{Heart}}$ mice became severely morbid in contrast to controls. Most strikingly, immunohistochemistry from cross-sectioned hearts harvested from these animals, revealed formation of neoplastic tumors, positive for alkaline phosphatase (AP) staining. Interestingly, the neoplasms primarily formed below the endocardial layer of the heart (Fig. 12B). Furthermore, Nanog^+ cells were clearly detectable in OSKM-IRES-GFP expressing cells within the neoplasms, clearly indicating that neoplasms were derived from cardiomyocytes (Fig. 14C). Next, surgically excised neoplasms were enzymatically dissociated and subjected to cell culture. Intriguingly, culture of these cells led to the growth of many colonies, which maintained Nanog expression even in the absence of Dox (Fig. 14D). These results demonstrate that sustained OSKM expression reprograms adult cardiomyocyte to nanog -expressing cells with iPSC characteristics in vivo, but requires much more time in comparison to other organs [164]. Formation of cardiac tumors also occurred in $i4F^{\text{Heart/mCherry}}$ mice, which harbor one but not two OSKM alleles and consequently express OSKM at lower levels in comparison to $i4F^{\text{Heart}}$ mice (Fig. 10). However, cardiac tumor formation occurred only after 7 weeks (Fig 14E, F). Similar to $i4F^{\text{Heart}}$ mice, the tumors exhibited Nanog expression. Importantly, activation of the H2BmCherry reporter confirmed that neoplasms were derived from Cre-recombinase expressing cardiomyocytes (Fig. 14G, H). In addition, and similar to $i4F^{\text{Heart}}$ mice, isolated cells from the $i4F^{\text{Heart/mCherry}}$ neoplasms formed Nanog -expressing colonies in the absence of

Dox in culture. Taken together, these data show that reprogramming of adult cardiomyocytes in vivo strongly depends both on levels and duration of OSKM expression.

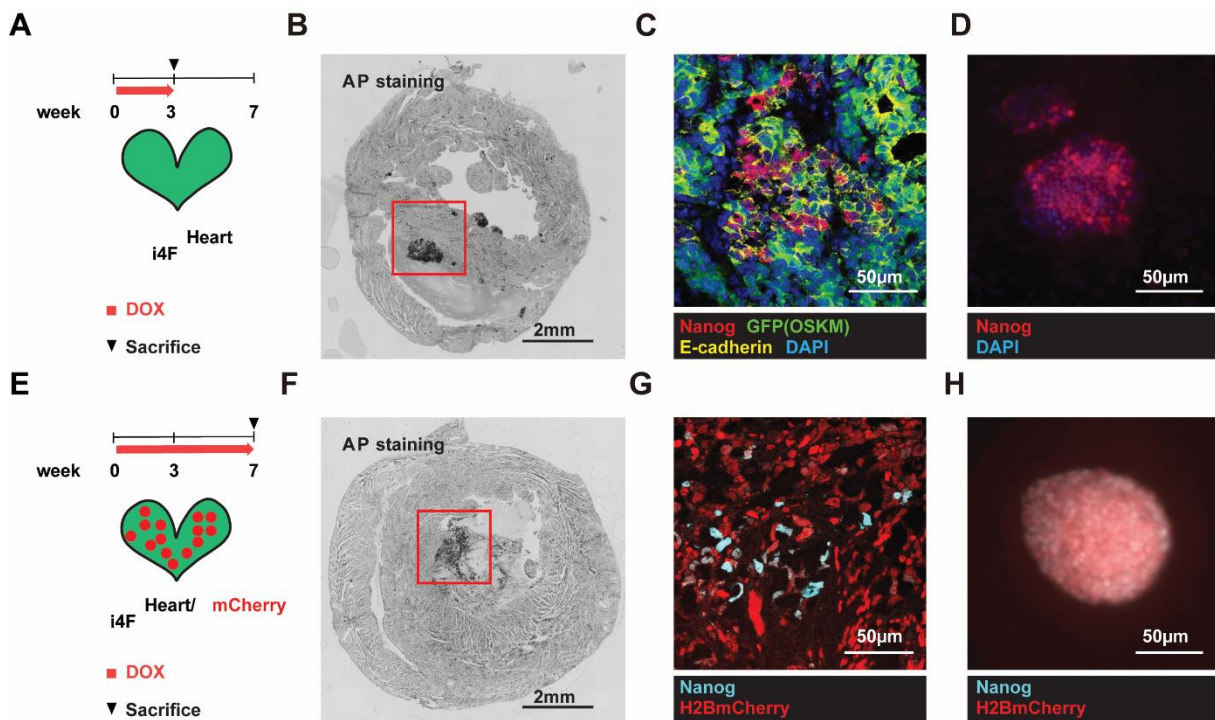


Fig. 14 Extended OSKM expression induces formation of heart tumors derived from adult cardiomyocytes.

(A) Schematic outline of sustained DOX treatment (3 weeks) in $i4F^{\text{Heart}}$ mice.

(B) Alkaline phosphatase staining of cardiomyocyte-derived neoplasms in the myocardium of $i4F^{\text{Heart}}$ mice treated with doxycycline. Scale bar = 2 mm; $n = 3$.

(C) Immunofluorescent staining of cardiac neoplasm from a cross-sectioned $i4F^{\text{Heart}}$ (from red inset in (B)). Nanog (red), E-cadherin (yellow), DAPI (blue) and OSKMIRES-GFP (green). Scale bar = 50 μm ; $n = 3$.

(D) Immunofluorescent image of a Nanog-expressing clone derived from a $i4F^{\text{Heart}}$ neoplasm (Nanog stained in red), DAPI marks DNA blue). Scale bar = 50 μm .

(E) Schematic outline of sustained DOX treatment (7 weeks) of $i4F^{\text{Heart/mCherry}}$ mice.

(F) Alkaline phosphatase staining of cardiomyocyte-derived neoplasm in the myocardium of $i4F^{\text{Heart/mCherry}}$ mice treated with doxycycline for 7 weeks. Scale bar = 2 mm; $n = 3$.

(G) Representative immunofluorescent staining of cardiac neoplasm from a cross-sectioned $i4F^{\text{Heart/mCherry}}$ heart (from red inset in (F)). Nanog (cyan) and H2BmCherry (red). Scale bar = 50 μm ; $n = 3$.

(H) Immunofluorescent image of Nanog-expressing clone (Nanog stained in blue) derived from an $i4F^{\text{Heart/mCherry}}$ neoplasm. (H2BmCherry marks nuclei in red). Scale bar = 50 μm .

Next, three clones from $i4F^{\text{Heart/mCherry}}$ mice were randomly selected and karyotyped. No chromosomal aberrations were detected, suggesting that genomic integrity was maintained in

the reprogrammed cardiomyocytes (Fig. 15A, B). Consistently, injection of $i4F^{\text{Heart/mCherry}}$ cells from one clone into blastocysts led to development of a healthy chimera in a foster mother (Fig. 15C, D). Taken together, these data formally demonstrate that adult cardiomyocytes can be fully reprogrammed to iPSCs *in vivo*.

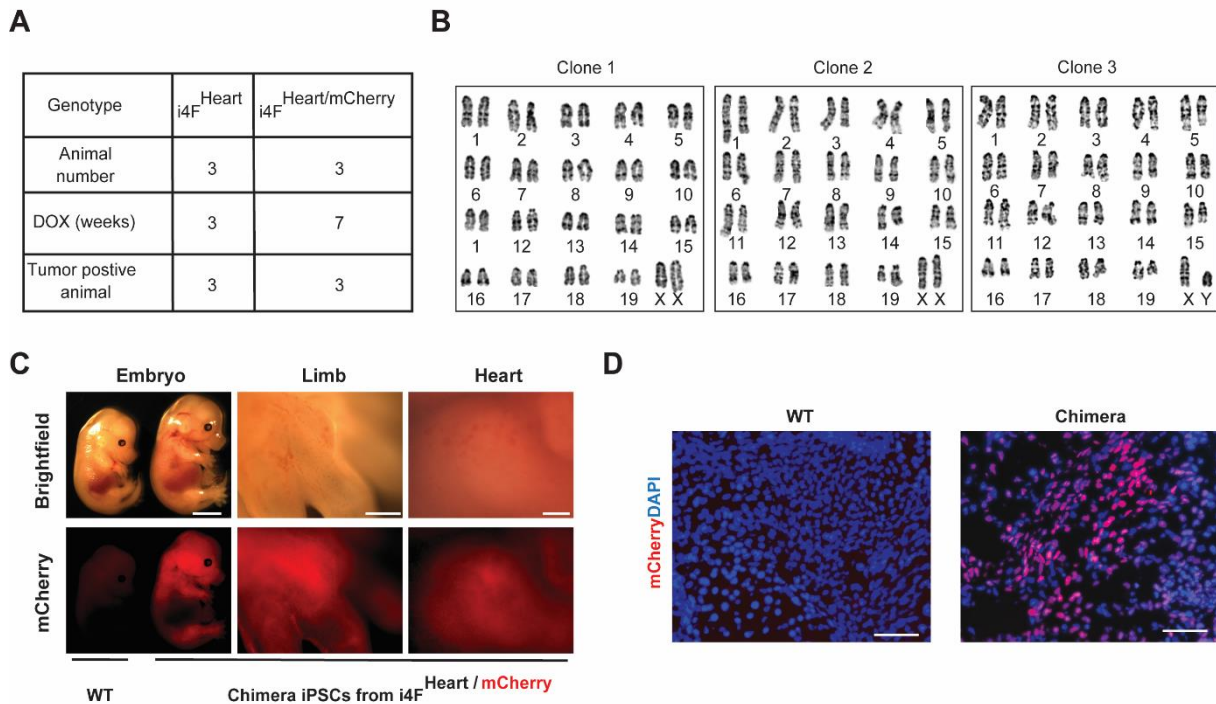


Fig. 15 Induction of pluripotency in adult cardiomyocytes by *in vivo* reprogramming.

(A) Quantification of tumor incidence in doxycycline-treated $i4F^{\text{Heart}}$ and $i4F^{\text{Heart/mCherry}}$ mice. (B) Karyotype analysis demonstrating normal chromosome content with no obvious deletions or duplications in 3 independent iPSC lines derived from adult $i4F^{\text{Heart/mCherry}}$ mice. (C and D) Formation of mouse chimera after blastocyst injection of Nanog-expressing cells isolated from heart tumors of adult $i4F^{\text{Heart/mCherry}}$ mice. Scale bar in (B)=1mm. H2BmCherry is visualized in red and DAPI in blue in section (D). Scale bar in (D)=50 μm .

The XMLC2 promoter is an early lineage marker that drives expression in the cardiac crescent during early development [184]. To confirm that solely adult cardiomyocytes express OSKM, we generated $i4F^{\text{aMHC-MCM}}$ mice, in which the OSKM expression is induced by the Myosin Heavy Chain promoter upon Dox treatment after Tamoxifen injection (Fig. 16A). At 8 weeks of age, $i4F^{\text{aMHC-MCM}}$ mice were subjected to Tamoxifen and subsequent Dox treatment as depicted in Fig. 16B. Four weeks after Dox treatment, hearts were dramatically enlarged compared to controls that had been subjected to Tamoxifen but not to Dox treatment (Fig. 16C). Strikingly, Tam/Dox-treated $i4F^{\text{aMHC-MCM}}$ mice exhibited formation of cardiac tumors similar to $i4F^{\text{Heart}}$ and $i4F^{\text{Heart/mCherry}}$ mice (Fig. 16D). Furthermore, a clear increase of aSMA^+ and PH3^+ expression was detected in cTnT^+ cardiomyocytes in the myocardium of

cross-sectioned hearts (Fig. 16E). These data indicate that cardiomyocytes dedifferentiate and reenter the cell-cycle in $i4F^{\alpha\text{MHC-MCM}}$ hearts upon Dox treatment. In addition to expression of alkaline phosphatase (Fig. 16D), cardiac tumors were also positive for Nanog and GFP cells and as such fully recapitulate the phenotype of $i4F^{\text{Heart}}$ and $i4F^{\text{Heart/mCherry}}$ mice (Fig. 16F).

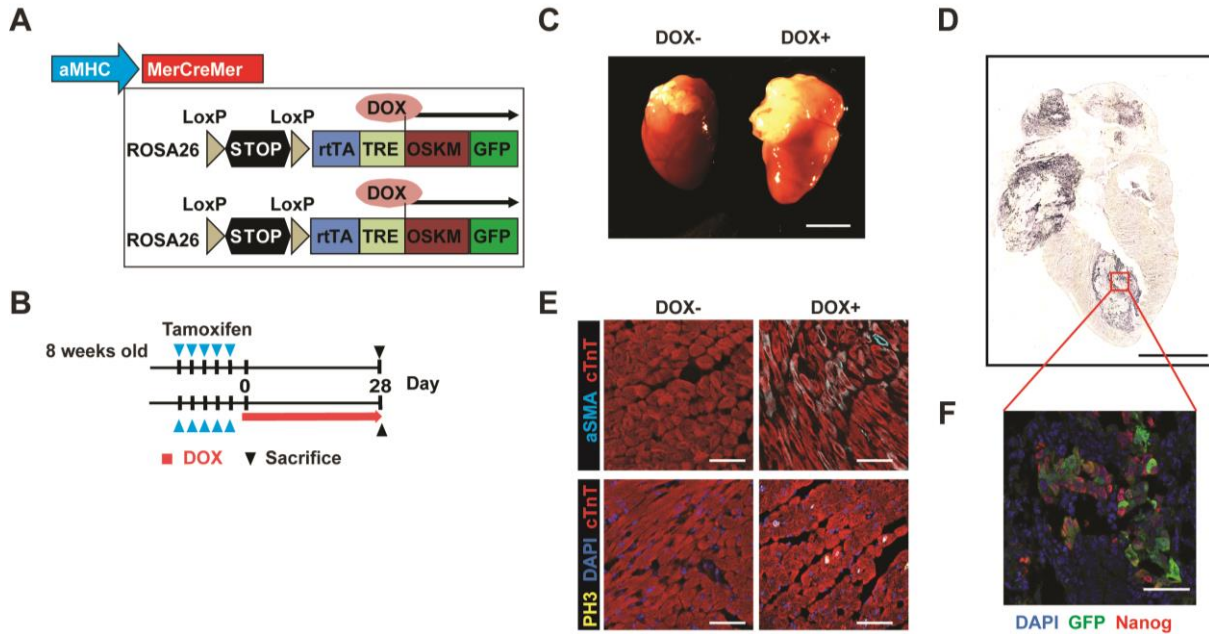


Fig. 16. Extended OSKM expression induces formation of cardiomyocyte-derived heart tumors in $i4F^{\alpha\text{MHC-MCM}}$ mice.

(A) Description of the transgenic $i4F^{\alpha\text{MHC-MCM}}$ mouse model.

(B) Schematic outline of tamoxifen and doxycycline treatments of $i4F^{\alpha\text{MHC-MCM}}$ mice.

(C) Brightfield image of whole hearts dissected from $i4F^{\alpha\text{MHC-MCM}}$ mice with and without doxycycline treatment. Scale bar=2 mm.

(D) Alkaline phosphatase staining of cardiomyocyte-derived neoplasms in the myocardium of $i4F^{\alpha\text{MHC-MCM}}$ mice treated with doxycycline. Scale bar=2 mm; n=4.

(E) Immunofluorescence staining of cross-sectioned hearts from tamoxifen-injected $i4F^{\alpha\text{MHC-MCM}}$ mice with and without doxycycline treatment for 28 days. Cardiac dedifferentiation is indicated by a-smooth muscle actin expression (cyan). Enhanced cell cycle activity is demonstrated by immunostaining of PH3 in counterstained cTnT-expressing cardiomyocytes (red). Scale bar=50 μm .

(F) Immunofluorescence staining of neoplasm from a cross-sectioned $i4F^{\alpha\text{MHC-MCM}}$ heart. Nanog (red), OSKMIRES-GFP (green) and DAPI (blue). Scale bar=50 μm ; n=4.

5.7. Temporarily-restricted OSKM expression promotes cardiomyocyte de-differentiation, proliferation and re-differentiation

So far it was shown that short-term OSKM expression promotes adult cardiomyocyte proliferation but that continuous OSKM expression leads to cardiac tumor formation in

$i4F^{\text{Heart}}$ and $i4F^{\text{Heart/mCherry}}$ mice. As the genetic system allows reversibility of OSKM expression it was hypothesized that it might be possible to enable cardiomyocytes to acquire proliferation competence without losing cardiomyocyte identity when OSKM expression is terminated before tumor formation. To test this idea, it was important to first determine the dynamics of OSKM protein expression from the polycistronic OSKM knock-in in $i4F^{\text{Heart}}$ mice upon Dox supply and withdrawal. To investigate this, Western blot analysis of Oct4 protein expression was performed from heart lysates of $i4F^{\text{Heart}}$ mice treated for different time periods with Dox. Oct4 protein was expressed as early as 2 days after administration of Dox but rapidly declined upon Dox withdrawal and was completely lost within one day (Fig 17A). This indicates that once halting supply of Dox, reprogramming of cardiomyocytes is arrested. Next, adult $i4F^{\text{Heart}}$ mice were subjected to different time periods of Dox treatment to determine an optimal condition wherein cardiomyocyte proliferation rates are significantly increased while maintaining functionality of $i4F^{\text{Heart}}$ hearts (Fig. 17B). Notably, signs of cardiomyocyte dedifferentiation and proliferation were not visible until after 3 days of continuous Dox treatment, although OSKM expression was detectable after treating $i4F^{\text{Heart}}$ mice for 2 days with Dox (Figure 17A). Early signs of cardiomyocyte dedifferentiation became apparent by 6 days of continuous Dox-treated in $i4F^{\text{Heart}}$ mice, indicated by occasional expression of αSMA (Fig. 17C). In addition, a significant increase of PH3 and AuroraB positive cardiomyocytes was indicated by immunofluorescent staining in heart cross sections and isolated cardiomyocytes (Fig. 17C-F). These data demonstrate that 6 days Dox treatment is sufficient to enable cardiomyocytes to reenter the cell cycle in adult $i4F^{\text{Heart}}$ mice. Furthermore, the data show that several days are required to induce OSKM-dependent dedifferentiation and proliferation. Strikingly, withdrawal of Dox after 6 days terminated OSKM expression after one day (Fig. 17A), which was followed by rapid loss of αSMA expression (Fig. 17C), indicating that short-term OSKM-induced cardiomyocyte dedifferentiation is a reversible process. Consistent with this, induced proliferation of cardiomyocytes was completely arrested within 4 days after Dox withdrawal (Fig. 17C, D).

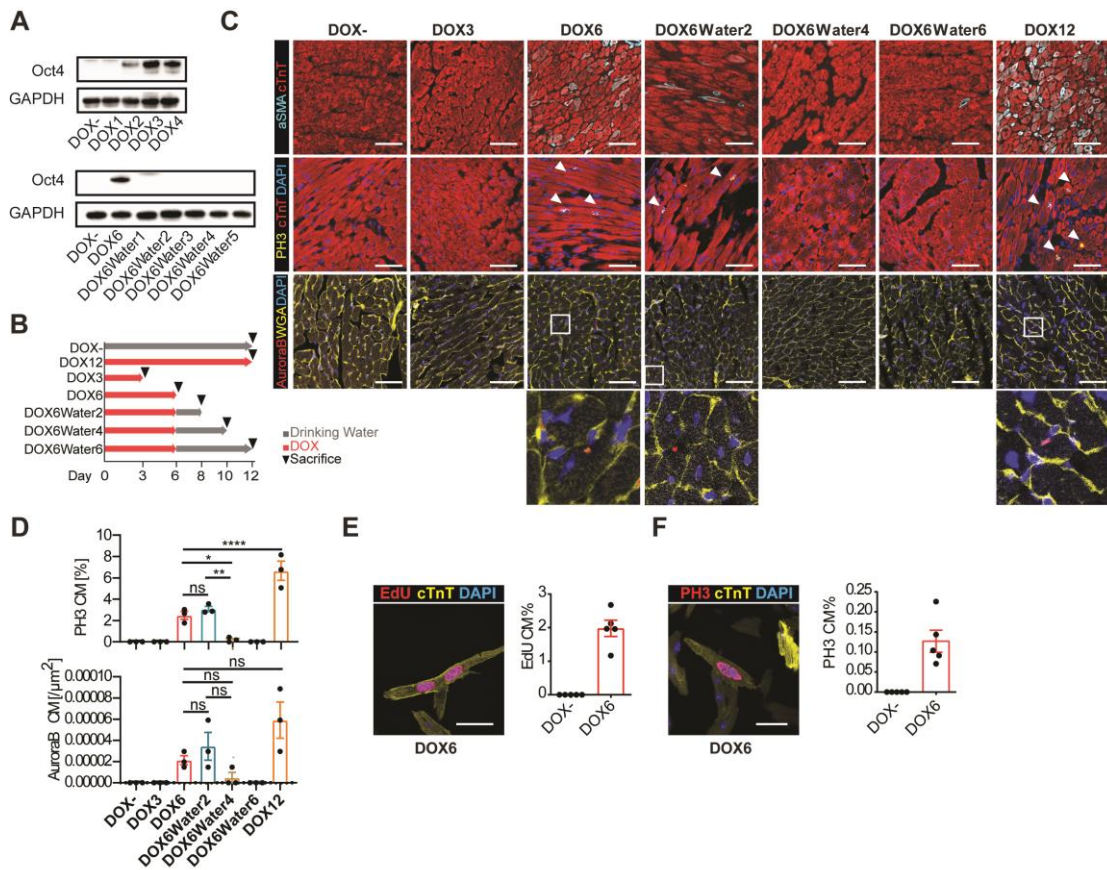


Fig. 17 Kinetics of de- and redifferentiation and proliferation of adult cardiomyocytes by doxycycline induced OSKM expression in vivo.

(A) Western blot images of Oct4 expression in hearts of i4FHeart mice upon doxycycline administration and withdrawal.

(B) Immunostaining of cross-sectioned adult hearts from i4F^{Heart} mice treated with doxycycline for indicated time lengths for cardiac dedifferentiation (a-smooth muscle actin (cyan), top panel), proliferation (PH3 (yellow) middle panel), and cytokinesis markers (Aurora B kinase (red) bottom panels). Scale bar=50 μ m.

(C) Quantification of PH3 positive cardiomyocytes as in (A). Error bars are s.e.m. p-values were calculated by One-Way ANOVA, n=3. ns P>0.05, *P<0.05, **P<0.01, ****P<0.0001.

(D) Quantification of Aurora B kinase positive cardiomyocytes as in (A). Error bars are s.e.m. p-values were calculated by One-Way ANOVA, n=3. ns P>0.05.

(E and F) Immunostaining of freshly isolated adult cardiomyocytes for EdU (E) and PH3 (F) from i4F^{Heart} mice treated for 6 days with doxycycline. Quantifications are shown on the right. Scale bar=10 μ m. n=5. Error bars are s.e.m.

Transcriptional profiles of the cardiomyocytes after withdrawal of Dox treatment were then determined and compared to the transcriptomes of cardiomyocytes treated with Dox for 6 and 12 days and to transcriptomes of cardiomyocytes from different development stages [182]. Similar to 12 days of continuous OSKM expression (Fig. 13), 6 days of continuous OSKM induced a gene expression profile strikingly similar to neonatal and E14.5 cardiomyocytes (Fig. 18A, B) as revealed by principal component and Pearson correlation analyses. As

expected, the changes of gene expression induced by OSKM expression were primarily related to cell proliferation and metabolism. Importantly, changes of gene expression levels were unidirectional and related to the length of Dox administration. For example, expression of the cell cycle regulators increased with prolonged Dox treatment whereas expression of genes related to fatty acid and/or beta-oxidation decreased. Notably, expression of Oct4, Sox2, Klf4 and c-Myc remained at the same levels. These data suggest that cardiomyocyte reprogramming is a stochastic process, which highly depends on the length of Dox administration. Importantly, gene expression changes were almost completely reverted upon Dox withdrawal (Fig. 18A-D) confirming that OSKM-induced cardiomyocyte dedifferentiation is a reversible process also at the level of gene expression. Changes in gene expression analysis were consistent the histological assessments.

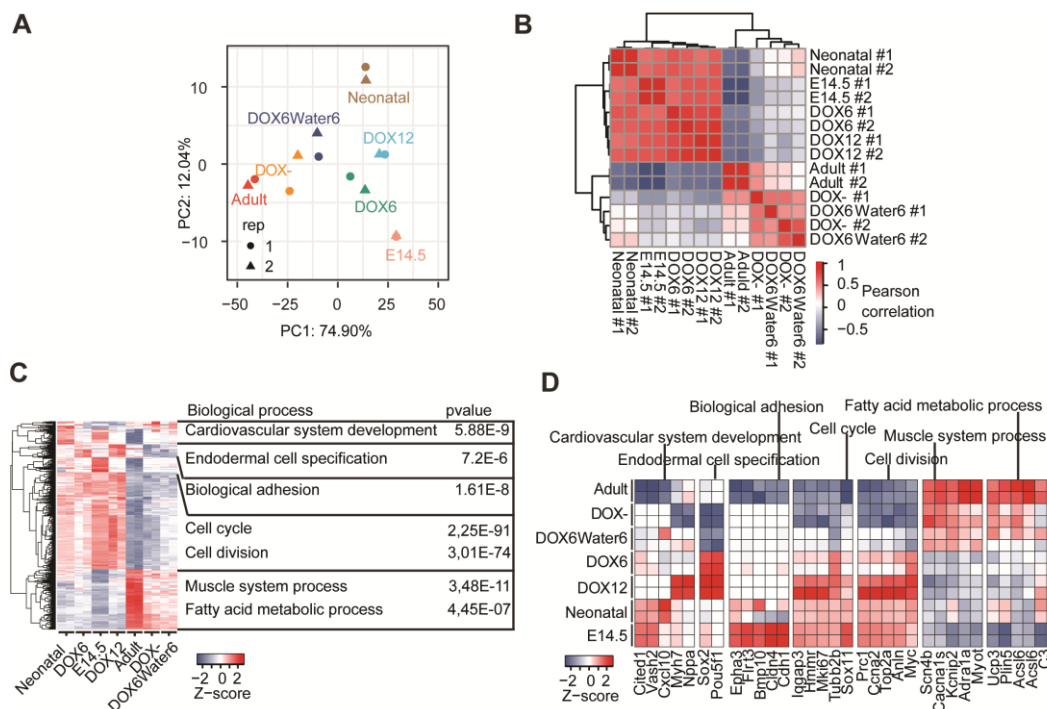


Fig. 18 Transcriptomic kinetics of de- and redifferentiation of adult cardiomyocytes by doxycycline induced OSKM expression in vivo.

(A and B) Principal component analysis (PCA) (A) and Pearson-correlation (B) of transcriptomes derived from isolated cardiomyocytes of Dox-treated $i4F^{\text{Heart}}$ mice. (C and D) Heatmaps of top differentially expressed genes according to GO classes.

To determine the effects of OSKM-induced dedifferentiation on heart function, functional magnetic resonance imaging (fMRI) measurements were performed in $i4F^{\text{Heart}}$ mice treated with the different Dox regimens. fMRI measurements creates serial images at different views

for evaluation of heart function such as left ventricle ejection fraction (LVEF), stroke volume (SV) and cardiac output (CO). Interestingly, short-term Dox treatment for 6 days did not cause significant changes of heart function in $i4F^{\text{Heart}}$ mice, indicated by unchanged SV and LVEF (Fig.19A-C). Moreover, heart functions remained normal when Dox treatment was terminated after 6 days (Fig.19A-C). In comparison to short-term Dox treatment, the 12 days Dox-treated $i4F^{\text{Heart}}$ mice displayed dramatic reduction of SV and LVEF (Fig.19A-C), consistent with pronounced dedifferentiation of cardiomyocytes. Notably, even after withdrawing Dox after they were treated with Dox for 12 days, $i4F^{\text{Heart}}$ mice became increasingly sick and died within two weeks (Fig.19D-E). Collectively, these results show that short-term OSKM expression for 6 days can elicit cardiomyocyte dedifferentiation and increase cardiomyocyte proliferation in $i4F^{\text{Heart}}$ mice without compromising heart function. In contrast, prolonged OSKM expression enhances cardiomyocyte dedifferentiation and induces higher cardiomyocyte proliferation rates, but simultaneously causes irreversible heart failure.

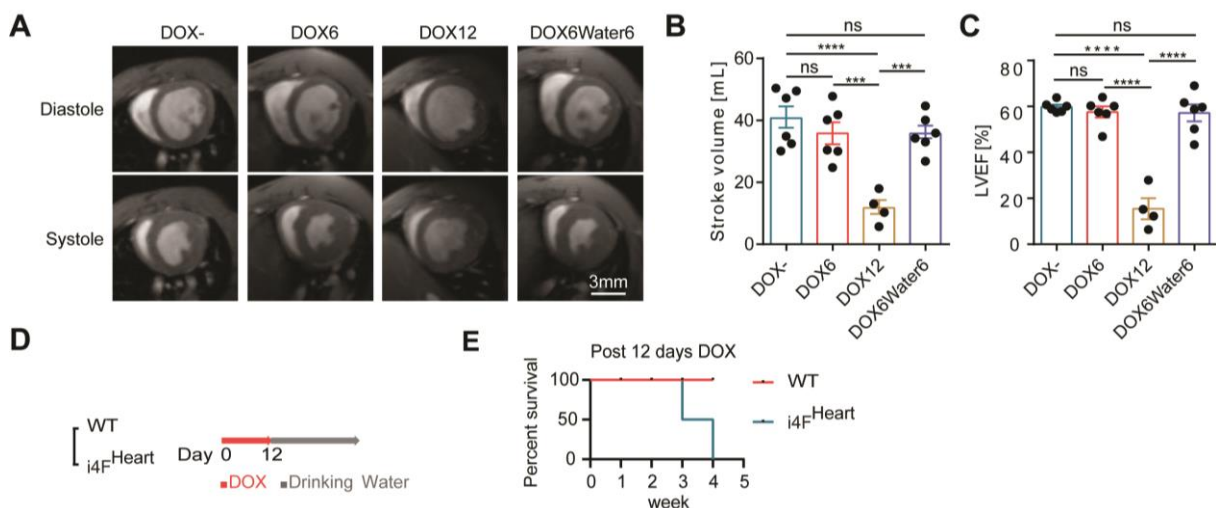


Fig. 19 Fig. S3. Effects of extended OSKM expression in the heart are not reversible.

(A) fMRI images of doxycycline-treated $i4F^{\text{Heart}}$ mice at end-systole and end-diastole.

(B, C) Cardiac stroke volumes (B) and left ventricle ejection fraction (C) of doxycycline-treated $i4F^{\text{Heart}}$ mice. n(DOX-)=6, n(DOX6)=6, n(DOX12)=4, n(DOX6Water6)=6. p-values were calculated by One-Way ANOVA. ns P>0.05, ***P<0.001, ****P<0.0001.

(D) Schematic outline of $i4F^{\text{Heart}}$ and wildtype mice with 12-day-Dox treatment and continue culturing without Dox.

(E) Kaplan-Meier survival curves of wildtype and $i4F^{\text{Heart}}$ mice treated with doxycycline for 12 days, followed by doxycycline withdrawal, n=4.

5.8. Partial OSKM expression promotes juvenile (P7) heart regeneration following apical resection

Sadek and colleagues found that significant heart regeneration occurs in 1-day-old neonatal mice after partial surgical resection of the cardiac apex. However, the regenerative capacity is lost in juvenile mice by 7 days of age, which is mainly attributed to progressive arrest of cardiomyocyte proliferation, concomitant to maturation [119]. Since transient expression of OSKM in cardiomyocyte stimulates proliferation without loss of cardiomyocyte identity, it was tested OSKM expression also enables cardiac repair in juvenile mice. To test this, the cardiac apex was resected in $i4F^{\text{Heart/mCherry}}$ P7 mice, followed by a 7 day Dox treatment regimen. In addition, mice were also injected intraperitoneally with EdU to measure cell proliferation (Fig. 20A). Control $i4F^{\text{Heart/mCherry}}$ mice underwent the same surgery but were not treated with Dox. Four weeks after apical resection and three weeks after Dox treatment the hearts were harvested and subjected to histological analyses. Consistent with previous reports, trichrome staining of cross-sectioned hearts from untreated $i4F^{\text{Heart/mCherry}}$ mice displayed severe fibrotic scarring which protruded into the endocardial layer at the cardiac apex [119] (Fig. 20B, C). In comparison, the size of fibrotic scars was significantly reduced in Dox-treated $i4F^{\text{Heart/mCherry}}$ mice (Fig. 20B, C). In addition, a significant increase of EdU incorporating H2BmCherry-labelled cardiomyocyte nuclei was observed in Dox-treated mouse hearts, compared to non-treated controls. Most interestingly, cardiomyocyte proliferation rates were highest at the border zone adjacent to the initial injury site (Fig. 20D, E), suggesting that the accompanying inflammatory response upon cardiac damage and the changes in the microenvironment promote cell cycle entry of partially reprogrammed cardiomyocytes. In summary, these results show that transient OSKM-expression efficiently extends the regenerative window of juvenile mice following amputation by induction of cardiomyocyte proliferation.

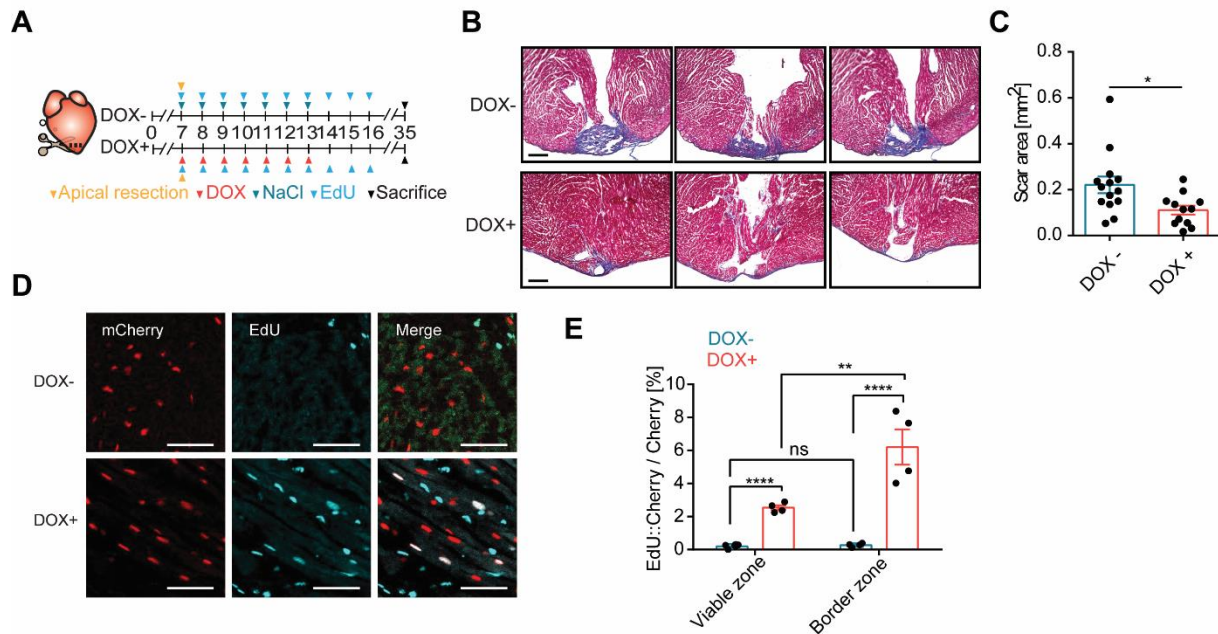


Fig. 20 OSKM enables regeneration of juvenile (P7) hearts.

(A) Schematic outline of treatments of juvenile (P7) $i4F^{\text{Heart/mCherry}}$ mice.

(B) Masson's trichrome-stain of cross-sectioned heart from $i4F^{\text{Heart/mCherry}}$ mice treated as in (A) showing fibrotic scar tissue in blue and healthy myocardium in red. Scale bar=200 μm .

(C) Quantification of scar size from (B). Scale bar=2 mm. Error bars are s.e.m., $n(\text{DOX-})=14$, $n(\text{DOX+})=12$. p -values were calculated by the unpaired Student's two-sided t-test. * $P<0.05$.

(D and E) Images (D) and quantification (E) of EdU incorporation (cyan) in H2BmCherry-labelled cardiomyocytes (red) at the injury site of $i4F^{\text{Heart/mCherry}}$ mice treated as in (A). Scale bar=50 μm . Error bars are s.e.m., $n=4$. p -values were calculated by Two-Way ANOVA. ns $P>0.05$, * $P<0.05$, ** $P<0.01$, *** $P<0.001$, **** $P<0.0001$.

5.9. Partial OSKM expression promotes adult heart regeneration and restore function following myocardial infarction

Next, it was tested whether transient reprogramming contributes to regeneration of adult hearts. To test this, cardiac damage was induced in $i4F^{\text{Heart}}$ by ligation of the left anterior descending artery (LAD) resulting in myocardial infarction (MI). Since MI rapidly induces cardiac remodeling, mice were treated with a 6-day-Dox regimen 6 days before MI (pretreatment, PT), one day after MI (acute treatment, AT) and 6 days after MI (therapeutic treatment, TT) (Fig. 21A).

Strikingly, hearts from Dox-treated $i4F^{\text{Heart}}$ mice displayed a significant decrease of scar size at 21 days after MI, compared with untreated controls under all tested conditions (Fig. 21A-C). To determine whether heart regeneration involves cardiomyocyte proliferation, EdU incorporation rates were scored in adult cardiomyocytes, in which PCM uniquely localizes to

the nuclear envelope [5, 71, 192]. A significant increase of EdU incorporating PCM1⁺ cardiomyocytes was observed in all treatment conditions (Fig. 21D-E). Notably, the highest rates of cardiomyocyte proliferation were observed at the border zone of pretreated and acutely treated infarcted i4F^{Heart} hearts (Fig. 21D, E). These results strongly indicate that transient OSKM-expression promotes heart regeneration via proliferation of pre-existing cardiomyocytes.

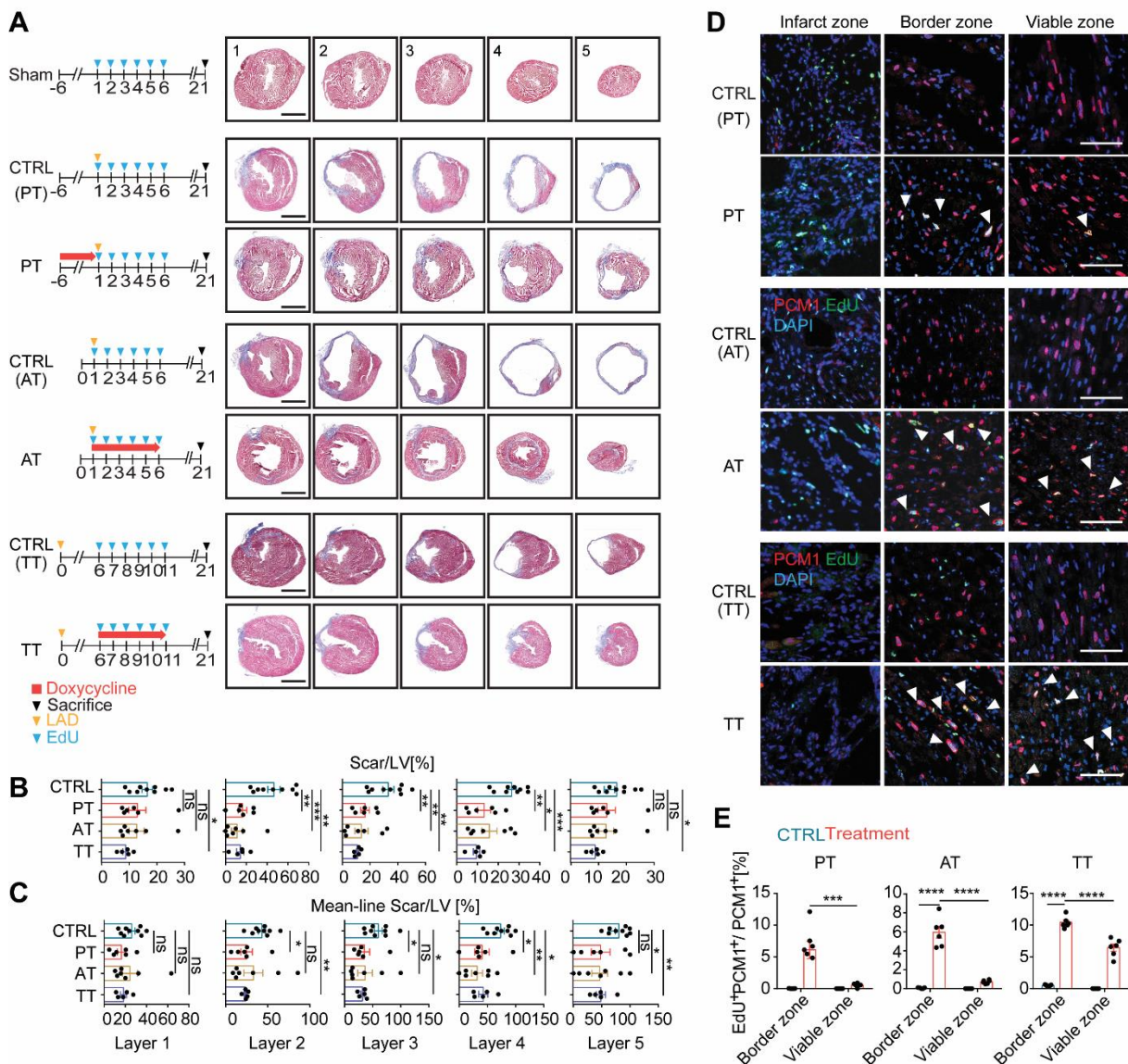


Fig. 21 Partial cardiomyocyte-specific reprogramming enables heart regeneration in adult mice.

(A) Schematic outline of Dox treatments of LAD-ligated i4F^{Heart} mice and Masson's trichrome-stained serial transverse sections showing fibrotic scar tissue (blue) and healthy

myocardium (red). A representative sham, non-infarcted heart is shown in the top panel. Scale bar=2mm.

(B) Quantification of scar size in left ventricles from (A). Error bars are s.e.m., n(CTRL)=9, n(PT)=6, n(AT)=7, n(TT)=6, p-values were calculated by One-Way ANOVA. ns P>0.05, *P<0.05, **P<0.01, ***P<0.001, ****P<0.0001.

(C) Quantification of scar midline infarct area length in left ventricles from (A). Error bars are s.e.m., n(CTRL)=9, n(PT)=6, n(AT)=7, n(TT)=6. p-values were calculated by One-Way ANOVA. ns P>0.05, *P<0.05, **P<0.01, ***P<0.001, ****P<0.0001.

(D and E) Images (D) and quantification (E) of EdU incorporation (green) in PCM1-positive CMs (red) at border, infarct and viable zones of LAD-ligated hearts from i4F^{Heart} mice, subjected to different doxycycline treatment regimens as in (A). Scale bar=50µm. Error bars are s.e.m., n=6, p-values were calculated by Two-Way ANOVA. ns P>0.05, *P<0.05, **P<0.01, ***P<0.001, ****P<0.0001.

Next, it was tested whether partial reprogramming might functionally protect cardiomyocytes from cell death after myocardial infarction. To this end, circulating levels of cTnI were measured and compared between the Dox-treated and untreated controls (24 hours after LAD ligation (Fig. 22A-C). No differences were observed between different groups, ruling out that OSKM expression enhances cardiomyocytes survival and protects the myocardium from damage. In addition, pre-treatment with Dox had no effect on the rate of MI-induced cardiomyocyte death as indicated by pronounced cleaved caspase 3 staining of cTnT+ cardiomyocytes in the infarcted zone. No differences were observed to non-treated controls (Fig. 22A-C).

Immunostaining against the pan-leukocyte marker CD45 in heart cross-sections did not reveal any differences between infarcted Dox-treated i4F^{Heart} mice and controls (Fig. 22D), which indicates that OSKM-expression does not dramatically alter the extent of inflammation upon infarction. The identity of individual immune cells was analyzed any further, leaving the possibility that OSKM expression modulates the quality of the inflammatory response. To investigate the integrity of the vasculature, CD31 (PECAM) and αSMA immunostainings were performed on cross-sections of infarcted hearts 49 days after LAD ligation in all treatment settings (Fig. 22E). As expected, cardiac vascularization was severely disrupted in the infarcted area of WT mice. Importantly, the residual infarcted areas of Dox treated i4F^{Heart} mice also displayed severe vascularization defects similar to infarcted WT mice. Therefore, partial cardiomyocyte-specific reprogramming does not induce neovascularization when a fibrotic scar is already formed. Taken together, these data strongly indicate that OSKM expression does not protect from MI-induced heart damage and enables adult heart repair through proliferation of pre-existing cardiomyocytes.

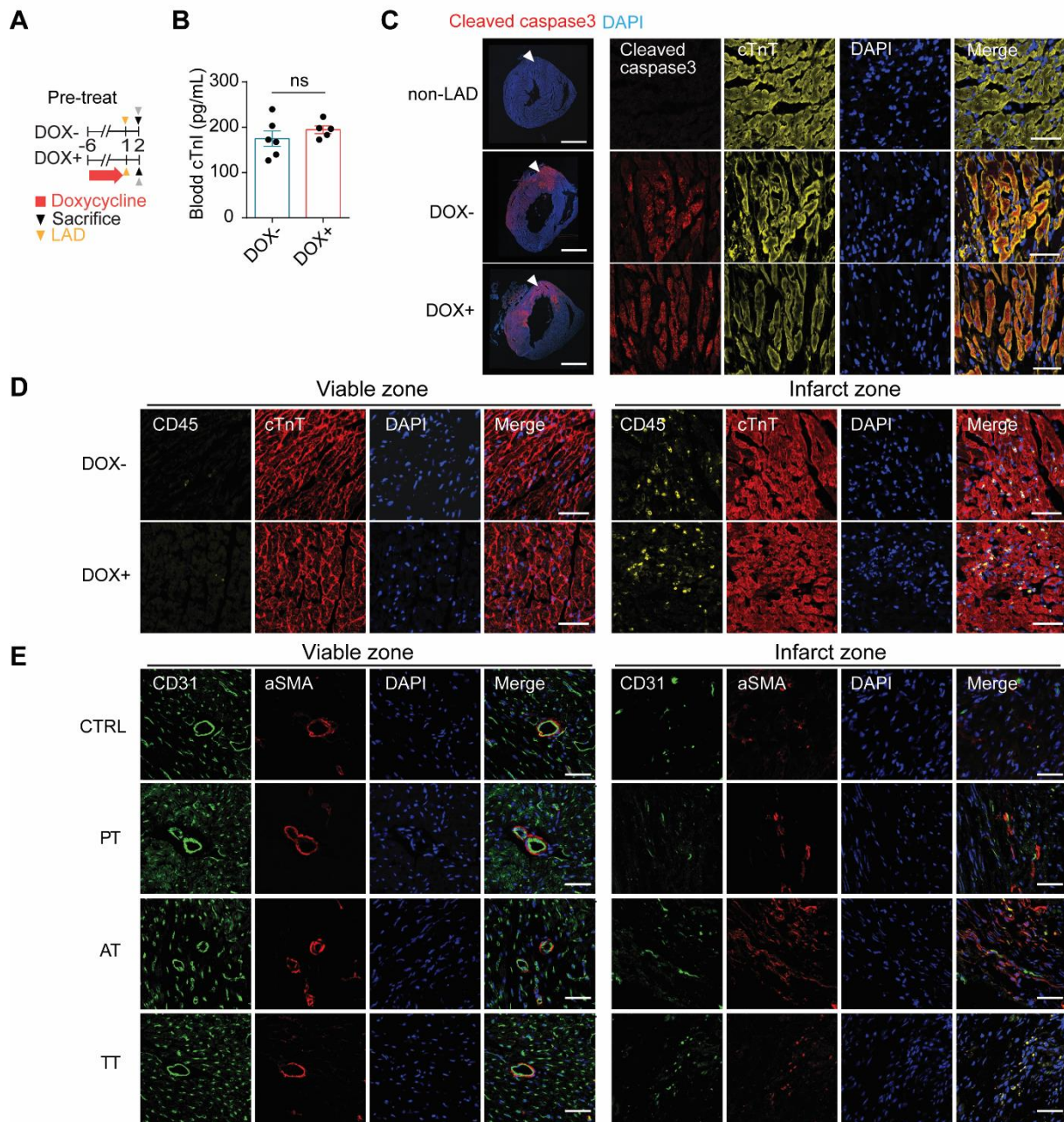


Fig. 22 Partial cardiomyocyte-specific reprogramming does not alter inflammatory and vascular responses in infarcted hearts.

(A) Schematic outline of treatment of LAD-ligated $i4F^{\text{Heart}}$ mice.

(B) Mice in different groups show no differences in cTnI serum levels (A). Error bars are s.e.m., $n=6$, p-values were calculated by the unpaired Student's two-sided t-test. ns $P>0.05$.

(C) Immunostaining for apoptotic cardiomyocytes in hearts of $i4F^{\text{Heart}}$ mice treated as in (A) Cleaved caspase-3 (red), cTnT (yellow) and nuclei by DAPI (blue). Scale bar in transverse sections=2mm. Scale bar in cross sections=50 μm .

(D) Immunostaining for the pan-leukocyte marker CD45 in hearts of $i4F^{\text{Heart}}$ mice treated as in (A) CD45 (yellow), cTnT (red) and nuclei by DAPI (blue). Scale bar=50 μm , $n=6$.

(E) Immunostaining for the vesicular marker CD31 and α SMA in hearts of $i4F^{\text{Heart}}$ mice treated as in (Fig. 22A) CD31 (green), α SMA (red) and nuclei by DAPI (blue). Scale bar=50 μ m, n=6.

To determine long-term effects of transient OSKM expression on heart function, serial functional magnetic resonance imaging (fMRI) measurements were performed up to 49 days after MI under all tested conditions (PT, AT and TT). Similar to earlier time points following MI (Fig. 21), reduced scar size (Fig. 23.A-C) and increased cardiomyocyte proliferation rates (Fig. 23D, E) were observed in hearts of Dox-treated $i4F^{\text{Heart}}$ mice. Intriguingly, fMRI revealed substantial improvement of all measured cardiac functions in $i4F^{\text{Heart}}$ mice treated with Dox before and during MI in contrast to control mice, which exhibited a continuous decrease of cardiac function up to 49 days. $i4F^{\text{Heart}}$ mice treated with Dox before and during MI exhibited significant restoration of left ventricle ejection fractions (LVEF), left ventricle stroke volumes (LVSV) and cardiac output (CO) levels over time. Notably, improvement of cardiac function was most prominent in pre-treated $i4F^{\text{Heart}}$ mice (Fig. 23F-L). Interestingly, mice treated with Dox 6 days after MI did not display significant improvement of cardiac function despite a substantial reduction in scar size. No effects on cardiac function were observed in Dox-treated WT mice (Fig. 24). As cardiac function was not completely restored in all settings, these data suggest that newly formed cardiomyocytes might not be fully functional or suboptimally arranged within the myocardium to exert full contractile force. Improving function of newly formed cardiomyocytes may allow to further narrow the gap between infarcted and sham-treated, non-infarcted hearts. In conclusion, this study shows that forced transient dedifferentiation and reprogramming of adult cardiomyocytes improves LV systolic function after MI, particularly when reprogramming is initiated as early as possible.

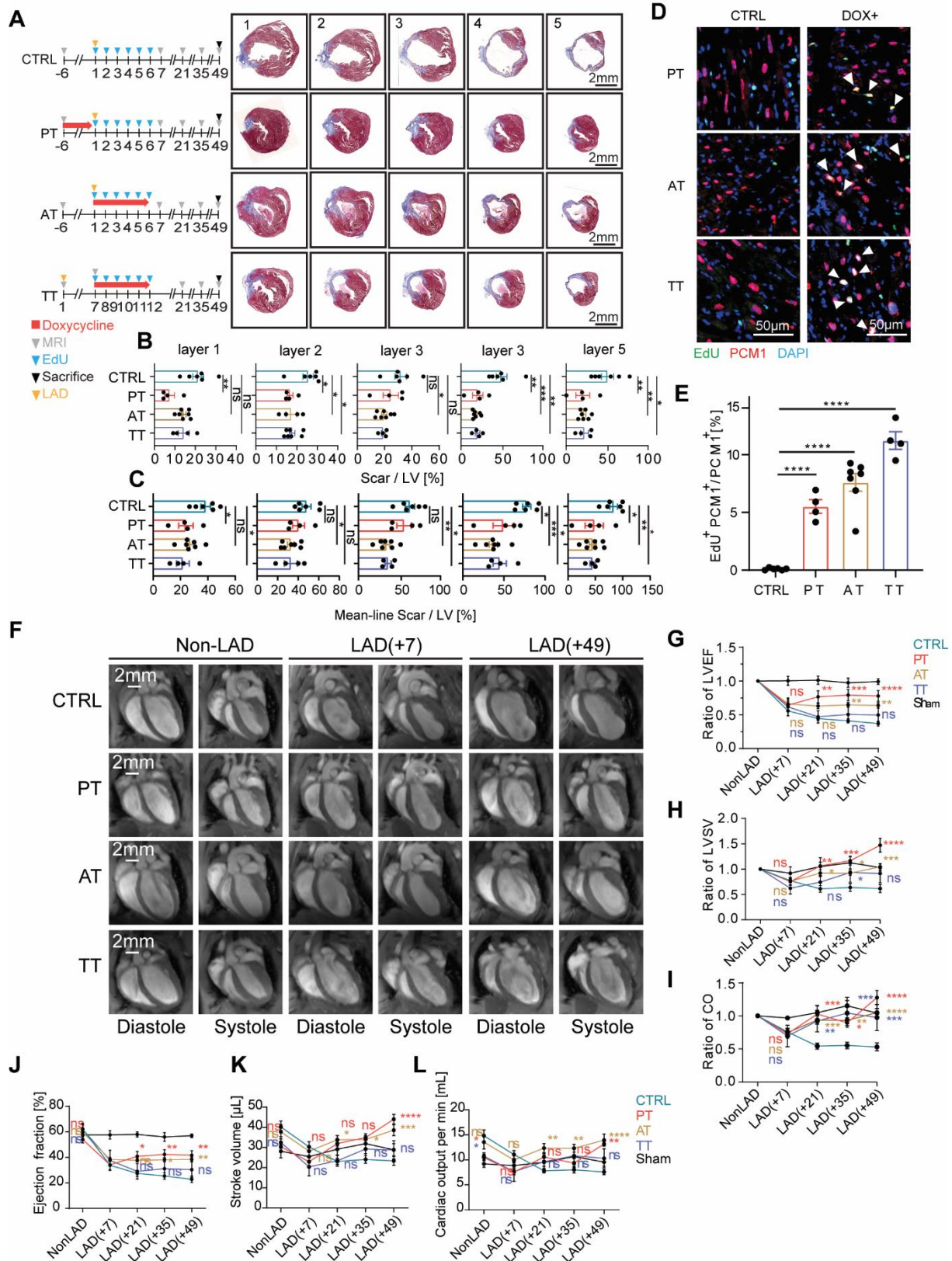


Fig. 23 Heart regeneration by partial cardiomyocyte-specific reprogramming. (A) Schematic outline of Dox treatments for LAD-ligated $i4F^{Heart}$ mice and Masson's trichrome-staining of serial transverse sections showing fibrotic scar tissue in blue and healthy myocardium in red.

(B) Quantification of scar size in left ventricles from (A). Error bars are s.e.m., n=6, p-values were calculated by One-Way ANOVA. ns P>0.05, *P<0.05, **P<0.01, ***P<0.001, ****P<0.0001.

(C) Quantification of scar midline infarct arc length in left ventricles from (A). Error bars are s.e.m., n=6. p-values were calculated by One-Way ANOVA. ns P>0.05, *P<0.05, **P<0.01, ***P<0.001, ****P<0.0001.

(D and E) Images (D) and quantification (E) of EdU incorporation (green) in PCM1⁺ cardiomyocytes (red and marked by arrows) at the border zone of LAD-ligated i4F^{Heart} hearts. (G, H and I) Serial MRI measurements showing ratios of relative changes of cardiac functions over time.

(J, K and L) Serial MRI measurements showing relative changes of cardiac functions over time.

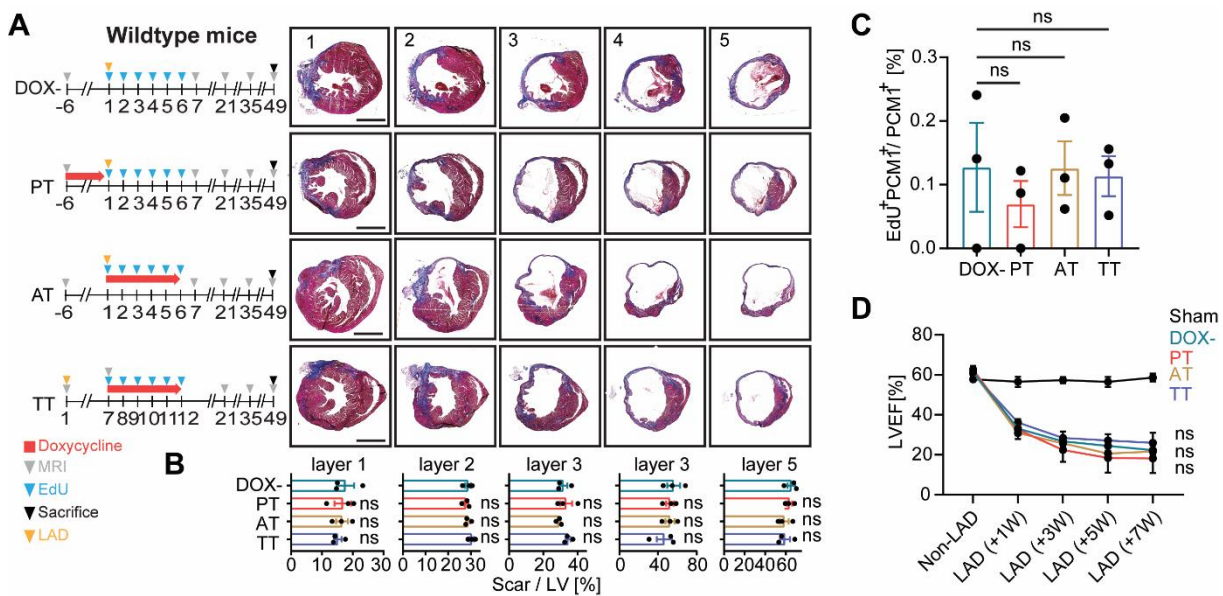


Fig. 24 Doxycycline does not affect heart regeneration.

(A) Schematic outline of doxycycline treatments of LAD-ligated wildtype mice and Masson's trichrome-stained serial transverse sections showing fibrotic scar tissue (blue) and healthy myocardium (red). Scale bar=2mm.

(B) Quantification of scar size in left ventricles from (A). Error bars are s.e.m., n=3, p-values were calculated by One-Way ANOVA. ns P>0.05.

(C) Quantification of EdU incorporation in PCM1-positive Cardiomyocytes (red) at border zones of LAD-ligated hearts from wildtype mice and subjected to different doxycycline treatment as in (A). Error bars are s.e.m., n=3, p-values were calculated by One-Way ANOVA. ns P>0.05.

(D) Serial MRI measurements showing absolute changes of LV ejection fraction. Error bars are s.e.m., n=3, p-values were calculated by One-Way ANOVA. ns P>0.05.

6. Discussion

6.1. Proliferation of cardiomyocytes

6.1.1. OSKM-induced dedifferentiation of cardiomyocytes

In this thesis, I demonstrated that cardiomyocyte-specific and transient reprogramming enables cardiomyocytes to acquire proliferation competence and thereby enables heart regeneration in adult mice. Enabling heart regeneration through induction of cardiomyocyte proliferation is considered as a promising means to restore heart function after myocardial damage. Much has been learned from the heart regenerative ability of lower vertebrates including zebrafish and more recently from the discovery that the neonatal mouse heart also owns considerable heart regenerative competence. Regardless of the species or the extent of cardiomyocyte renewal upon cardiac damage, heart regeneration appears to always rely on the division of preexisting cardiomyocytes [28, 119]. During heart regeneration in zebrafish, proliferating cardiomyocytes show a lower density of assembled sarcomeres [193] and some electrophysiological functions are disabled [68]. Furthermore, proliferating cardiomyocytes prefer carbohydrates instead of fatty acids for energy generation [194] and express genes that are normally expressed at earlier stages of cardiac development. Here, I could clearly show that all of these processes are induced upon OSKM expression in adult cardiomyocytes as they gain proliferative and hence regeneration competence. Stimulation or enhancement of cardiomyocyte proliferation seems always associated with dedifferentiation [195]. Therefore, this study supports the idea that dedifferentiation itself facilitates induction of cardiomyocyte proliferation. Interestingly, exposure of isolated adult cardiomyocytes to culture conditions also results in spontaneous cardiomyocyte dedifferentiation. However, despite the fact that cardiomyocytes dedifferentiate in both pathophysiological and culture conditions [196], cardiomyocytes usually do to reenter the cell cycle under pathological conditions [197, 198].

Currently, many strategies to elicit cardiomyocyte proliferation converge on manipulation of the Hippo-YAP signaling pathway or on hyper-activation of cell-cycle regulators [199]. However, the increase of cardiomyocyte proliferation rates by these two strategies are relatively low resulting in only moderate heart regeneration in respect to both tissue renewal and improvement of heart functions after cardiac injury. Since neither Hippo-YAP signaling

nor cell cycle regulators are normally not directly involved in cellular (de-)differentiation processes, it is conceivable that stronger dedifferentiation effectors might be needed to enhance the reentry of cardiomyocytes into the cell cycle. In support of this idea, Kisby et al., reported that transient overexpression of OSKM can increase proliferation rates of neonatal rat cardiomyocytes in vitro [200]. In extension to these findings, I demonstrated that sustained overexpression of OSKM fully rewinds the developmental program of murine neonatal cardiomyocytes to the pluripotent state in vivo. Most strikingly, forced expression of OSKM also elicits cardiomyocyte dedifferentiation and proliferation in both juvenile (P7) and adult cardiomyocytes, which at these developmental time points are widely accepted as division incompetent. Along this line, the rates of induced cardiomyocyte proliferation appeared to depend strongly on the developmental stage, since the rates of induced cardiomyocyte proliferation upon OSKM-expression decreases with maturation and age.

It was also shown in this study that the degree of dedifferentiation strongly depends on the length and dosage of OSKM expression. The longer and higher OSKM is expressed in cardiomyocytes, the more they dedifferentiate and the more they proliferate. Dedifferentiation was essentially detected by the wide-spread and progressive loss of cardiomyocyte differentiation markers and an increase of de-differentiation markers and cell cycle related genes. In comparison to previous reports, wherein dedifferentiation is usually determined by the expression of only relatively few genes related to heart development such as *Acta2*, *Myh7* and *Nppa*, here I disclosed that 40% of all genes involved in heart development are re-activated upon short-term OSKM expression. Transcriptome analyses revealed that partially reprogrammed, regenerative competent adult cardiomyocytes are strikingly similar to embryonic and neonatal cardiomyocytes that still harbor proliferative capacity. The developmental program could be rewound even further by sustained OSKM expression which eventually even led to complete cardiomyocyte reprogramming and formation of rapidly dividing pluripotent tumor cells. Together with the observation that cardiomyocyte-specific OSKM expression elicits the highest rates of induced cardiomyocyte proliferation reported to date, these findings prove that the efficiency of cell-cycle reentry and rates of cardiomyocyte proliferation are directly correlated with the extent of dedifferentiation. Consistent with this, shortly after birth when physiological enlargement of heart size is mediated in part by divisions of not yet completely mature cardiomyocytes, proliferation drops rapidly, concomitant with cardiomyocyte maturation and hypertrophic growth [201].

6.1.2. Cytokinesis of bi-nucleated cardiomyocytes

It should be noted that the switch from cardiomyocyte hyperplasia to hypertrophy coincides with division of cardiomyocyte nuclei without cell divisions, resulting in cardiomyocytes with more than one nucleus. The inherent multinucleation of cardiomyocytes thus provides a significant hurdle to distinguish nuclear divisions from true cell divisions when aiming to detect cardiomyocyte proliferation by immunohistochemical staining. Here, I performed live video microscopy and thereby provided unambiguous and direct evidence of cardiomyocyte division. So far, only two reports have provided time-lapse movies indicating division of adult cardiomyocytes in vitro by NRG1 treatment or forced expression of CDK1, respectively. [122, 140]. Interestingly, it has been suggested that bi- or multi-nucleation of cardiomyocytes provides a significant barrier towards their division, since because only division of mononucleated cardiomyocytes was observed so far [122, 189].

Here, it was formally demonstrated that bi-nucleated cardiomyocytes can in fact undergo mitosis and cytokinesis when manipulated appropriately. Most interestingly, it was found that OSKM induce bi-nucleated cardiomyocytes to enter cytokinesis without duplication of nuclei, thereby giving rise to two mono-nucleated daughters. It is tempting speculate that bi-nucleated cardiomyocytes reside in a poised state and are halted in the cell cycle, preventing them to complete cytokinesis after nuclear duplication. Rewinding the developmental program through OSKM expression appears to release this brake, reactivating the cell cycle and allowing “completion” of the halted cell division process. If this hypothesis is true, identification of the molecular mechanisms that are responsible for acquisition of the “paused” state as well as those that enable “pause release” may provide a new angle to support division of multi-nucleated cardiomyocytes for heart repair.

6.2. Cardiomyocyte reprogramming

6.2.1. OSKM induced heart tumors

In this study it was demonstrated that continuous and cardiomyocyte-specific expression of OSKM leads to the formation of heart tumors containing pluripotent cells. This observation is remarkable and changes our current view on reprogramming biology because reprogramming of cells that are considered to be non-proliferative such as adult cardiomyocytes, neurons and

skeletal muscle cells has never been shown. Since the first iPSCs were generated by forced OSKM expression in proliferating MEFs in 2006, many studies thereafter have perpetually claimed that OSKM-dependent reprogramming is strongly dependent on the proliferation rates of the donor cell, providing an explanation why cardiomyocytes, neurons and skeletal muscle fibers could not be reprogrammed so far. This assertion was reinforced by observations in i4F mice, in which OSKM expression can only be induced at the organismal level in all cells of a mouse body. In these mice, teratomas only emerge in proliferative tissues but never in low proliferative organs including heart, skeletal muscle and brain [164, 165]. These observations raised the hypothesis that low dividing cells either do not possess reprogramming competence or alternatively that low dividing cells need longer duration of OSKM expression to be reprogrammed. This idea is supported by the report that reprogramming is stochastic and highly depends on inherent proliferation rates that strongly differ between cell types [162].

However, OSKM-expressing i4F mice develop teratomas within one to two weeks and are severely morbid or die. By using a cardiomyocyte-specific Cre-Recombinase allele, I could show that i4F^{Heart} and i4F^{Heart/mCherry} mice, which enable cardiomyocyte-specific reprogramming, circumvents preceding morbidities that occur upon ubiquitous expression in OSKM in i4F mice. Essentially, this genetic setup allows to investigate long-term effects of OSKM-expression at a cell autonomous level and in cardiomyocytes *in vivo*.

I demonstrated that 3 weeks and 7 weeks of continuous cardiomyocyte-specific OSKM expression are necessary to induce formation of pluripotent heart tumors, in i4F^{Heart} and i4F^{Heart/mCherry} mice *in vivo*, respectively. This is a significantly longer time compared to *in vivo* reprogramming in other proliferative organs in i4F mice [164]. Following the hypothesis that low proliferative rate cells required longer stochastic phase, if it is true, the cardiomyocyte reprogramming indicates cell cycle is not completely arrested in adult cardiomyocytes. Or if the hypothesis is false, it suggests OSKM expression enable induce adult cardiomyocytes reenter cell cycle even if they fully lose proliferative capacity.

Interestingly, Belmonte and colleagues claimed in a previous report that heterozygous i4F mice carrying a single copy of the OSKM fail to generate iPSCs *in vivo*. However it is important to mention that the duration and dosage of OSKM expression was not revealed [171]. In contrast to this claim, I showed here that both i4F^{Heart} and i4F^{Heart/mCherry} mice, carrying one or two alleles of the OSKM cassette, respectively, both develop cardiomyocyte-

derived heart tumors through sustained OSKM expression. Importantly, $i4F^{\text{Heart/mCherry}}$ mice carrying a single copy of OSKM require much longer time of OSKM-expression to form heart tumors in comparison with $i4F^{\text{Heart}}$ mice. This is important because it indicates that both the dosage and duration of OSKM is important to avoid the risk of tumor formation when using this method to elicit cell proliferation.

6.2.2. The cells in cardiomyocytes derived heart tumor

Most interestingly, the cardiomyocyte derived heart tumors observed in $i4F^{\text{Heart}}$ and $i4F^{\text{Heart/mCherry}}$ mice contained cells expressing the pluripotency marker Nanog, of which some were positive for the epithelial marker E-cadherin. Notably, Nanog positive iPSCs isolated from these tumors contained normal karyotypes and were capable to contribute to chimera formation upon injection into blastocysts. This strongly suggests that iPSCs originate from cardiomyocytes that are mono-nucleated and not bi- or multinucleated. However, it needs to be taken into account that bi-nucleated adult cardiomyocytes may also divide and give rise to two mono-nucleated daughters upon OSKM expression in vitro. This raises the possibility that bi-nucleated cardiomyocytes could provide a source for in vivo generated iPSCs. Although it will be difficult to unequivocally prove this type of division in vivo, it would support the hypothesis of a ‘pause’ and ‘release’ mechanism of induced cardiomyocyte cytokinesis.

Interestingly, I observed many E-cadherin positive but Nanog negative cells, which surrounded the pluripotent Nanog positive cells within cardiac tumors. Since E-cadherin is an epithelial marker, this observation strongly suggests that OSKM expression converts adult cardiomyocytes to an intermediate, epithelial-like state before acquiring pluripotency. This is consistent with the fact that epithelialization appears to be required for reprogramming towards pluripotency [202]. Epithelialization seems to be a commonality of all known cell types that are on the way to become iPSCs, providing a strong clue to further understand the mechanisms of how cardiomyocytes undergo cell fate conversion.

6.2.3. Morphological and molecular changes during cardiomyocytes reprogramming

The profound morphological changes that adult cardiomyocytes undergo during reprogramming are particularly remarkable because cardiomyocytes are large in comparison to all other known reprogrammable cell types. Moreover, in the adult mouse heart, cardiomyocytes display a rigid rod-shape structure [203] and are approximately 100-200 μm in length while iPSCs are only approximately 12 μm in width. Because OSKM expression in cardiomyocytes enables formation of tumors containing iPSCs, it is surprising that adult cardiomyocytes completely change the morphology and decrease their size by at least ten-fold. It will be exciting to understand the mechanisms that enable cell and survival during such profound morphological rearrangements and obvious disintegration of their structural units.

Forced OSKM expression in cardiomyocytes seems to elicit a stepwise reversion of heart developmental processes. In the converse situation, wherein ESCs are differentiated into mature cardiomyocytes, the morphology changes in the opposite direction. It is widely accepted that epigenetic modifications, which determine gene expression programs, essentially instruct how ESCs undergo morphological changes as they differentiate. Essentially, the reversibility between starting and endpoints of cardiomyocyte/ES cell fates and the step-wise nature of reprogramming, during which the epigenome is dynamically changed while OSKM expression levels are constant in $i4F^{\text{Heart}}$ mice, is strikingly reminiscent to recursive functions (Fig. 25). In analogy, I propose that the dynamics of cardiomyocyte reprogramming can be interpreted as a recursion function during which OSKM expression continuously alters the “function of cell identity” as cells reprogram to acquire a new terminal cell fate over time.

Function:

```

Cardiomyocyte( $\int$  Epigenetics)
{
   $f1(\int$  Epigenetics) =  $\int$  Gene expression
   $f2(\int$  Gene expression) =  $\int$  Epigenetics'
  Return ( Cardiomyocyte( $\int$  Epigenetics') )
}
    
```

OSKM expression

```

Embryonic stem cell( $\int$  Epigenetics)
{
   $f1(\int$  Epigenetics) =  $\int$  Gene expression
   $f2(\int$  Gene expression) =  $\int$  Epigenetics'
  Return (Embryonic stem cell( $\int$  Epigenetics') )
}
    
```

Model:

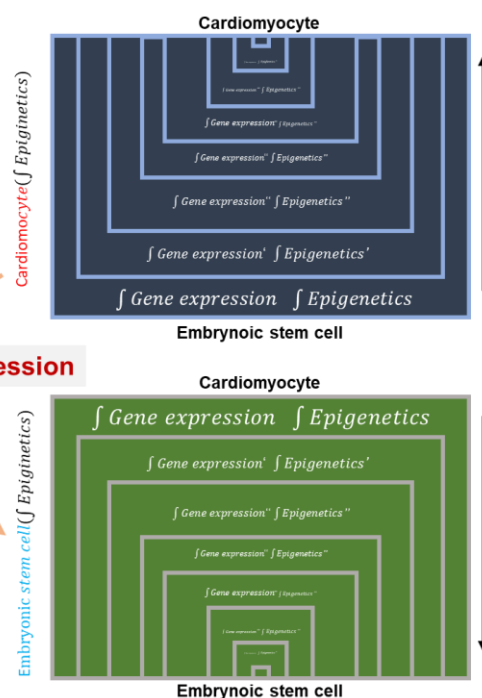


Fig. 25 The recursive function (programming) reflects progressive alterations of epigenetics and gene expression along with differentiation and reprogramming. ‘Cardiomyocyte’ is the initial function and adult cardiomyocyte is the infinite, wherein differentiation of embryonic stem cell rely on mutual effects from epigenetics and gene expression. Once OSKM expression, the main function and its’ infinite are converted to embryonic stem cell, which is caused by alteration of epigenetics and gene expression.

6.2.4. Tissue environment and cardiomyocyte reprogramming

Here, it was shown that OSKM expression converts adult cardiomyocytes to iPSCs in vivo. However, adult cardiomyocytes were not reprogrammed to pluripotency in culture despite continuous OSKM expression for up to three months. This difference suggests that the tissue environment is functionally important for reprogramming of cardiomyocytes. Environmental factors that promote reprogramming in vivo are apparently missing in culture conditions employed in this study. Conversely, it is possible that factors which are specifically inhibitory towards reprogramming of cardiomyocytes are contained in the reprogramming medium. Along this line, it has been shown by Abad et al. that iPSCs generated by in vivo reprogramming are more similar to ESCs than those generated in vitro. It was also shown in the same study that in vivo generated iPSCs own totipotent characteristics, which suggests that OSKM-dependent reprogramming in vivo can rewind the developmental program even

further than previously thought and is supported by microenvironmental cues [164]. Consistent with this assumption, it was later shown that *in vivo* reprogramming elicits senescence in some cells, which secrete the cytokine interleukin 6 (IL6) into the microenvironment, thereby increasing the efficiency of OSKM-dependent reprogramming of adjacent cells [204]. Interestingly, I did not find any evidence for senescent cells by virtue of p21 expression in i4F^{Heart} mice, which only express OSKM in cardiomyocytes and no other cell type. This suggests that full reprogramming of cardiomyocytes might not require IL6 or that other yet unknown factors promote cardiomyocyte reprogramming. I could show that OSKM-dependent dedifferentiation of adult cardiomyocytes elicits cardiac remodeling. Cardiac remodelling includes changes in the extracellular matrix [205] and immune responses [206]. It is conceivable that secondary factors associated with cardiac remodeling events contribute to and facilitate reprogramming *in vivo*. If true, identification of such factors by secretome or proteome analyses in reprogramming hearts may help to prevent the associated risk of tumor formation while enhancing adult cardiomyocyte proliferation for heart regeneration.

6.3. Reversibility of OSKM-dependent dedifferentiation

A important finding of this study is that dedifferentiated cardiomyocytes in reprogrammed hearts re-differentiate and essentially restore normal gene expression patterns when OSKM expression is terminated. Reprogramming does not fully erase the cardiomyocyte program, which is probably critical for reacquisition of the previously differentiated state. It is remarkable that the length and dosage of OSKM expression determines a point of no return, after which cardiomyocyte cannot re-differentiate anymore (Fig. 26). It will be important to understand whether and to what extent the heart environment itself is cardiogenic and can support redifferentiation of the reprogrammed fetal-like cardiomyocytes when OSKM expression is terminated. Loss of such a favorable environment upon prolonged OSKM expression might contribute to the failure of cardiomyocytes to re-differentiate.

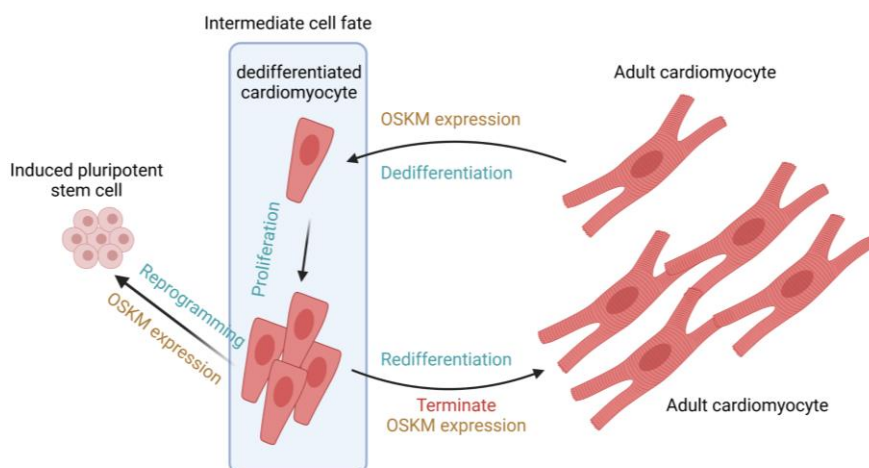


Fig. 26 Schematic diagram of OSKM-mediated conversion of adult cardiomyocytes into an intermediate state. Dedifferentiated cardiomyocytes can proliferate, be reprogrammed with prolonged OSKM expression and redifferentiate to adult cardiomyocyte by terminating OSKM expression.

Previously it was reported that partial reprogramming rejuvenates cells by reversion of age-associated epigenetic hallmarks while the differentiated status of cells is not significantly altered. However, the latter claim was not supported by differential gene expression analyses and in comparison to “young” counterparts of “old” tissues and cells [171, 172]. How and to what extent gene expression and epigenetic rejuvenation patterns correlate and to what degree they are reversible during partial reprogramming remains an open question. In this regard, it is likely that significant differences between different cell types and tissues exist. Moreover, how epigenetic rejuvenation and/or whether defined epigenetic landscapes determine the biological clock of an organism are exciting questions for future studies. In respect to rejuvenated cardiomyocytes, it will be interesting to understand whether and how redifferentiated expression patterns correlate with reacquisition of epigenetic tags that are altered during aging such as DNA methylation patterns [207, 208] or certain histone modifications[209]. While heart function is not significantly influenced by short-term, transient OSKM expression in cardiomyocytes, sustained OSKM expression causes heart failure. When dedifferentiation of cardiomyocytes goes too far, the subsequent decrease of heart function cannot be reverted upon termination of OSKM expression, resulting in death of the animal. This indicates that the microenvironment of the heart cannot support re-differentiation when dedifferentiation of cardiomyocytes exceeds a certain threshold. Therefore, identifying mechanisms and means that facilitate and enhance redifferentiation will

be as important as a full understanding of the dedifferentiation processes that instate the rejuvenated, proliferation and regenerative competent state.

6.4. Perspectives

Overall, the most important discovery made in this thesis is that the mammalian heart acquires significant regenerative potential by acquisition of a fetal-like state through transient and cardiomyocyte-specific expression of OSKM. Thus, the study opens exciting new perspectives to enable heart regeneration in humans. However, when considering to apply this concept for safe clinical applications, at least three major issues need to be solved. First, the precise mechanisms of OSKM-dependent dedifferentiation and redifferentiation need to be fully elucidated. The second issue is to find ways to increase regenerative efficiency. And the last is to find efficient and safe delivery systems that will allow reversible and specific expression of OSKM in human cardiomyocytes.

6.4.1. Mechanism of partial cardiomyocyte reprogramming

Although transient OSKM-dependent reprogramming can promote heart regeneration, it also bares critical risks. Here, it was shown that extended OSKM expression does not allow redifferentiation of dedifferentiated cardiomyocytes, resulting in irreversible heart failure. Furthermore, cardiac tumors form when cardiomyocytes undergo full reprogramming. Therefore, in order to provide perspectives for therapy, it is of great importance to understand the exact mechanisms of OSKM-dependent cardiomyocyte de- and redifferentiation.

If OSKM expression is terminated early enough, transcriptomic patterns of partially reprogrammed, dedifferentiated cardiomyocytes can be reverted. I did not observe a decrease of left ventricular ejection fraction in $i4F^{\text{Heart}}$ mice when OSKM was expressed for 6 days. Moreover, cardiac tumor formation did not occur over a two-month follow up. However, longer follow-up times are needed, since not all deregulated genes fully reacquire their previous expression levels when OSKM expression was terminated. Conceivably, abnormal expression levels might result in cardiomyocyte dysfunction and consequential cardiac disease over extended time periods. This possibility is particularly obvious for incompletely reverted gene expression pathways that are related to mitochondria homeostasis and oxidative phosphorylation. Along this line, I showed that OSKM expression elicits a progressive metabolic shift towards glycolysis from oxidative phosphorylation, which is the main energy supply of cardiomyocytes. If expression of many critical genes related to oxidative

phosphorylation cannot be fully restored, a shortage of energy production might occur, impairing long-term contractility of adult cardiomyocytes. Metabolic remodeling is associated with heart failure [210], which illustrates this concern. Long-term OSKM expression (12 days) accelerates metabolic remodeling, which may enhance the risk for heart failure and lethality. Therefore, the therapeutic window, during which reprogramming can induce beneficial, regenerative effects, is relatively small. Of course, identifying specific dosages and durations of OSKM expression will be important to provide any therapeutic perspective of OSKM expression for inducing heart-regenerative capacity. However, understanding the precise molecular mechanisms as to when and especially how the benefits of OSKM expression turn into detrimental effects will be much more informative. Preventing deregulation of genes that are not required for partial reprogramming but critical for heart functions might be a possible solution. Alternatively, identifying factors that could support and accelerate the cardiomyocyte de- and redifferentiation processes might provide leverage to make heart repair processes faster than the development and manifestation of an adverse cardiopathogenic state.

Along this line, it might be possible to directly target epigenetic pathways that are controlled by OSKM to promote cardiomyocyte proliferation, essentially bypassing the function of OSKM. Such a concept is supported by the idea that OSKM-induced somatic cell reprogramming is essentially an epigenetic process that is amenable to acceleration by epi-metabolic adjustments [157]. More importantly, this study demonstrates that epigenetic alterations in cardiomyocytes happen in cardiomyocytes due to OSKM expression, since I showed that adult cardiomyocytes can transit between adult and fetal-like states by reversible reprogramming. Even more compellingly, I could show that adult cardiomyocytes can fully reprogram to karyotypically normal pluripotent cells capable of chimera formation.

Similar to the reasons stated above, it is tempting to speculate that some epigenetic alterations are not reversible, which could lead to heart dysfunction, since many cardiac diseases are also correlated with epigenetic dysregulation of cardiomyocytes. Prominent examples include distinct changes of CpG methylations that are associated with chronic dilated cardiomyopathy [211] or cardiomyocyte-specific deletion of the H3K79 methyltransferase DOT1L which leads to cardiac remodeling and cardiomyocyte death [212]. Interestingly, DOT1L itself has been shown to be necessary for OSKM-dependent reprogramming [213]. It remains unknown whether long-term OSKM expression in cardiomyocytes leads to irreversible epigenetic alterations. Owing to the potential impact of epigenetic alterations as an underlying cause of cardiac disease, it will be important to identify the precise epigenetic underpinnings of

cardiomyocyte reprogramming and to understand to what extent epigenetic modifications are reversible as an outlook towards developing safe clinical applications.

Clearly, obtaining a deeper understanding of the reprogramming of cardiomyocytes will be decisive. In addition to this, and just as important, will be a better understanding of the functions and roles of non-myocyte cell types that contribute to maintenance of cardiac homeostasis and that will very likely play important roles during the acquisition of a regenerative state. Such non-myocyte cell types include fibroblasts, endothelial cells, adipocytes, smooth muscle cells and neuronal cells [2] that are important for physical connections [214], paracrine signaling [215] and autocrine signaling [216] within the heart and with cardiomyocytes specifically.

In this context it is particularly fascinating that partial reprogramming reduces scar sizes after myocardial infarction. This is important because cardiac fibrosis is a direct consequence of myocardial damage [217]. Myocardial infarction normally results in cardiomyocyte death, which promotes differentiation of cardiac fibroblasts to myofibroblasts [218]. These cells secrete pro-inflammatory cytokines [219] and direct remodelling of the extracellular matrix (ECM), preventing cardiac rupture [220]. However, depending on the extent of myocardial damage, excessive cardiac fibrosis will aggravate cardiac pathology and exacerbate heart failure. Therefore, understanding how partial reprogramming influences the crosstalk between cardiomyocytes and fibroblasts in reducing scar size will provide key insights into normal and improved mechanisms of heart repair.

Intriguingly, although OSKM expression occurs in all cardiomyocytes throughout the heart, cardiomyocyte proliferation predominantly occurred at the border zone of infarcted heart adjacent to the injury site where a scar would normally form. It is tempting to speculate that infiltrating immune cells and/or non-myocytes that are activated or recruited to the infarct site might secrete factors to support proliferation of reprogrammed cardiomyocytes. This idea is consistent with the observation that cardiomyocyte proliferation was much more pronounced in vivo than in in vitro cultures, wherein such factors putatively emanating from the infarcted microenvironment are missing. Identifying such factors may create exciting new angles and approaches for heart therapy.

6.4.2. Timing of OSKM expression for heart regeneration

For the heart regeneration studies I initiated short-term OSKM expression at three different time points, which were prior to MI (pretreatment), immediately following MI (acute treatment), and one week after MI (therapeutic treatment). Interestingly, cardiomyocyte proliferation rates increased in all settings along with decreased scar formation. A short window of OSKM expression is therefore sufficient to allow cardiomyocytes to proliferate and repopulate the damaged area with new cardiomyocytes where scarring would normally occur.

Dedifferentiated cardiomyocytes proliferate to repair injured heart due to OSKM expression, although OSKM expression is terminated before induction of MI in the pretreatment setting. This strongly suggests that the acquired fetal-like state of cardiomyocytes itself endows the adult heart with a certain degree of regenerative capacity and is responsive to myocardial damage, similar to the regenerative neonatal heart. In the pretreatment condition, cardiomyocytes are already sufficiently dedifferentiated, creating regenerative-competent state before myocardial damage occurs. However, in clinically relevant settings, patients will seek treatment after a myocardial infarction has already occurred. Thus, it is very important that heart function was not restored, although the therapeutic intervention decreased the relative fibrotic scar size after myocardial infarction. This raises the questions whether it is feasible to restore heart function in human patients solely by transient OSKM expression and more specifically, why heart function cannot be restored when transient OSKM expression is initiated at later time points and cardiomyocyte proliferation takes place.

It needs to be noted that for all treatment settings I employed a 6-day regimen to induce cardiomyocyte dedifferentiation. Lower dosage and/or shorter duration of OSKM expression might be required to enable functional recovery after myocardial infarction in the therapeutic setting. This idea might appear counterintuitive at first but is based on the fact that myocardial infarction alone is sufficient to induce a significant degree of cardiomyocyte dedifferentiation and remodelling [221, 222]. This knowledge, together with the observation that effects of OSKM expression for longer than 6 days are not reversible anymore, raise the possibility that the 6-day regimen in the therapeutic setting will surpass the point of reversibility.

Cardiomyocytes in the border zone are already dedifferentiated to a certain extent and thus might be pushed too far by 6-days of OSKM expression, preventing redifferentiation. This idea is supported by the observation that cardiomyocyte proliferation rates were markedly

higher in the therapeutic setting compared to the pretreatment and acute treatment settings. It will be important to fully characterize cardiomyocytes at distinct stages of reprogramming and in different settings (e.g. before, during and after infarction) to better understand if and how partial reprogramming can be therapeutically utilized to improve cardiac function even at later time points.

It needs to be noticed that after cardiac injury, the damaged heart essentially forms a new microenvironment, which is already established before OSKM expression is induced in the therapeutic model. The new microenvironment supports healing and fibroblast-dependent scarring and this is needed to rapidly reach a steady state that enables organismal survival. However, this goes along with immediate reduction of heart function and essentially an overall change of heart morphology. Thus, despite of the increase in cardiomyocyte proliferation, heart function may never be completely restored after damage, simply because the injured heart and cardiovascular system have already acquired a new but altered state, involving widespread changes and involving many different cell types. These changes cannot be reverted by only increasing cardiomyocyte proliferation. Once a new balance has been established, changes are more difficult to accomplish. Therefore, it is important to discriminate between prevention of pathological phenotypes by regeneration and reversal of established pathologies. In other words, once a damaged system acquires stability, it will be difficult to completely undo established changes.

Nevertheless, there are approaches that together with partial reprogramming may help to conquer the obstacles of treating heart failure, which might include identifying optimized OSKM-expression conditions concerning dosage and duration as explained above. Simultaneously removing fibrotic tissues together with transient OSKM-expression might provide another reasonable means to restore heart function of already damaged hearts. This could be achieved by introduction of engineered T cells that can specifically target and reduce cardiac fibrosis [223] which has been shown to improve cardiac functions of injured hearts [223, 224]. It will be exciting to combine these two approaches in future studies, which together might create an efficient method for heart repair.

6.5.2. Delivery

This study is a proof-of concept demonstrating that significant heart regeneration can be achieved by controlled OSKM expression in transgenic mice.

Harnessing this concept for future clinical applications, requires alternative strategies that enable exogenous delivery of OSKM into human cardiomyocytes. A promising strategy for the delivery of transgenes is the use of engineered recombinant adeno-associated virus (rAAV). Indeed, a series of gene therapies involving rAAVs have already been applied in clinic trials, such as the delivery of rAAV2-CFTR for treatment of cystic fibrosis [225], rAAV2-FIX for hemophilia B [226], rAAV2-RPE65 for Leber congenital amaurosis RPE-65 deficiency [227], rAAV2-hAAT for AAT deficiency [228], and rAAV9-smn1 for spinal muscle atrophy type 1 [229]. Notably, the rAAV2-RPE65 and rAAV9-smn1 based therapies have been approved by the Food and Drug Administration (FDA) in 2017 and 2020, respectively, clearly indicating the therapeutic promise of rAAV-based gene therapies for a wide range of human diseases.

Delivering rAAV to express OSKM for therapeutic purposes however faces the problem that Oct4, Sox2, Klf4 and cMyc own a tumorigenic potential, especially when expressed in cells that are inherently proliferative [171]. Therefore, it will be especially important to secure cardiomyocyte-specific expression of rAAV. It is possible to generate rAAVs with different tissue-specific tropisms such as AAV6 and AAV9 serotypes that show higher tropism for cardiomyocytes. More recently, it was shown that AAVs with highly specific tropisms can be generated by directed evolution, providing perspective for cardiomyocyte-specific expression of OSKM [230, 231]. An alternative strategy to rAAV-based gene delivery might be the delivery of lipid nanoparticle-mRNAs directly into cells. Such methods have been developed and are under clinical evaluation. They are used to target cancer, genetic diseases and virus infections, the most prominent example is the use of mRNA vaccines against coronavirus disease 2019 (COVID-19). Strategies exist to make lipid-nanoparticles cell type specific but the technology requires further efforts to become more specific and fail-proof.

Lastly, the effects of OSKM expression in human adult cardiomyocytes essentially remain unknown. A first step will be to confirm the concepts of inducing cardiomyocyte proliferation by transient OSKM expression in human cells. Inducing OSKM-expression in engineered heart tissues derived from human iPSCs [232, 233] or cardiac organoids [234] will be useful to gain first insights. Many important and exciting questions related to the mechanisms and translational potential of partial reprogramming for cardiac regeneration remain to be answered. This study paves a novel avenue of research to exploit future possibilities to accomplish mammalian heart regeneration.

Acknowledgements

I would like to express my deepest gratitude to my supervisor Dr. Johnny Kim, who gave me the chance to perform this fantastic project. He used his sincerity, encouragement, and inexhaustible passion to support me through my entire PhD journey. I am thankful for him to give me enough freedom and source to learn technologies. Those brainstorming sessions with him are the precious gifts of my life.

I would like to express my sincere gratitude to Director Prof. Dr. Thomas Braun and associate colleagues, Dept. Cardiac Development and Remodeling, Max Planck Institute for Heart and Lung Research, for providing me this chance and supporting my study in institute.

I am grateful to have worked with the members in AG.Kim, Giovanni Maroli, Felipe Luettmann, Krishna Sreenivasan, Jiasheng Zhong, Lisa Röhn and Lea Frauendorfer. And I am really appreciate the supports from all of you.

I have to express my gratitude to Astrid Wietelmann and Ursula Hofmann, who patiently taught me to use the magnetic resonance imaging machine for measurements.

I am thankful to Marion Wiesnet for kindly sharing her experience and all wonderful discussions about critical technical skills, cardiomyocyte isolation and LAD ligation.

I am grateful to be supported by wonderful colleagues, especially Stefan Guenther, Susanne Kreutzer and Sonja Krueger for technical support.

I am happy to have met friends in the institute, and I enjoyed sharing ideas with each other.

I must thank my previous supervisor Ralf Jauch, for introducing me to this fantastic institute. And I am so delighted for publishing the ePOU project with his support.

Special thanks goes to my partner Qing Zhang, who always supported me. Sincere thanks goes also to my mother Yan Xiang, father Min Chen and grandmother Ruiqiu Luo.

List of abbreviation.

Unit

°C	°C centigrade Celsius
µg	microgram, 10 ⁻⁶ g
µL	Microliter
µm	micrometer, 10 ⁻⁶ m
µM	micromole(s), 10 ⁻⁶ mole(s)
bp	bp base pairs
cm	Centimetre
g	gram(s)
h	hour(s)
kbp	kilo base pair(s)
kDa	kiloDalton
L	liter(s)
M	Molar
Mg	Milogram
min	minute(s)
mL	milliliter, 10 ⁻³ L
mM	millimole(s), 10 ⁻³ mole(s)
mm	millimeter, 10 ⁻³ m
ng	nanogram(s), 10 ⁻⁹ g
pmol	Picomole, 10 ⁻¹² moles
rpm	rotations per minute
s	second(s)
T	Tesla
V	Volts

Materials

AAV9	Adeno-associated virus 9
AP	Alkaline phosphatase
APS	Ammoniumperoxodisulfat
BDM	2,3-Butanedione monoxime
BSA	Bovine serum albumin
cDNA	Complementary DNA
CO ₂	Carbon dioxide
DAPI	4',6-diamidino-2-phenylindole

DEPC	Diethylpyrocarbonate
DMEM	Dulbecco's modified eagle medium
DMSO	Dimethyl sulfoxide
DNA	Deoxyribonucleic acid
dNTP	Deoxyribonucleotide triphosphate
Dox	Doxycycline
DTT	Dithiothreitol
EDTA	Ethylenediaminetetraacetic acid
EdU	5-ethynyl-2'-deoxyuridine
ELISA	Enzyme-linked immunosorbent assay
FBS	Fetal bovine serum
HEPES	4-(2-Hydroxyethyl)-1-piperazineethanesulfonic acid
KSR	Knockout serum replacement
LB	Luria-bertani
LIF	Leukemia inhibitory factor
MES	2-(<i>N</i> -morpholino)ethanesulfonic acid
mRNA	Messenger RNA
OCT	Optimal cutting temperature medium
PBS	Phosphate-buffered saline
PBST	Phosphate-buffered saline with Triton X-100
PFA	Paraformaldehyde
PVDF	Polyvinylidene fluoride
RNA	Ribonucleic acid
SDS	Sodium dodecyl sulfate
SDS-PAGE	Sodium dodecyl sulfate-polyacrylamide gel electrophoresis
TAM	Tamoxifen
TBST	Tris buffered saline with tween-20
TE	Tris-EDTA
TEMED	Tetramethylethylenediamine
Tris	Tris(hydroxymethyl)aminomethane
WGA	Wheat germ agglutinin

Gene and protein

Acta2	Actin alpha 2, smooth muscle
aSMA	Actin alpha 2, smooth muscle
CD31	Platelet endothelial cell adhesion molecule
CD45	Protein tyrosine phosphatase, receptor type, C
CDKIs	Cyclin-dependent kinase inhibitors
CDKs	Cyclin-dependent kinases
c-Myc	Myc proto-oncogene, bhlh transcription factor
cTnT	Cardiac troponin T

Cx43	Connexin 43
ErbB2	Erb-b2 receptor tyrosine kinase 2
ErbB4	Erb-b2 receptor tyrosine kinase 4
ESRRG	Estrogen related receptor gamma
FoxM1	Forkhead box m1
G1	Gap1
G2	Gap2
GAPDH	Glyceraldehyde-3-phosphate dehydrogenase
Gata4	GATA Binding protein 4
GFP	Green fluorescent protein
GMT	Gata4, Mef2c, and Tbx5
GMTH	Gata4, Mef2c, Tbx5, and Hand2
Hand2	Heart and neural crest derivatives expressed 2
Hoxb13	Homeobox B13
HP1 β	Heterochromatin Protein 1 β
Id1	Inhibitor Of DNA Binding 1, HLH Protein
IL6	Interleukin 6
Klf4	Kruppel like factor 4
M	Mitosis
Mef2c	Mef2c antisense rna 1
Meis1	Meis homeobox 1
MESP1	Mesoderm posterior bhlh transcription factor 1
miR-1	Microrna 1-1
miR133	Microrna 133
Myh7	Myosin heavy chain 7
MYOCD	Myocardin
Myod1	Myogenic differentiation 1
Nppa	Natriuretic peptide a
NRG1	Neuregulin 1
Oct4	Pou class 5 homeobox 1
OSK	Oct4, Sox2, and Klf4
OSKM	Oct4, Sox2, Klf4 and c-Myc
p16	Cyclin dependent kinase inhibitor 2a
p21	Cyclin dependent kinase inhibitor 1a
p21Waf1	CDK-interacting protein 1
p27	Cyclin dependent kinase inhibitor 1b
p27Kip1	Cyclin-dependent kinase inhibitor 1B
p57Kip2	Cyclin-dependent kinase inhibitor 1C
PCM1	Pericentriolar material 1
PDK1	Pyruvate dehydrogenase kinase 1
PH3	Phosphorylated histone 3
PI3K	Phosphatidylinositol-4,5-bisphosphate 3-kinase
S	Synthesis
Sox2	Sry-box transcription factor 2

Tbx5	T-box transcription factor 5
Tnni1	Troponin i1, slow skeletal type
Yap	Yes1 associated transcriptional regulator
YAP5SA	Five serine (S) to alanine (A) mutation in YAP
ZFPM2	Zinc finger protein, Fog family member 2

Cell

ESC-CM	Embryonic stem cell-derived cardiomyocytes
HEK293T	Human embryonic kidney 293 cells with SV40 large T antigen
iPSC-CM	Induced pluripotent stem cell-derived cardiomyocytes
iPSCs	Induced pluripotent cells
MEF	Mouse embryonic fibroblasts
MNCs	Bone marrow-derived mononuclear
MSCs	Bone marrow-derived (stromal) mesenchymal stem cells
PSC-CM	Pluripotent stem cell-derived cardiomyocytes

Other abbreviations

%	Percentage
AT	Acute treatment
ATAC-seq	Assay for Transposase-Accessible Chromatin using sequencing
fMRI	Functional magnetic resonance imaging
G1	Gap1
G2	Gap2
IP	Intraperitoneal
LV	Left ventricle
LVEF	Left ventricle ejection fraction
LVSV	Left ventricle stroke volume
M	Mitosis
PT	Pre-treatment
RNA-seq	RNA sequencing
rtTA	Reverse tetracycline-controlled transactivator
S	Synthesis
Tet-on	Tetracycline-controlled transcriptional activation, turn on
TRE	Tetracycline response element
TT	Therapeutic treatment
WT	Wild type

References

1. Vivien, C.J., J.E. Hudson, and E.R. Porrello, *Evolution, comparative biology and ontogeny of vertebrate heart regeneration*. NPJ Regen Med, 2016. **1**: p. 16012.
2. Litvinukova, M., et al., *Cells of the adult human heart*. Nature, 2020. **588**(7838): p. 466-472.
3. Taylor, E.W., D. Jordan, and J.H. Coote, *Central control of the cardiovascular and respiratory systems and their interactions in vertebrates*. Physiological Reviews, 1999. **79**(3): p. 855-916.
4. Levine, H.J., *Rest heart rate and life expectancy*. J Am Coll Cardiol, 1997. **30**(4): p. 1104-6.
5. Bergmann, O., et al., *Evidence for cardiomyocyte renewal in humans*. Science, 2009. **324**(5923): p. 98-102.
6. Ayub, M.T. and D. Kalra, *Coronary Microvascular Dysfunction and the Role of Noninvasive Cardiovascular Imaging*. Diagnostics (Basel), 2020. **10**(9).
7. Buckingham, M., S. Meilhac, and S. Zaffran, *Building the mammalian heart from two sources of myocardial cells*. Nat Rev Genet, 2005. **6**(11): p. 826-35.
8. Tam, P.P., et al., *The allocation of epiblast cells to the embryonic heart and other mesodermal lineages: the role of ingression and tissue movement during gastrulation*. Development, 1997. **124**(9): p. 1631-42.
9. Bulatovic, I., et al., *Human fetal cardiac progenitors: The role of stem cells and progenitors in the fetal and adult heart*. Best Pract Res Clin Obstet Gynaecol, 2016. **31**: p. 58-68.
10. Sylva, M., M.J. van den Hoff, and A.F. Moorman, *Development of the human heart*. Am J Med Genet A, 2014. **164A**(6): p. 1347-71.
11. Del Monte-Nieto, G., et al., *Control of cardiac jelly dynamics by NOTCH1 and NRG1 defines the building plan for trabeculation*. Nature, 2018. **557**(7705): p. 439-445.
12. Le Garrec, J.F., et al., *Quantitative analysis of polarity in 3D reveals local cell coordination in the embryonic mouse heart*. Development, 2013. **140**(2): p. 395-404.
13. Sedmera, D., et al., *Developmental patterning of the myocardium*. Anat Rec, 2000. **258**(4): p. 319-37.
14. Buijtendijk, M.F.J., P. Barnett, and M.J.B. van den Hoff, *Development of the human heart*. Am J Med Genet C Semin Med Genet, 2020. **184**(1): p. 7-22.
15. Gavaghan, M., *Cardiac anatomy and physiology: a review*. AORN J, 1998. **67**(4): p. 802-22; quiz 824-8.
16. Sen, T., et al., *Which Coronary Lesions Are More Prone to Cause Acute Myocardial Infarction?* Arq Bras Cardiol, 2017. **108**(2): p. 149-153.
17. Reimer, K.A., et al., *The wavefront phenomenon of ischemic cell death. 1. Myocardial infarct size vs duration of coronary occlusion in dogs*. Circulation, 1977. **56**(5): p. 786-94.
18. Bunch, T.J., S.H. Hohnloser, and B.J. Gersh, *Mechanisms of sudden cardiac death in myocardial infarction survivors: insights from the randomized trials of implantable cardioverter-defibrillators*. Circulation, 2007. **115**(18): p. 2451-7.

19. Jenca, D., et al., *Heart failure after myocardial infarction: incidence and predictors*. ESC Heart Fail, 2021. **8**(1): p. 222-237.
20. Virani, S.S., et al., *Heart Disease and Stroke Statistics-2021 Update: A Report From the American Heart Association*. Circulation, 2021. **143**(8): p. e254-e743.
21. Goldman, J.A. and K.D. Poss, *Gene regulatory programmes of tissue regeneration*. Nat Rev Genet, 2020. **21**(9): p. 511-525.
22. Morgan, T.H., *Experimental studies of the regeneration of Planaria maculata*. Roux's archives of developmental biology, 1898. **7**(2): p. 364-397.
23. Candia Carnevali, M.D., et al., *Cellular and molecular mechanisms of arm regeneration in crinoid echinoderms: the potential of arm explants*. Dev Genes Evol, 1998. **208**(8): p. 421-30.
24. Reddy, P.C., A. Gungi, and M. Unni, *Cellular and Molecular Mechanisms of Hydra Regeneration*. Results Probl Cell Differ, 2019. **68**: p. 259-290.
25. Ham, R.G. and R.E. Eakin, *Time sequence of certain physiological events during regeneration in hydra*. J Exp Zool, 1958. **139**(1): p. 33-53.
26. Pfefferli, C. and A. Jazwinska, *The art of fin regeneration in zebrafish*. Regeneration (Oxf), 2015. **2**(2): p. 72-83.
27. Simon, A. and E.M. Tanaka, *Limb regeneration*. Wiley Interdiscip Rev Dev Biol, 2013. **2**(2): p. 291-300.
28. Poss, K.D., L.G. Wilson, and M.T. Keating, *Heart regeneration in zebrafish*. Science, 2002. **298**(5601): p. 2188-90.
29. Wosczyzna, M.N. and T.A. Rando, *A Muscle Stem Cell Support Group: Coordinated Cellular Responses in Muscle Regeneration*. Dev Cell, 2018. **46**(2): p. 135-143.
30. Michalopoulos, G.K. and M.C. DeFrances, *Liver regeneration*. Science, 1997. **276**(5309): p. 60-6.
31. Michalopoulos, G.K., *Principles of liver regeneration and growth homeostasis*. Compr Physiol, 2013. **3**(1): p. 485-513.
32. Fausto, N., J.S. Campbell, and K.J. Riehle, *Liver regeneration*. Hepatology, 2006. **43**(2 Suppl 1): p. S45-53.
33. Takeo, M., W. Lee, and M. Ito, *Wound healing and skin regeneration*. Cold Spring Harb Perspect Med, 2015. **5**(1): p. a023267.
34. Rafii, S., J.M. Butler, and B.S. Ding, *Angiocrine functions of organ-specific endothelial cells*. Nature, 2016. **529**(7586): p. 316-25.
35. Oates, P.S. and A.R. West, *Heme in intestinal epithelial cell turnover, differentiation, detoxification, inflammation, carcinogenesis, absorption and motility*. World J Gastroenterol, 2006. **12**(27): p. 4281-95.
36. Lee, L.P., P.Y. Lau, and C.W. Chan, *A simple and efficient treatment for fingertip injuries*. J Hand Surg Br, 1995. **20**(1): p. 63-71.
37. Lemperle, G., M. Schwarz, and S.M. Lemperle, *Nail regeneration by elongation of the partially destroyed nail bed*. Plast Reconstr Surg, 2003. **111**(1): p. 167-72; discussion 173.
38. Ohta, M. and M. Saito, *[Regeneration of bone marrow tissue. Growth and differentiation of hematopoietic stem cells and the role of bone marrow microenvironment on hematopoiesis]*. Hum Cell, 1991. **4**(3): p. 212-21.
39. Stocum, D.L. and J.A. Cameron, *Looking proximally and distally: 100 years of limb regeneration and beyond*. Dev Dyn, 2011. **240**(5): p. 943-68.
40. Brockes, J.P. and A. Kumar, *Comparative aspects of animal regeneration*. Annu Rev Cell Dev Biol, 2008. **24**: p. 525-49.
41. Chernoff, E.A., et al., *Urodele spinal cord regeneration and related processes*. Dev Dyn, 2003. **226**(2): p. 295-307.

42. Simkin, J., et al., *The mammalian blastema: regeneration at our fingertips*. *Regeneration (Oxf)*, 2015. **2**(3): p. 93-105.
43. Seifert, A.W., et al., *Skin shedding and tissue regeneration in African spiny mice (Acomys)*. *Nature*, 2012. **489**(7417): p. 561-5.
44. Williams-Boyce, P.K. and J.C. Daniel, Jr., *Comparison of ear tissue regeneration in mammals*. *J Anat*, 1986. **149**: p. 55-63.
45. Williams-Boyce, P.K. and J.C. Daniel, Jr., *Regeneration of rabbit ear tissue*. *J Exp Zool*, 1980. **212**(2): p. 243-53.
46. Li, C., et al., *Deer antler--a novel model for studying organ regeneration in mammals*. *Int J Biochem Cell Biol*, 2014. **56**: p. 111-22.
47. Borgens, R.B., *Mice regrow the tips of their foretoes*. *Science*, 1982. **217**(4561): p. 747-50.
48. Singer, M., et al., *Open finger tip healing and replacement after distal amputation in rhesus monkey with comparison to limb regeneration in lower vertebrates*. *Anat Embryol (Berl)*, 1987. **177**(1): p. 29-36.
49. Douglas, B.S., *Conservative management of guillotine amputation of the finger in children*. *Aust Paediatr J*, 1972. **8**(2): p. 86-9.
50. Gerber, T., et al., *Single-cell analysis uncovers convergence of cell identities during axolotl limb regeneration*. *Science*, 2018. **362**(6413).
51. Lehoczky, J.A., B. Robert, and C.J. Tabin, *Mouse digit tip regeneration is mediated by fate-restricted progenitor cells*. *Proc Natl Acad Sci U S A*, 2011. **108**(51): p. 20609-14.
52. Rinkevich, Y., et al., *Germ-layer and lineage-restricted stem/progenitors regenerate the mouse digit tip*. *Nature*, 2011. **476**(7361): p. 409-13.
53. Stewart, S. and K. Stankunas, *Limited dedifferentiation provides replacement tissue during zebrafish fin regeneration*. *Dev Biol*, 2012. **365**(2): p. 339-49.
54. Tu, S. and S.L. Johnson, *Fate restriction in the growing and regenerating zebrafish fin*. *Dev Cell*, 2011. **20**(5): p. 725-32.
55. Singh, S.P., J.E. Holdway, and K.D. Poss, *Regeneration of amputated zebrafish fin rays from de novo osteoblasts*. *Dev Cell*, 2012. **22**(4): p. 879-86.
56. Chien, K.R., et al., *Regenerating the field of cardiovascular cell therapy*. *Nat Biotechnol*, 2019. **37**(3): p. 232-237.
57. Dumont, N.A., et al., *Satellite Cells and Skeletal Muscle Regeneration*. *Compr Physiol*, 2015. **5**(3): p. 1027-59.
58. Preussner, J., et al., *Oncogenic Amplification of Zygotic Dux Factors in Regenerating p53-Deficient Muscle Stem Cells Defines a Molecular Cancer Subtype*. *Cell Stem Cell*, 2018. **23**(6): p. 794-805 e4.
59. Tomasetti, C., B. Vogelstein, and G. Parmigiani, *Half or more of the somatic mutations in cancers of self-renewing tissues originate prior to tumor initiation*. *Proc Natl Acad Sci U S A*, 2013. **110**(6): p. 1999-2004.
60. Patel, J. and M.N. Sheppard, *Pathological study of primary cardiac and pericardial tumours in a specialist UK Centre: surgical and autopsy series*. *Cardiovasc Pathol*, 2010. **19**(6): p. 343-52.
61. Grebenc, M.L., et al., *Primary cardiac and pericardial neoplasms: radiologic-pathologic correlation*. *Radiographics*, 2000. **20**(4): p. 1073-103; quiz 1110-1, 1112.
62. Castillo, J.G. and G. Silvay, *Characterization and management of cardiac tumors*. *Semin Cardiothorac Vasc Anesth*, 2010. **14**(1): p. 6-20.
63. Cano-Martinez, A., et al., *Functional and structural regeneration in the axolotl heart (Ambystoma mexicanum) after partial ventricular amputation*. *Arch Cardiol Mex*, 2010. **80**(2): p. 79-86.

64. Chablais, F., et al., *The zebrafish heart regenerates after cryoinjury-induced myocardial infarction*. BMC Dev Biol, 2011. **11**: p. 21.
65. Gonzalez-Rosa, J.M., et al., *Extensive scar formation and regression during heart regeneration after cryoinjury in zebrafish*. Development, 2011. **138**(9): p. 1663-74.
66. Witman, N., et al., *Recapitulation of developmental cardiogenesis governs the morphological and functional regeneration of adult newt hearts following injury*. Dev Biol, 2011. **354**(1): p. 67-76.
67. Kikuchi, K., et al., *Primary contribution to zebrafish heart regeneration by gata4(+) cardiomyocytes*. Nature, 2010. **464**(7288): p. 601-5.
68. Wang, J., et al., *The regenerative capacity of zebrafish reverses cardiac failure caused by genetic cardiomyocyte depletion*. Development, 2011. **138**(16): p. 3421-30.
69. Maliken, B.D. and J.D. Molkentin, *Undeniable Evidence That the Adult Mammalian Heart Lacks an Endogenous Regenerative Stem Cell*. Circulation, 2018. **138**(8): p. 806-808.
70. Senyo, S.E., et al., *Mammalian heart renewal by pre-existing cardiomyocytes*. Nature, 2013. **493**(7432): p. 433-6.
71. Bergmann, O., et al., *Dynamics of Cell Generation and Turnover in the Human Heart*. Cell, 2015. **161**(7): p. 1566-75.
72. van Berlo, J.H., et al., *c-kit+ cells minimally contribute cardiomyocytes to the heart*. Nature, 2014. **509**(7500): p. 337-41.
73. Nadal-Ginard, B., G.M. Ellison, and D. Torella, *Absence of evidence is not evidence of absence: pitfalls of cre knock-ins in the c-Kit locus*. Circ Res, 2014. **115**(4): p. 415-8.
74. Murry, C.E., H. Reinecke, and L.M. Pabon, *Regeneration gaps: observations on stem cells and cardiac repair*. J Am Coll Cardiol, 2006. **47**(9): p. 1777-85.
75. Wilhelm, M.J., *Long-term outcome following heart transplantation: current perspective*. J Thorac Dis, 2015. **7**(3): p. 549-51.
76. Rose, E.A., et al., *Long-term use of a left ventricular assist device for end-stage heart failure*. N Engl J Med, 2001. **345**(20): p. 1435-43.
77. Bristow, M.R., et al., *Cardiac-resynchronization therapy with or without an implantable defibrillator in advanced chronic heart failure*. N Engl J Med, 2004. **350**(21): p. 2140-50.
78. Yacoub, M., *Cardiac donation after circulatory death: a time to reflect*. Lancet, 2015. **385**(9987): p. 2554-6.
79. Huang, P., et al., *Induction of functional hepatocyte-like cells from mouse fibroblasts by defined factors*. Nature, 2011. **475**(7356): p. 386-9.
80. Vierbuchen, T., et al., *Direct conversion of fibroblasts to functional neurons by defined factors*. Nature, 2010. **463**(7284): p. 1035-41.
81. Tarlow, B.D., et al., *Bipotential adult liver progenitors are derived from chronically injured mature hepatocytes*. Cell Stem Cell, 2014. **15**(5): p. 605-18.
82. Yanger, K., et al., *Robust cellular reprogramming occurs spontaneously during liver regeneration*. Genes Dev, 2013. **27**(7): p. 719-24.
83. Thorel, F., et al., *Conversion of adult pancreatic alpha-cells to beta-cells after extreme beta-cell loss*. Nature, 2010. **464**(7292): p. 1149-54.
84. Davis, R.L., H. Weintraub, and A.B. Lassar, *Expression of a single transfected cDNA converts fibroblasts to myoblasts*. Cell, 1987. **51**(6): p. 987-1000.
85. Qian, L., et al., *In vivo reprogramming of murine cardiac fibroblasts into induced cardiomyocytes*. Nature, 2012. **485**(7400): p. 593-8.
86. Song, K., et al., *Heart repair by reprogramming non-myocytes with cardiac transcription factors*. Nature, 2012. **485**(7400): p. 599-604.
87. Nam, Y.J., et al., *Reprogramming of human fibroblasts toward a cardiac fate*. Proc Natl Acad Sci U S A, 2013. **110**(14): p. 5588-93.

88. Wada, R., et al., *Induction of human cardiomyocyte-like cells from fibroblasts by defined factors*. Proc Natl Acad Sci U S A, 2013. **110**(31): p. 12667-72.
89. Fu, J.D., et al., *Direct reprogramming of human fibroblasts toward a cardiomyocyte-like state*. Stem Cell Reports, 2013. **1**(3): p. 235-47.
90. Cao, N., et al., *Conversion of human fibroblasts into functional cardiomyocytes by small molecules*. Science, 2016. **352**(6290): p. 1216-20.
91. Klose, K., M. Gossen, and C. Stamm, *Turning fibroblasts into cardiomyocytes: technological review of cardiac transdifferentiation strategies*. FASEB J, 2019. **33**(1): p. 49-70.
92. Aly, R.M., *Current state of stem cell-based therapies: an overview*. Stem Cell Investig, 2020. **7**: p. 8.
93. Taylor, D.A., et al., *Regenerating functional myocardium: improved performance after skeletal myoblast transplantation*. Nat Med, 1998. **4**(8): p. 929-33.
94. He, K.L., et al., *Autologous skeletal myoblast transplantation improved hemodynamics and left ventricular function in chronic heart failure dogs*. J Heart Lung Transplant, 2005. **24**(11): p. 1940-9.
95. Farahmand, P., et al., *Skeletal myoblasts preserve remote matrix architecture and global function when implanted early or late after coronary ligation into infarcted or remote myocardium*. Circulation, 2008. **118**(14 Suppl): p. S130-7.
96. Menasche, P., *Cell therapy trials for heart regeneration - lessons learned and future directions*. Nat Rev Cardiol, 2018. **15**(11): p. 659-671.
97. Assmus, B., et al., *Transplantation of Progenitor Cells and Regeneration Enhancement in Acute Myocardial Infarction (TOPCARE-AMI)*. Circulation, 2002. **106**(24): p. 3009-17.
98. Strauer, B.E., et al., *Repair of infarcted myocardium by autologous intracoronary mononuclear bone marrow cell transplantation in humans*. Circulation, 2002. **106**(15): p. 1913-8.
99. Leistner, D.M., et al., *Transplantation of progenitor cells and regeneration enhancement in acute myocardial infarction (TOPCARE-AMI): final 5-year results suggest long-term safety and efficacy*. Clin Res Cardiol, 2011. **100**(10): p. 925-34.
100. Surder, D., et al., *Effect of Bone Marrow-Derived Mononuclear Cell Treatment, Early or Late After Acute Myocardial Infarction: Twelve Months CMR and Long-Term Clinical Results*. Circ Res, 2016. **119**(3): p. 481-90.
101. Hare, J.M., et al., *Comparison of allogeneic vs autologous bone marrow-derived mesenchymal stem cells delivered by transendocardial injection in patients with ischemic cardiomyopathy: the POSEIDON randomized trial*. JAMA, 2012. **308**(22): p. 2369-79.
102. Heldman, A.W., et al., *Transendocardial mesenchymal stem cells and mononuclear bone marrow cells for ischemic cardiomyopathy: the TAC-HFT randomized trial*. JAMA, 2014. **311**(1): p. 62-73.
103. Tano, N., et al., *Epicardial placement of mesenchymal stromal cell-sheets for the treatment of ischemic cardiomyopathy; in vivo proof-of-concept study*. Mol Ther, 2014. **22**(10): p. 1864-71.
104. Kehat, I., et al., *Electromechanical integration of cardiomyocytes derived from human embryonic stem cells*. Nat Biotechnol, 2004. **22**(10): p. 1282-9.
105. Ishida, M., et al., *Transplantation of Human-induced Pluripotent Stem Cell-derived Cardiomyocytes Is Superior to Somatic Stem Cell Therapy for Restoring Cardiac Function and Oxygen Consumption in a Porcine Model of Myocardial Infarction*. Transplantation, 2019. **103**(2): p. 291-298.
106. Shiba, Y., et al., *Human ES-cell-derived cardiomyocytes electrically couple and suppress arrhythmias in injured hearts*. Nature, 2012. **489**(7415): p. 322-5.

107. Fernandes, S., et al., *Human embryonic stem cell-derived cardiomyocytes engraft but do not alter cardiac remodeling after chronic infarction in rats*. J Mol Cell Cardiol, 2010. **49**(6): p. 941-9.
108. Shiba, Y., et al., *Electrical Integration of Human Embryonic Stem Cell-Derived Cardiomyocytes in a Guinea Pig Chronic Infarct Model*. J Cardiovasc Pharmacol Ther, 2014. **19**(4): p. 368-381.
109. Liu, Y.W., et al., *Human embryonic stem cell-derived cardiomyocytes restore function in infarcted hearts of non-human primates*. Nat Biotechnol, 2018. **36**(7): p. 597-605.
110. Chong, J.J., et al., *Human embryonic-stem-cell-derived cardiomyocytes regenerate non-human primate hearts*. Nature, 2014. **510**(7504): p. 273-7.
111. van Laake, L.W., et al., *Human embryonic stem cell-derived cardiomyocytes survive and mature in the mouse heart and transiently improve function after myocardial infarction*. Stem Cell Res, 2007. **1**(1): p. 9-24.
112. Kawamura, M., et al., *Feasibility, safety, and therapeutic efficacy of human induced pluripotent stem cell-derived cardiomyocyte sheets in a porcine ischemic cardiomyopathy model*. Circulation, 2012. **126**(11 Suppl 1): p. S29-37.
113. Liu, Y.W., et al., *Erratum: Human embryonic stem cell-derived cardiomyocytes restore function in infarcted hearts of non-human primates*. Nat Biotechnol, 2018. **36**(9): p. 899.
114. Guo, R., et al., *Stem cell-derived cell sheet transplantation for heart tissue repair in myocardial infarction*. Stem Cell Res Ther, 2020. **11**(1): p. 19.
115. Kawamura, M., et al., *Enhanced survival of transplanted human induced pluripotent stem cell-derived cardiomyocytes by the combination of cell sheets with the pedicled omental flap technique in a porcine heart*. Circulation, 2013. **128**(11 Suppl 1): p. S87-94.
116. Kawamura, M., et al., *Enhanced Therapeutic Effects of Human iPS Cell Derived-Cardiomyocyte by Combined Cell-Sheets with Omental Flap Technique in Porcine Ischemic Cardiomyopathy Model*. Sci Rep, 2017. **7**(1): p. 8824.
117. Liew, L.C., B.X. Ho, and B.S. Soh, *Mending a broken heart: current strategies and limitations of cell-based therapy*. Stem Cell Res Ther, 2020. **11**(1): p. 138.
118. Becker, R.O., S. Chapin, and R. Sherry, *Regeneration of the ventricular myocardium in amphibians*. Nature, 1974. **248**(5444): p. 145-7.
119. Porrello, E.R., et al., *Transient regenerative potential of the neonatal mouse heart*. Science, 2011. **331**(6020): p. 1078-80.
120. Zhu, W., et al., *Regenerative Potential of Neonatal Porcine Hearts*. Circulation, 2018. **138**(24): p. 2809-2816.
121. Haubner, B.J., et al., *Functional Recovery of a Human Neonatal Heart After Severe Myocardial Infarction*. Circ Res, 2016. **118**(2): p. 216-21.
122. Bersell, K., et al., *Neuregulin1/ErbB4 signaling induces cardiomyocyte proliferation and repair of heart injury*. Cell, 2009. **138**(2): p. 257-70.
123. D'Uva, G., et al., *ERBB2 triggers mammalian heart regeneration by promoting cardiomyocyte dedifferentiation and proliferation*. Nat Cell Biol, 2015. **17**(5): p. 627-38.
124. Fan, R., N.G. Kim, and B.M. Gumbiner, *Regulation of Hippo pathway by mitogenic growth factors via phosphoinositide 3-kinase and phosphoinositide-dependent kinase-1*. Proc Natl Acad Sci U S A, 2013. **110**(7): p. 2569-74.
125. Heallen, T., et al., *Hippo pathway inhibits Wnt signaling to restrain cardiomyocyte proliferation and heart size*. Science, 2011. **332**(6028): p. 458-61.
126. Halder, G. and R.L. Johnson, *Hippo signaling: growth control and beyond*. Development, 2011. **138**(1): p. 9-22.

127. Morikawa, Y., et al., *Dystrophin-glycoprotein complex sequesters Yap to inhibit cardiomyocyte proliferation*. Nature, 2017. **547**(7662): p. 227-231.
128. Leach, J.P., et al., *Hippo pathway deficiency reverses systolic heart failure after infarction*. Nature, 2017. **550**(7675): p. 260-264.
129. von Gise, A., et al., *YAP1, the nuclear target of Hippo signaling, stimulates heart growth through cardiomyocyte proliferation but not hypertrophy*. Proc Natl Acad Sci U S A, 2012. **109**(7): p. 2394-9.
130. Monroe, T.O., et al., *YAP Partially Reprograms Chromatin Accessibility to Directly Induce Adult Cardiogenesis In Vivo*. Dev Cell, 2019. **48**(6): p. 765-779 e7.
131. Hirose, K., et al., *Evidence for hormonal control of heart regenerative capacity during endothermy acquisition*. Science, 2019. **364**(6436): p. 184-188.
132. Bassat, E., et al., *The extracellular matrix protein agrin promotes heart regeneration in mice*. Nature, 2017. **547**(7662): p. 179-184.
133. Eulalio, A., et al., *Functional screening identifies miRNAs inducing cardiac regeneration*. Nature, 2012. **492**(7429): p. 376-81.
134. Huang, W., et al., *Loss of microRNA-128 promotes cardiomyocyte proliferation and heart regeneration*. Nat Commun, 2018. **9**(1): p. 700.
135. Tao, Y., et al., *miR-199a-3p promotes cardiomyocyte proliferation by inhibiting Cd151 expression*. Biochem Biophys Res Commun, 2019. **516**(1): p. 28-36.
136. Liu, N., et al., *microRNA-133a regulates cardiomyocyte proliferation and suppresses smooth muscle gene expression in the heart*. Genes Dev, 2008. **22**(23): p. 3242-54.
137. Malumbres, M. and M. Barbacid, *Cell cycle, CDKs and cancer: a changing paradigm*. Nat Rev Cancer, 2009. **9**(3): p. 153-66.
138. Pasumarthi, K.B., et al., *Targeted expression of cyclin D2 results in cardiomyocyte DNA synthesis and infarct regression in transgenic mice*. Circ Res, 2005. **96**(1): p. 110-8.
139. Bicknell, K.A., C.H. Coxon, and G. Brooks, *Forced expression of the cyclin B1-CDC2 complex induces proliferation in adult rat cardiomyocytes*. Biochem J, 2004. **382**(Pt 2): p. 411-6.
140. Shapiro, S.D., et al., *Cyclin A2 induces cardiac regeneration after myocardial infarction through cytokinesis of adult cardiomyocytes*. Sci Transl Med, 2014. **6**(224): p. 224ra27.
141. Di Stefano, V., et al., *Knockdown of cyclin-dependent kinase inhibitors induces cardiomyocyte re-entry in the cell cycle*. J Biol Chem, 2011. **286**(10): p. 8644-8654.
142. Mohamed, T.M.A., et al., *Regulation of Cell Cycle to Stimulate Adult Cardiomyocyte Proliferation and Cardiac Regeneration*. Cell, 2018. **173**(1): p. 104-116 e12.
143. Cheng, Y.Y., et al., *Reprogramming-derived gene cocktail increases cardiomyocyte proliferation for heart regeneration*. EMBO Mol Med, 2017. **9**(2): p. 251-264.
144. Ebel, H., et al., *Divergent siblings: E2F2 and E2F4 but not E2F1 and E2F3 induce DNA synthesis in cardiomyocytes without activation of apoptosis*. Circ Res, 2005. **96**(5): p. 509-17.
145. Mahmoud, A.I., et al., *Meis1 regulates postnatal cardiomyocyte cell cycle arrest*. Nature, 2013. **497**(7448): p. 249-253.
146. Nguyen, N.U.N., et al., *A calcineurin-Hoxb13 axis regulates growth mode of mammalian cardiomyocytes*. Nature, 2020. **582**(7811): p. 271-276.
147. Wang, W.E., et al., *Dedifferentiation, Proliferation, and Redifferentiation of Adult Mammalian Cardiomyocytes After Ischemic Injury*. Circulation, 2017. **136**(9): p. 834-848.
148. Takahashi, K., et al., *Induction of pluripotent stem cells from adult human fibroblasts by defined factors*. Cell, 2007. **131**(5): p. 861-72.

149. Aasen, T., et al., *Efficient and rapid generation of induced pluripotent stem cells from human keratinocytes*. Nat Biotechnol, 2008. **26**(11): p. 1276-84.
150. Ye, Z., et al., *Human-induced pluripotent stem cells from blood cells of healthy donors and patients with acquired blood disorders*. Blood, 2009. **114**(27): p. 5473-80.
151. Unzu, C., et al., *Human Hepatocyte-Derived Induced Pluripotent Stem Cells: MYC Expression, Similarities to Human Germ Cell Tumors, and Safety Issues*. Stem Cells Int, 2016. **2016**: p. 4370142.
152. Bar-Nur, O., et al., *Epigenetic memory and preferential lineage-specific differentiation in induced pluripotent stem cells derived from human pancreatic islet beta cells*. Cell Stem Cell, 2011. **9**(1): p. 17-23.
153. Quattrocelli, M., et al., *Intrinsic cell memory reinforces myogenic commitment of pericyte-derived iPSCs*. J Pathol, 2011. **223**(5): p. 593-603.
154. Ruiz, S., et al., *High-efficient generation of induced pluripotent stem cells from human astrocytes*. PLoS One, 2010. **5**(12): p. e15526.
155. Miyoshi, N., et al., *Defined factors induce reprogramming of gastrointestinal cancer cells*. Proc Natl Acad Sci U S A, 2010. **107**(1): p. 40-5.
156. Kotini, A.G., et al., *Functional analysis of a chromosomal deletion associated with myelodysplastic syndromes using isogenic human induced pluripotent stem cells*. Nat Biotechnol, 2015. **33**(6): p. 646-55.
157. Kim, K.P., et al., *Permissive epigenomes endow reprogramming competence to transcriptional regulators*. Nat Chem Biol, 2021. **17**(1): p. 47-56.
158. Soufi, A., et al., *Pioneer transcription factors target partial DNA motifs on nucleosomes to initiate reprogramming*. Cell, 2015. **161**(3): p. 555-568.
159. Leichsenring, M., et al., *Pou5f1 transcription factor controls zygotic gene activation in vertebrates*. Science, 2013. **341**(6149): p. 1005-9.
160. Li, R., et al., *A mesenchymal-to-epithelial transition initiates and is required for the nuclear reprogramming of mouse fibroblasts*. Cell Stem Cell, 2010. **7**(1): p. 51-63.
161. Wernig, M., et al., *c-Myc is dispensable for direct reprogramming of mouse fibroblasts*. Cell Stem Cell, 2008. **2**(1): p. 10-2.
162. Hanna, J., et al., *Direct cell reprogramming is a stochastic process amenable to acceleration*. Nature, 2009. **462**(7273): p. 595-601.
163. Buganim, Y., D.A. Faddah, and R. Jaenisch, *Mechanisms and models of somatic cell reprogramming*. Nat Rev Genet, 2013. **14**(6): p. 427-39.
164. Abad, M., et al., *Reprogramming in vivo produces teratomas and iPSC cells with totipotency features*. Nature, 2013. **502**(7471): p. 340-5.
165. Haenebalcke, L., et al., *The ROSA26-iPSC mouse: a conditional, inducible, and exchangeable resource for studying cellular (De)differentiation*. Cell Rep, 2013. **3**(2): p. 335-41.
166. Marion, R.M., et al., *Telomeres acquire embryonic stem cell characteristics in induced pluripotent stem cells*. Cell Stem Cell, 2009. **4**(2): p. 141-54.
167. Marion, R.M., et al., *A p53-mediated DNA damage response limits reprogramming to ensure iPSC cell genomic integrity*. Nature, 2009. **460**(7259): p. 1149-53.
168. Suhr, S.T., et al., *Mitochondrial rejuvenation after induced pluripotency*. PLoS One, 2010. **5**(11): p. e14095.
169. Lapasset, L., et al., *Rejuvenating senescent and centenarian human cells by reprogramming through the pluripotent state*. Genes Dev, 2011. **25**(21): p. 2248-53.
170. Manukyan, M. and P.B. Singh, *Epigenome rejuvenation: HP1beta mobility as a measure of pluripotent and senescent chromatin ground states*. Sci Rep, 2014. **4**: p. 4789.
171. Ocampo, A., et al., *In Vivo Amelioration of Age-Associated Hallmarks by Partial Reprogramming*. Cell, 2016. **167**(7): p. 1719-1733 e12.

-
172. Lu, Y., et al., *Reprogramming to recover youthful epigenetic information and restore vision*. Nature, 2020. **588**(7836): p. 124-129.
173. Sarkar, T.J., et al., *Transient non-integrative expression of nuclear reprogramming factors promotes multifaceted amelioration of aging in human cells*. Nat Commun, 2020. **11**(1): p. 1545.
174. Rodriguez-Matellan, A., et al., *In Vivo Reprogramming Ameliorates Aging Features in Dentate Gyrus Cells and Improves Memory in Mice*. Stem Cell Reports, 2020. **15**(5): p. 1056-1066.
175. Ackers-Johnson, M., et al., *A Simplified, Langendorff-Free Method for Concomitant Isolation of Viable Cardiac Myocytes and Nonmyocytes From the Adult Mouse Heart*. Circ Res, 2016. **119**(8): p. 909-20.
176. Itah, R., I. Gitelman, and C. Davis, *A replacement for methoxyflurane (Metofane) in open-circuit anaesthesia*. Lab Anim, 2004. **38**(3): p. 280-5.
177. Nakada, Y., et al., *Hypoxia induces heart regeneration in adult mice*. Nature, 2017. **541**(7636): p. 222-227.
178. Mahmoud, A.I., et al., *Surgical models for cardiac regeneration in neonatal mice*. Nat Protoc, 2014. **9**(2): p. 305-11.
179. Dobin, A., et al., *STAR: ultrafast universal RNA-seq aligner*. Bioinformatics, 2013. **29**(1): p. 15-21.
180. Liao, Y., G.K. Smyth, and W. Shi, *featureCounts: an efficient general purpose program for assigning sequence reads to genomic features*. Bioinformatics, 2014. **30**(7): p. 923-30.
181. Anders, S. and W. Huber, *Differential expression analysis for sequence count data*. Genome Biol, 2010. **11**(10): p. R106.
182. Greco, C.M., et al., *DNA hydroxymethylation controls cardiomyocyte gene expression in development and hypertrophy*. Nat Commun, 2016. **7**: p. 12418.
183. Abe, T., et al., *Establishment of conditional reporter mouse lines at ROSA26 locus for live cell imaging*. Genesis, 2011. **49**(7): p. 579-90.
184. Breckenridge, R., et al., *Pan-myocardial expression of Cre recombinase throughout mouse development*. Genesis, 2007. **45**(3): p. 135-44.
185. Schwenk, F., U. Baron, and K. Rajewsky, *A cre-transgenic mouse strain for the ubiquitous deletion of loxP-flanked gene segments including deletion in germ cells*. Nucleic Acids Res, 1995. **23**(24): p. 5080-1.
186. Jackson, T., et al., *The c-myc proto-oncogene regulates cardiac development in transgenic mice*. Mol Cell Biol, 1990. **10**(7): p. 3709-16.
187. Rizzi, R., et al., *Post-natal cardiomyocytes can generate iPS cells with an enhanced capacity toward cardiomyogenic re-differentiation*. Cell Death Differ, 2012. **19**(7): p. 1162-74.
188. Bywater, M.J., et al., *Reactivation of Myc transcription in the mouse heart unlocks its proliferative capacity*. Nat Commun, 2020. **11**(1): p. 1827.
189. Patterson, M., et al., *Frequency of mononuclear diploid cardiomyocytes underlies natural variation in heart regeneration*. Nat Genet, 2017. **49**(9): p. 1346-1353.
190. Muralidhar, S.A., et al., *Harnessing the power of dividing cardiomyocytes*. Glob Cardiol Sci Pract, 2013. **2013**(3): p. 212-21.
191. Lopaschuk, G.D., R.L. Collinsnakai, and T. Itoi, *Developmental-Changes in Energy Substrate Use by the Heart*. Cardiovascular Research, 1992. **26**(12): p. 1172-1180.
192. Vukusic, K., et al., *The Atrioventricular Junction: A Potential Niche Region for Progenitor Cells in the Adult Human Heart*. Stem Cells Dev, 2019. **28**(16): p. 1078-1088.
193. Jopling, C., et al., *Zebrafish heart regeneration occurs by cardiomyocyte dedifferentiation and proliferation*. Nature, 2010. **464**(7288): p. 606-9.

194. Sleep, E., et al., *Transcriptomics approach to investigate zebrafish heart regeneration*. J Cardiovasc Med (Hagerstown), 2010. **11**(5): p. 369-80.
195. Zhu, Y., et al., *What we know about cardiomyocyte dedifferentiation*. J Mol Cell Cardiol, 2021. **152**: p. 80-91.
196. Liu, H., et al., *Disassembly of myofibrils and potential imbalanced forces on Z-discs in cultured adult cardiomyocytes*. Cytoskeleton (Hoboken), 2016. **73**(5): p. 246-57.
197. Ausma, J., et al., *Dedifferentiated cardiomyocytes from chronic hibernating myocardium are ischemia-tolerant*. Mol Cell Biochem, 1998. **186**(1-2): p. 159-68.
198. Szibor, M., et al., *Remodeling and dedifferentiation of adult cardiomyocytes during disease and regeneration*. Cell Mol Life Sci, 2014. **71**(10): p. 1907-16.
199. Payan, S.M., F. Hubert, and F. Rochais, *Cardiomyocyte proliferation, a target for cardiac regeneration*. Biochim Biophys Acta Mol Cell Res, 2020. **1867**(3): p. 118461.
200. Kisby, T., et al., *Transient reprogramming of postnatal cardiomyocytes to a dedifferentiated state*. PLoS One, 2021. **16**(5): p. e0251054.
201. Guo, Y. and W.T. Pu, *Cardiomyocyte Maturation: New Phase in Development*. Circ Res, 2020. **126**(8): p. 1086-1106.
202. Pei, D., et al., *Mesenchymal-epithelial transition in development and reprogramming*. Nat Cell Biol, 2019. **21**(1): p. 44-53.
203. Judd, J., J. Lovas, and G.N. Huang, *Isolation, Culture and Transduction of Adult Mouse Cardiomyocytes*. J Vis Exp, 2016(114).
204. Mosteiro, L., et al., *Tissue damage and senescence provide critical signals for cellular reprogramming in vivo*. Science, 2016. **354**(6315).
205. Berk, B.C., K. Fujiwara, and S. Lehoux, *ECM remodeling in hypertensive heart disease*. J Clin Invest, 2007. **117**(3): p. 568-75.
206. Mortensen, R.M., *Immune cell modulation of cardiac remodeling*. Circulation, 2012. **125**(13): p. 1597-600.
207. Gilsbach, R., et al., *Dynamic DNA methylation orchestrates cardiomyocyte development, maturation and disease*. Nat Commun, 2014. **5**: p. 5288.
208. Gilsbach, R., et al., *Distinct epigenetic programs regulate cardiac myocyte development and disease in the human heart in vivo*. Nat Commun, 2018. **9**(1): p. 391.
209. Akerberg, B.N., et al., *A reference map of murine cardiac transcription factor chromatin occupancy identifies dynamic and conserved enhancers*. Nat Commun, 2019. **10**(1): p. 4907.
210. Neubauer, S., *The failing heart--an engine out of fuel*. N Engl J Med, 2007. **356**(11): p. 1140-51.
211. Meder, B., et al., *Epigenome-Wide Association Study Identifies Cardiac Gene Patterning and a Novel Class of Biomarkers for Heart Failure*. Circulation, 2017. **136**(16): p. 1528-1544.
212. Nguyen, A.T., et al., *DOTIL regulates dystrophin expression and is critical for cardiac function*. Genes Dev, 2011. **25**(3): p. 263-74.
213. Onder, T.T., et al., *Chromatin-modifying enzymes as modulators of reprogramming*. Nature, 2012. **483**(7391): p. 598-602.
214. Noorman, M., et al., *Cardiac cell-cell junctions in health and disease: Electrical versus mechanical coupling*. J Mol Cell Cardiol, 2009. **47**(1): p. 23-31.
215. Accornero, F., et al., *Placental growth factor regulates cardiac adaptation and hypertrophy through a paracrine mechanism*. Circ Res, 2011. **109**(3): p. 272-80.
216. Segers, V.F.M. and G.W. De Keulenaer, *Autocrine Signaling in Cardiac Remodeling: A Rich Source of Therapeutic Targets*. J Am Heart Assoc, 2021. **10**(3): p. e019169.
217. Rockey, D.C., P.D. Bell, and J.A. Hill, *Fibrosis--a common pathway to organ injury and failure*. N Engl J Med, 2015. **372**(12): p. 1138-49.

218. van den Borne, S.W., et al., *Myocardial remodeling after infarction: the role of myofibroblasts*. Nat Rev Cardiol, 2010. **7**(1): p. 30-7.
219. Porter, K.E. and N.A. Turner, *Cardiac fibroblasts: at the heart of myocardial remodeling*. Pharmacol Ther, 2009. **123**(2): p. 255-78.
220. Pellman, J., J. Zhang, and F. Sheikh, *Myocyte-fibroblast communication in cardiac fibrosis and arrhythmias: Mechanisms and model systems*. J Mol Cell Cardiol, 2016. **94**: p. 22-31.
221. Kubin, T., et al., *Oncostatin M is a major mediator of cardiomyocyte dedifferentiation and remodeling*. Cell Stem Cell, 2011. **9**(5): p. 420-32.
222. Dispersyn, G.D., et al., *Dissociation of cardiomyocyte apoptosis and dedifferentiation in infarct border zones*. Eur Heart J, 2002. **23**(11): p. 849-57.
223. Aghajanian, H., et al., *Targeting cardiac fibrosis with engineered T cells*. Nature, 2019. **573**(7774): p. 430-433.
224. Van der Borght, K., et al., *Myocardial Infarction Primes Autoreactive T Cells through Activation of Dendritic Cells*. Cell Rep, 2017. **18**(12): p. 3005-3017.
225. Wagner, J.A., et al., *Efficient and persistent gene transfer of AAV-CFTR in maxillary sinus*. Lancet, 1998. **351**(9117): p. 1702-3.
226. Nathwani, A.C., et al., *Adenovirus-associated virus vector-mediated gene transfer in hemophilia B*. N Engl J Med, 2011. **365**(25): p. 2357-65.
227. Russell, S., et al., *Efficacy and safety of voretigene neparvovec (AAV2-hRPE65v2) in patients with RPE65-mediated inherited retinal dystrophy: a randomised, controlled, open-label, phase 3 trial*. Lancet, 2017. **390**(10097): p. 849-860.
228. Brantly, M.L., et al., *Phase I trial of intramuscular injection of a recombinant adeno-associated virus serotype 2 alpha1-antitrypsin (AAT) vector in AAT-deficient adults*. Hum Gene Ther, 2006. **17**(12): p. 1177-86.
229. Mendell, J.R., et al., *Single-Dose Gene-Replacement Therapy for Spinal Muscular Atrophy*. N Engl J Med, 2017. **377**(18): p. 1713-1722.
230. Maheshri, N., et al., *Directed evolution of adeno-associated virus yields enhanced gene delivery vectors*. Nat Biotechnol, 2006. **24**(2): p. 198-204.
231. Tabebordbar, M., et al., *Directed evolution of a family of AAV capsid variants enabling potent muscle-directed gene delivery across species*. Cell, 2021. **184**(19): p. 4919-4938 e22.
232. Ronaldson-Bouchard, K., et al., *Advanced maturation of human cardiac tissue grown from pluripotent stem cells*. Nature, 2018. **556**(7700): p. 239-243.
233. Tiburcy, M., et al., *Defined Engineered Human Myocardium With Advanced Maturation for Applications in Heart Failure Modeling and Repair*. Circulation, 2017. **135**(19): p. 1832-1847.
234. Hofbauer, P., et al., *Cardioids reveal self-organizing principles of human cardiogenesis*. Cell, 2021. **184**(12): p. 3299-3317 e22.